Tire-soil interaction analysis of forest machines

Karthik Prakash

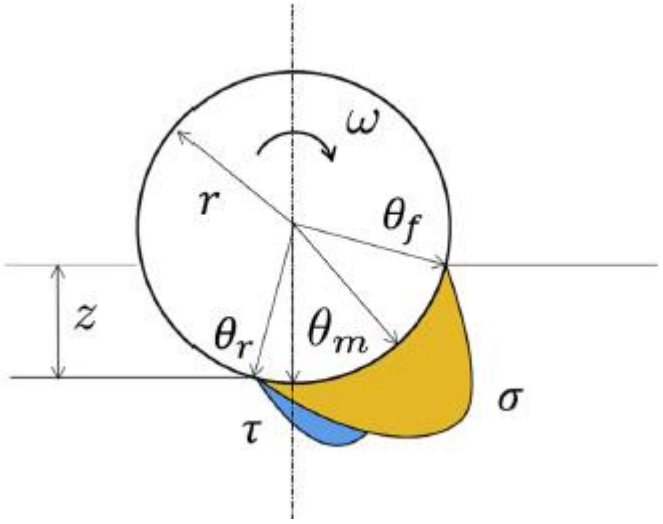

Master of Science Thesis MMK 2014:15 MKN 105
KTH Industrial Engineering and Management
Machine Design
SE-100 44 STOCKHOLM

Examensarbete MMK 2014:15 MKN 105

KTH Industriell teknik och management

Analys av däck-maskinteraktionen hos skogmaskiner

Karthik Prakash

Godkänt	Examinator	Handledare
2014-06-04	Ulf Sellgren	Ulf Sellgren
	Uppdragsgivare	Kontaktperson
	Skogforsk	Björn Löfgren

Sammanfattning

Kortvirkesmetoden är en mekaniserad för skogsavverkning. Det är en två-maskinsprocess, som utförs av en skördare och en skotare. Skotaren kan orsaka skador på marken, som exempelvis spårbildning och markpackning. Det har blivit allt viktigare att skydda skogen från de marskador orsakade av tunga maskiner. Detta är en initiell studie av samspelet mellan mark och hjul på en lastad skotare.

Olika WES-baserade spårdjupsmodeller har jämförts för att värdera deras förmåga att prediktera spårdjupen. Nya modeller har också utvecklats för att uppskatta relationen mellan spårdjup och flera hjulpassager. Modeller som kan prediktera kontakttrycket mellan däcket och marken, samt däckets markkontaktarea har studerats. Olika relationer för att bestämma mobilitetsparametrarna har också studerats.

Rötter spelar en viktig roll för att öka markens bärighet och att skydda den. Rötternas effekt på markens bärighet har behandlats i examensarbetet. Labbtester med tallrötter har genomförts för att bestämma deras armeringseffekt. Modeller som kan användas för att prediktera rötternas effekter har också studerats.

Ett första steg för att kunna kombinera WES- och Bekker-modeller har utförts, tillgängliga modeller som korrelerar WES- och Bekker-modeller har behandlats och en uppsättning relationer som relaterar de båda modellerna har härletts.
Effekten av halka i samband med nedsjunkning har studerats med hjälp av både WES- och Bekkerbaserade modeller. Dynamiksimuleringsprogramet MSC Adams har använts för att simulera skotarmodellen för att bestämma dess lämplighet för spårdjupsförutsägelse. Adams har använts för att studera vilken effekt olika däcktryck och hastighet har på spårdjupet.

Nyckelord: Bekker, skogsmark, skotare, spårdjup, WES

Master of Science Thesis MMK 2014:15 MKN 105

KTH Industrial Engineering and Management

Tire –soil interaction analysis of forest machines

Karthik Prakash

Approved	Examiner	Supervisor
2014-06-04	Ulf Sellgren	Ulf Sellgren
	Commissioner	Contact person
	Skogforsk	Björn Löfgren

Abstract

Cut-to-length logging is a mechanized method for delimbing trees and cutting them to length. It is a two-machine operation; taken care by a harvester and a forwarder. The forwarder can cause soil rutting, soil compaction and other detrimental after effects. Therefore it has become vital to protect the forest floor from destructive effects of heavy machines. This initiated the study to delve more into the interaction between the loaded forwarder wheel and the soil.

Various WES based rut depth models has been compared to validate its effectiveness in predicting the rut depths. New models have been developed to estimate the rut depth produced by the multipass effect of wheels. Models that could predict the contact pressure between the tire and soil as well as the tire soil contact area has been studied. Various relations to determine the mobility parameters have also been studied. The ones that are suitable to predict mobility parameters have been identified.

Roots play a major role in reinforcing the soil and protecting them. This extra reinforcement provided by roots has been taken into account in the thesis work. Lab test with pine tree roots have been carried out to determine the extra reinforcement supplied. Models that are capable of predicting the reinforcement effects due to roots have also been looked into.

An initial step towards connecting WES and Bekker models have been done; available models correlating both WES and Bekker models have been analysed and finally a set of relations connecting both have been derived.

The effect of slip on sinkage has been studied with the help of both WES and Bekker based models. Multibody simulation software MSC Adams has been used to simulate the forwarder model to determine its suitability for rut depth prediction. Adams has been employed to study the effect of tire inflation pressure and velocity on rut depth.

Keywords: Bekker, forwarder, forest soil, rutting, WES

FOREWORD

I express my heartfelt gratitude to all the people who extended their unconditional support and help during the course of the thesis work.

First and the foremost, I would like to express my sincere gratitude to Professor Ulf Sellgren, my professor, the internal supervisor and more over an excellent mechanical engineer. The guidance and suggestions provided by Ulf was a major source of inspiration to this work.

I thank Dr. Björn Löfgren from Skogforsk for believing in me to carry out this work. His inputs during the pulse meetings were very constructive.

Abdurasul Pirnazarov, without this person the work would not have reached its final phase. The insights he provided into the field of terramechanics is invaluable. I am indebted to Abdurasul for spending long hours discussing various aspects of the projects and providing valuable inputs. I would like to thank him from the bottom of my heart for all the help he has done as well as for lending valuable literatures associated with the work.

I would like to thank Professor Kjell Andersson for all the help he provided during the Adams modeling stage.

I express my sincere thanks to Abboos Ismailov for the help he offered during Adams simulation.

Madura Wijekoon, R&D Product Development Coordinator in Trelleborg, is another person I am indebted to for all the tire technical documents he provided. I greatly appreciate the helping hand he provided to clear various doubts.

I thank Revathi Palaniappan for sorting all my queries associated with various aspects of the project.

I am grateful to Praveen R. Nair for clearing various doubts associated with Adams simulations.

I express my sincere gratitude and reverence towards my parents, C.M.Prakash and Haripriya Prakash, for their unconditional love and support.

Finally, I dedicate this work to the Omnipotent and the Omnipresent for helping me to reach this stage.

''If you perform the sacrifice of doing your duty, you do not have to do anything else. Devoted to duty, man attains perfection.'' – The Bhagavad Gita

Karthik Prakash

Stockholm, 06-2014

NOMENCLATURE

The abbreviations used in the thesis report are mentioned here

Abbreviations

ADAMS	Automatic Dynamic Analysis of Mechanical Systems
ANN	Artificial Neural Network
CI	Cone Index
DEM	Digital Elevation Model
DEM	Discrete Element Method
FBM	Fiber Bundle Model
FEM	Finite Element Method/Finite Element Modelling
MBS	Multi Body Simulation
MPC	Multi-Pass Coefficient
NGP	Nominal Ground Pressure
WES	Waterways Experiment Station
WMR	Wheeled Mobility Robots

TABLE OF CONTENTS

1 INTRODUCTION

This chapter is intended to give a concise idea on what the thesis work is about, the delimitations and the method employed to complete the work.

1.1 Background

Cut-to-length logging is a mechanized method for delimbing trees and cutting them to length, especially in Europe. It is a two-machine operation, where a harvester fells trees, delimbs it and breaks them. While the forwarder transports the logs to areas accessible by trucks so as to move them to a processing facility. When the forwarder moves over the soil it can cause soil rutting. The passage of a forwarder can cause soil compaction, as an after effect, it affects the nutrient content of the soil, increases soil erosion, soil instability and reduced tree growth (Sutherland, 2003).

One of the prominent indications of soil damage by vehicle traffic is the excessive soil deformation or soil rutting (R.L.Raper, 2005). Soil ruts caused by the traffic of the forest machines adversely influence the soil and vegetation and vehicle mobility. Regular vehicle traffic through the forest induces soil compaction, it also affect the growth and distribution of roots. The ruts formed in steep terrains can pave the way for drastic erosion. The ruts formed can persist for years and affect the growth of seedlings and cause degradation of soil properties, which include soil horizon mixing and topsoil removal (Picchio et al., 2012) .

Estimating and modelling soil damage, soil rutting and compaction is given high importance due to the destruction of root systems which results in soil erosion (M.Saarilahti, 2002). Therefore it has become vital to predict the rutting due to machines and thereby protect the forest floor from destructive effects of heavy machines. The forest machines have to be gentle to the ground, so that it does not affect the soil properties and the root system needed for a sustainable environment.

It is an accepted fact that modelling of an off-road vehicle and the terrain is complex and difficult (Wong, 2010). Empirical methods are bought into light in such situations. In empirical modelling, the vehicle is tested in terrains that simulate the working condition where the vehicle is supposed to work. Then the results of the test, vehicle parameters and terrain parameters are empirically co-related. US Army Waterways Experiment Station (WES) follows this approach that depends on Cone Index as the prime input variable. Here, the vehicle mobility is explained by mobility parameters and connected empirically to wheel numeric, which describes the tire-soil interaction.

Tire-soil interaction can also be done through parametric analysis, Mieczysław Gregory Bekker (1905 – 1989) is one of the prominent figures in this field and his methods are widely followed. This method was primarily based on the inputs obtained from the Bevameter

technique. Bevameter technique is primarily based on elasticity theory and soil friction and cohesion factors (Saarilahti, 2002).

According to Wong (Wong, 2010), WES models are useful for preliminary assessment of the mobility of off-road vehicles. They cannot be extrapolated to terrain and vehicles on which tests have not been carried out. But, the model allows the evaluation of off-road vehicle mobility using very small number of variables, as compared to Bekker models, that uses many inputs.

Roots attribute a part of the forest floor bearing capacity. The extra reinforcement provided by the roots to soil depends on their mechanical properties, morphology and their distribution (Cofie, 2001). Tree roots could provide an extra reinforcement to the stability of hill slopes (Abe & Ziemer, 1991). The quantification of reinforcement provided by roots play a very prominent role in evaluating impacts caused to forest floor due to various forest machines. Various root modelling studies have been carried out to predict the exact the value of reinforcement provided by roots.

The Multi-body simulation software, MSC Adams plays an important role in predicting various impacts caused to the terrain by the motion of forwarder. Adams comes in handy when various models of forest machines need to be tested against their potential impacts to the ground. Adams calculation is based on the Bekker's theory. They could be used to predict the sinkage caused in the soil due to the vehicle. Various soft tire models are available that could be fine-tuned for the purpose.

1.2 Purpose

The main purpose of this thesis work is to evaluate the effectiveness of the WES based models in estimating tire-soil interaction. As present with any empirical models, the WES models are not always in line with the test data obtained by experiments. Here, the WES models developed is compared with the field test data obtained from the tests carried out in Tierp, Sweden. Work is carried out to refine the existing WES based models so as to bring it close to the field test data. Parametric models, based on Bekker's method will be studied. Work has been done to obtain a correlation between the WES model and Bekker model, this will aid for the proper transformation from one model to another.

Another area of investigation as part of the work is to study the effectiveness of using the multi-body simulation software MSC Adams to predict the rut depths caused by the forwarder. The results from Adams single wheel test will be connected to various WES models to evaluate if they produce same results. High priority will be given to refining WES based models and analytical/empirical analysis.

The following work will be carried out as part of the master thesis:

- Compute the rut depths, ground pressure, contact area and mobility parameters from available WES models of forwarder tires. Compare the rut depth, ground pressure and contact area with the field test data carried out on the forwarder at Tierp, Sweden.
- Investigate the effect of ''Novel wheel mobility number'' proposed by S. Hegazy & C.Sandu on the WES models of rut depths. And compare the results obtained with test data.
- Calculate the variation of the constants in the wheel numerics with respect to the Cone Index.
- Examine the effect of slip sinkage.
- Effect of root reinforcement and root orientation on soil shear strength will be studied with the help of available root testing machine and an evaluation of root reinforcement models with test data will be done. Rut depth of soils without roots and with roots will be modeled.
- WES and Bekker based model will be correlated to aid the transformation of one model to another.
- Study of the Adams soft-soil module will be carried to determine its feasibility. Effects of inflation pressure and velocity on rut depth will be studied with Adams simulation.

1.3 Delimitations

The delimitations of the project are as follows:

- Comparison of mobility parameters with test data is not carried out.
- The analysis will be limited to tires.
- The modeling is based on soft terrain.
- Dynamics effects acting will not be taken into account due to the low speed of the machine.
- Effects of turning radius and transmissions systems on rut depths have not been taken into account.

1.4 Method

A time schedule was prepared to keep the project in track and it was ensured that the time plan is followed. To start with, extensive literature collection was carried out. Literatures about various topics in terramechanics were collected and they were sorted out according to the topic, for example, WES models, rut depths, foot print area etc…

Next, with the aid of the available literature, the empirical WES models were created in Matlab R2013a. Comparison between various WES models and field test data was carried out in Matlab. The information obtained from selected literatures was implemented in the available WES models to find if there is any interesting result.

Results obtained by implementing the new wheel numeric suggested by S. Hegazy & C.Sandu were compared to the test data. The variations of the constants in the equations were also analyzed with respect to cone index. Tire soil contact pressure and tire soil contact area was also studied with the aid of various models.

The effect of root reinforcement was studied with the help of available instrumentation and the results were compared to existing root reinforcement models. The effect of slip on sinkage was studied and a new method to predict the rut depth of a forwarder by taking slip into account is proposed.

A new relation connecting the WES and Bevameter methods has been developed. Simultaneously, the available correlation between both models has been analyzed.

The Komatsu model was simulated in Adams to evaluate the software's suitability in rut depth prediction. Effect on tire inflation pressure and tire velocity was studied with the aid of Adams.

The project work was carried out at KTH Royal Institute of Technology, Stockholm, in the department of Machine design by collaborating with Skogforsk, the research body for the Swedish forestry sector. Regular contact with the internal project supervisor, Ph.D. students and external supervisor at Skogforsk was maintained through pulse meetings and emails.

2 FRAME OF REFERENCE

This chapter describes the area's that were looked into to gain an insight into various aspects of the thesis work.

2.1 Terramechanics

For a long time, the development of evaluating off-road vehicles has been based on 'cut and try' methods. Dr. M.G.Bekker's works, Theory of Land Locomotion in 1965, Off-the-Road-Locomotion and Introduction to Terrain-Vehicle Systems in 1960's paved the way for the proper and systematic development of off-road vehicle studies. His works laid the foundation for the distinct branch of applied mechanics called 'Terramechanics' (Wong, 1984)

According to J. Y. Wong (2010), '' In a broad sense, terramechanics is the study of the overall performance of a machine in relation to its operating environment-the terrain''. Terramechanics can be subdivided into Terrain-vehicle mechanics and Terrain-implement mechanics.

Terrain-vehicle mechanics is associated with the tractive performance of a vehcile traversing through an unprepared terrain, as well its ride quality, handling, water crossing etc over such terrains. On the other hand, Terrain-implement mechanics takes into account the performance of terrain-working machinery, like soil cultivating and earth moving equipments.

The terramechanic concepts can applied in the development, evaluation and selection of the following (Wong, 2010)

- Vehcile concpets and configurations
- Running gear of a vehicle
- Steering and suspension system
- Power transmission and distribution
- Handling, ride quality and performance

2.2 Tire-soil interaction models

Vehicle designers and researchers need to estimate the behaviour of vehicles in various soil conditions, tire-soil interaction models becomes an aid at such a point. Terramechanic models play a prominent role in estimating vehicle mobility as well as the effects of vehicle passes over various terrains. Wheel sinkage and penetration force estimation is very important to determine traction, motion resistance, soil compaction, rut depth etc...; all such parameters can be estimated through the available tire-soil interaction models. Tire- soil interaction models range from completely empirical to analytical. The proper selection of the terramechanics model depends on various factors. The model used depends on the intended

purpose and as well as environmental, economic and operational constraints (Wong, 2010). Vehicle-terrain interaction needs to be properly understood to select the proper vehicle as well as to tune its design variables to meet the requirements for its proper operation (Wong, 2010).

2.2.1 Empirical Models

Empirical models aid in the development of terrain-tire interaction by testing vehicles in terrains that best describe the operating environment. The results of such experiments are then co-related empirically. WES based modelling best describes this form of terrain-tire modelling, Cone Index is the primary input data used here. Empirical models are only applicable to vehicles that are tested in similar operating conditions, and cannot be extrapolated to other types of vehicles and operating terrain. Also to generate a reliable empirical model that could be utilized for a variety of situations, it demands a large chunk of input data. Also, empirical approach does not give details about the fundamental physical behaviour of soil (Ansorge, 2007).

In WES based model, an instrument called cone-penetrometer is used to obtain the parameter called 'cone index', which is the primary input to the WES based modelling. Cone Index represents the resistance to penetration into the terrain per unit cone base area. The cone penetrometer developed by WES has a 30^0 cone angle with 3.23 cm^2 base area. In WES method soil bearing capacity is linked to the cone index, so cone index can be viewed as an indicator of the bearing capacity (Saarilahti, 2002). Vehicle performance in clay and sand can be assessed by taking into account the gradient of cone index with respect to penetration depth (Wong, 2010).

In the WES approach two types of dimensionless parameters that depend on CI are employed; mobility parameters and wheel numeric. Vehicle mobility is explained by mobility parameters and wheel-soil interaction by wheel numerics.

2.2.1.1Mobility parameters

The mobility parameters used are:

- Pull coefficient or net traction coefficient or drawbar pull coefficient
- Rolling resistance coefficient
- Traction coefficient or thrust coefficient or gross traction coefficient

$$\mu_P = \frac{P}{W} \tag{1}$$

$$\mu_R = \frac{P_R}{W} \tag{2}$$

$$\mu_T = \frac{Q}{r_r W} \tag{3}$$

where

μ_P = pull coefficient

μ_R = rolling resistance coefficient

μ_T = traction coefficient

P = drawbar pull kN

P_R = rolling resistance to movement in kN

W = wheel load in kN

Q = wheel torque in kNm

r_r = rolling radius of wheel in m

2.2.1.2 Wheel numeric

Wheel numeric is a simplified model of wheel-soil interaction based on dimensionless parameters. The use of wheel numeric led to simple semi-empirical wheel models that act as the input in WES models for determining the mobility parameters like (Saarilahti, 2002):

- Torque
- Towed force
- Drawbar pull
- Sinkage

Various wheel numerics have been developed by various authors. Most of the wheel numerics are developed for cohesive soils, because majority of mobility issues are encountered in cohesive soils. The input variable for determining the wheel numerics include:

- Tire width
- Tire diameter
- Tire deflection
- Tire section width

Only the main wheel numerics that have been used in this project are only described. The wheel numeric that is commonly used is the one proposed by Turnage (1978). It includes factors like, contact pressure, tire deflection and tire width factor.

$$N_{CI} = \frac{CIbd}{W}\sqrt{\frac{\delta}{h}}\frac{1}{1+\frac{b}{2d}} \tag{4}$$

Another wheel numeric proposed by Wismer and Luth (1973) was suggested by Maclaurin to be better than the one described by himself:

$$C = \frac{CIbd}{W} \tag{5}$$

The predicition capability of the Wismer and Luth (1973) quation was improved by Freitag's incorporation of the term $\sqrt{\frac{\delta}{h}}$.

$$N_{CC} = \frac{CIbd}{W}\sqrt{\frac{\delta}{h}} \tag{6}$$

Where

CI= cone index in kPa

h = tire section height in m

b= tire width in m

d = tire diameter in m

W = wheel load in Kn

δ = tire deflection

2.2.2 Parametric analysis

M. G. Bekker pioneered in developing mathematical model for parametric analysis (Wong, 2010). The earliest model that paved the way for the development of Bekker model was developed by Bernstein and Goriatchkin (Bekker, 1956). The Bekker based method is based on the results obtained from the test carried out by the instrument, Bevameter. Pressure-sinkage and shear stress-shear displacement characteristics are primarily used in parametric analysis. There are 2 kinds of test in bevameter based method, to assess the normal and shear stress exerted on the soil by the vehicle, the plate penetration test and the shear test. Bekker based models are widely used to predict the motion characteristics of Martian rovers (Iagnemma, et al., 2011). Multi body simulation subroutines in ADAMS based on Bekker model have been developed to cater to the needs of the mobility prediction on Martian rovers (Zhou, et al., 2013).

Bernstein-Goriatchkin equation is the basic empirical equation used in Terramechanics to predict the pressure-sinkage relationship between a rigid-plate load and sinkage (Lyasko, 2010).

$$p = kz^n \tag{7}$$

Where,

p= pressure

z = sinkage

k and n= constants

Bekker derived Equation 8 by replacing k with k_c and k_ϕ.

$$p = \left(\frac{k_c}{B} + k_\phi \right) z^n \tag{8}$$

Where,

k_c = cohesive modulus of deformation

k_ϕ = friction modulus of deformation

n = dimensionless exponent of load-sinkage curve

B = tire width in m

Equation 8 was tested and validated with many types of soils with various plate sizes and traction devices, and is the most commonly used equation now. The modulus of deformation and sinkage exponent are depended on the soil-plate and load system. They have different values for different soils and can be estimated by load-sinkage curve fitting method. To determine the values, either plate, vehicles or complicated equipment's not used in classical soil mechanics should be employed. An important fact that should be taken into consideration is that, these constants should not under any circumstances be used to evaluate tractive performance of vehicles outside the load range it was tested without experimental verification (Lyasko, 2010), that is, the values of these constants cannot be extrapolated outside the boundary of the test conditions.

The versatility of the parametric model has a flip side also. Bekker model cannot be applied to smaller vehicles which has a tire diameter less than or equal to 50 cm or those that experience less than 45 N of normal load. Bekker mentions that sinkage equation is suitable only at conditions where sinkage-to-wheel diameter ratio is small, so that the contact patch is flat (Spenko & Meirion-Griffith, 2011). It has also been pointed out the Bekker based approach is not completely suitable when applied to WMR. WMR violates all the conditions that Bekker used in developing his model. The pressure-sinkage expressions developed are based on static state experiments and cannot be used to describe the dynamic terramechanics activities (Ding, et al., 2014).

In order to get a deeper idea about what is happening when a wheel moves over soil surface; better understanding about the flow pattern of the soil in longitudinal direction and the soil deformation should be studied in detail (Wong, 1967). The works of Bekker assumes that the flow of soil beneath a penetrating narrow plate is entirely sideways, but research carried out by Onafeko & Reece (1964) and Wong (1967) have shown that it is not the same.

Photogrpahic methods have been employed by Wong, (1967) to study the longitudinal movement of clay and sand below both wide and narrow tires. Through the same experiments he had demonstrated the effect of slip on sinkage, that is sinkage increases with slip and identified the different flow patterns in clay and sand.

2.3 Mathematical models

Mathematical models are based on plasticity theory and soil strength parameters, it is more appropriate for scientific programmes (M.Saarilahti, 2002).Mathematical tools have been used to study about the non-homogeneous behaviour of soil in tire-soil interaction analysis, plasticity theory has been employed to delve more into the interaction (Karafiath, 1975). Mathematical models demand laboratory test to obtain soil strength parameters, which is considered as its downside.

2.4 Computational models

Computational methods based on FEM and DEM is available to analyse terramechanics problems. They can provide in-depth details about specific aspects of terrain-soil interaction, through heavy computation. Obtaining precise information associated with tire-terrain interaction could help to determine how tire type and natural conditions affect the tractive performance. The empirical models available over simplify tire soil interaction, whereas finite element models could model terrain-tire interaction in an extensive way without implementing many assumptions (Xia, 2010). Xia (Xia, 2010) has generated a finite strain hyperelasticity model for modeling rubber materials and has proved that soil compaction and tire mobility can be estimated by implementing finite element modelling.

Finite element and Finite volume methods are employed to estimate traction characteristics of tire interacting with snow and soil. Lagrangian finite element method and Eulerian finite volume method (Choi, et al., 2012) are increasingly becoming popular. Discrete element models are also used to aid in the study of tire-terrain interaction of lunar rovers (Shioji, et al., 2010). DEM cannot handle modelling and solving highly nonlinear multibody systems such as tractors, robots, tracked vehicles etc. (Melanz, et al., 2014). But, several parameters like ratio of shear stress to normal stress have to be provided as input to computational based methods, which is not feasible (Wong, 2010). More issues need to be resolved before computational based methods can become as proper substitute for the other models mentioned above. Work associated with three and two-dimensional numerical simulations of tire soil interaction are being done, and have been found that three dimensional effects did not affect much the result of analysis in clays, but in sands, the results of such analysis plays a significant role (Hambleton & Drescher, 2009).

2.5 Roots

Tree roots play a vital role in providing reinforcement to soil. Roots can highly improve the stability of the hill slopes as well as stream banks. Root soil mechanics have been studied in detailed by authors like Wu et al.,1988, Waldron & Dakessian., 1981, Gray & Barker, 2013. Authors like Thomas & Pollen-Bankhead (2009);Bengough & Mullins (1991); Wilatt & Sulistyaningsih (1990); Abe & Ziemer (1991); Wästerlund (1989) have contributed extensively to the reinforcement effect provided by roots to the soil shear strength. Timber harvesting and clear-cutting affects the rooting strength, as an after effect it may cause slope failures (Bishop & Stevens.,1964, Brown & Sheu.,1975, Wu, 1976). According to Wästerlund (1989), the strength of the root bark varies with season. At least 200 to 500 m roots per m^{-2} guards the top soil layer.

2.5.1 Root reinforcement modelling

Roots provide an extra shear resistance to soil thereby improving the shear resistance of the soil; root reinforcement depends on the number of roots as well as size of roots (Abe & Ziemer, 1991). Tree age could also determine the amount of reinforcement effect, young tress usually provide greater soil cohesion (Genet, et al., 2008). Plant roots improve root reinforcement by increasing apparent cohesion; this will result in slope stability (Schmidt, et al. 2001, Van Beek, et al. 2005). Simple perpendicular root models is used to evaluate the reinforcement effect provided by roots (Wu et al., 1988).The Wu model is based on the assumption that each root will fail in tension simultaneously, but Riestenberg (1994) found that the roots doesn't fail simultaneously. Thomas & Pollen-Bankhead, 2009 developed a new FBM based model to take into account the gradual break down of each root. They also evaluated the root architecture effect on the extra strength provided by the roots.

2.6 Soil Damage

Forest soils are very sensitive to disturbances caused due to forest machines. The machines used in forestry applications are becoming heavier and powerful. Axle loads on such machines can reach till 300 kN (Håkansson, 1994). Forwarders are the heaviest equipment in forestry operations, which weigh from 15 to 40 tons, and require highest volume of traffic (Labell & Jaeger, 2006). The major soil damage caused by the passage of heavy forest machines are soil rutting and soil compaction. These two damages affect the soil structure and as an after effect it can cause a wide range of issues like, erosion, loss of soil stability etc...Most of the structural changes caused by the heavy machines are irreversible. Horn, et al., (2004), has given a very vivid description about the impacts caused by such machines.

When the applied load from the machine exceeds the maximum strength the soil can with stand, rutting occurs and as result forest productivity will be badly affected which can further cause the sediments to flow into open water body (Michigan.gov, 2014). When the stress acting on the soil exceeds the internal strength of the soil, known as precompression stress;

there will be plastic deformation of the soil. Excessive rutting acts an indicator to change the forest operations to avoid further damage to the forest floor.

The mechanical stress applied affecting the soil due to the forestry machines acts in three dimensions and makes the soil compacted. Soil compaction, similar to soil rutting, can affect the growth of tress and other plants. Proper planning of machine loads, machine routes, frequency of travel etc. needs to done to minimize soil compaction (Sakai, et al., 2008). Soil compaction causes reduced plant growth, because it reduces water infiltration and nutrient exchange. The degree of compaction is highest at top 30 cm of soil profile (Labell & Jaeger, 2006). The stress induced in the soil may reach 400 kPa while the machine works on a slope. Depending on the operating conditions, even vehicles with relatively less mass can produce stress level as high as very heavy forest machines (Horn, et al., 2004). The soil stresses affects the pore network, the result of which is to waken the stable soil particles. The compaction rate of wheeled vehicles is higher when compared to tracked ones.

Due to the forest machinery activities, the air permeability will also decrease. This can lead to reduced biomass production, water runoff and stagnant water sites that result in reduced plant growth.

To conclude, it has to be accepted that the forestry operations cannot be carried out without compacting the soil and inducing structural damage to the soil by the running gear. As suggested by Horn, et al.,(2004), wheel and skid track should be used and the existing network of compacted area has to utilized in proper manner for all the forestry activities, so that the unwheeled and noncompacted areas are not disturbed anymore.

2.7 Multi-body simulation

A multi-body system contains interconnected rigid or flexible bodies/masses, each of which may undergo various kinds of displacements. The bodies are connected to each other through joints, spring dampers etc… Multi-body simulation is used in a range of areas, starting mainly from automotive, biomechanics, product development and extending till the simulation of Martian rovers. In this thesis work, the multi-body simulation software MSC Adams is used to evaluate the effect the forwarder has on the forest soil; mainly the sinkage/rut-depth. MSC Adams could evaluate the dynamics of moving parts as well as find how loads and forces are distributed in a body, various modules are available in Adams that helps to study more about vibrations, fatigue etc... (MSC Software, 2014).In the thesis work, Adams soft soil module will be used to evaluate the co-relation between the WES and Bekker model for a loaded single wheel.

2.7.1 Adams soft-soil tire and road models

The multibody simulation software MSC Adams takes care of the terrain-soil interaction with the help of soft-soil tire and road models. The property files representing the soft-soil tire model as well as road model should be used together to simulate the interaction. The files

available in the software library were used in this project to study the tire-soil interaction. The soil behaviour can be changed by modifying the values of soil properties in the road file.

2.8 Digital soil modelling

An interesting area of study is the digital modelling of the terrain or the soft-soil. DEM is an engaging area where studies have been carried out in detail to model soft-soil terrain. The soil surface can be described using digital elevation grid; the height information at specific horizontal coordinates can be defined by grid nodes of a rectangular mesh grid.

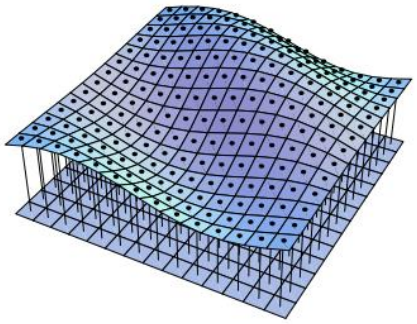

Figure 1 DEM grids

In the DEM method, a continuous section of soil is considered as matrix of rectangular soil columns, each of which is identified by a specific height value that is stored in a two-dimensional grid structure. The center of each soil column is mentioned as heightfield vertex and each of the specific nodes can be assigned specific soil property values. These property values can be changed accordingly as loading and unloading occurs in the soil during time. A collision algorithm detects if a rigid object has collided with the surface when a ray casted from bottom of the column intersect the rigid object before it hits the vertex. Flag's will be set to imply the movement of columns and the height difference will be stored.

With such a method the time-dependent elastic and plastic response of the soil can be taken into account, e.g. multi-pass effects. The vertical strain in each soil grid node can be used to find the sinkage; and the grid heights can be updated to take into account change in soil characteristics after a wheel pass. Imitating the soil in such a manner helps to treat the soil as non-homogeneous in the vertical direction; this is more in-line with reality.

Calculation of sinkage, energy and power can be made on a soil node basis and the resultant can be obtained by summing up the contribution from each node. It has to be kept in mind that such an analysis won't take into account the soil and pore fluid flow; this may produce a variation when comparing the results with test data.

3 DATA COLLECTION

The data's collected to carry out the detailed analysis has been briefly described in this chapter.

3.1 Test machines

The field tests were done for two machines, namely, Rottne F13s and Komatsu 860. Both the machines were tested in loaded and unloaded conditions; the loads are mentioned in Appendix A2. Komatsu 860 was tested for three band track configurations also. Band tracks have not been taken into account in this thesis work.

Figure 2 Rottne F13s and Komatsu 860Test tracks

The tests were done in Tierp, Sweden. Both the machines were tested in straight paths and S-shaped paths. Tests in S-tracks were done to estimate the effect in rut depths due to shear, as turning radius and velocity has an effect on rut depth. Komatsu 860 has been tested with band tracks on straight as well as S-shaped curves.

3.2 Pressure measurement

To measure pressure exerted by the machines on the ground, three pressure sensors were placed at an interval of 15 cm below the ground surface. The sensors were connected to a data acquisition system to store the measured pressure data.

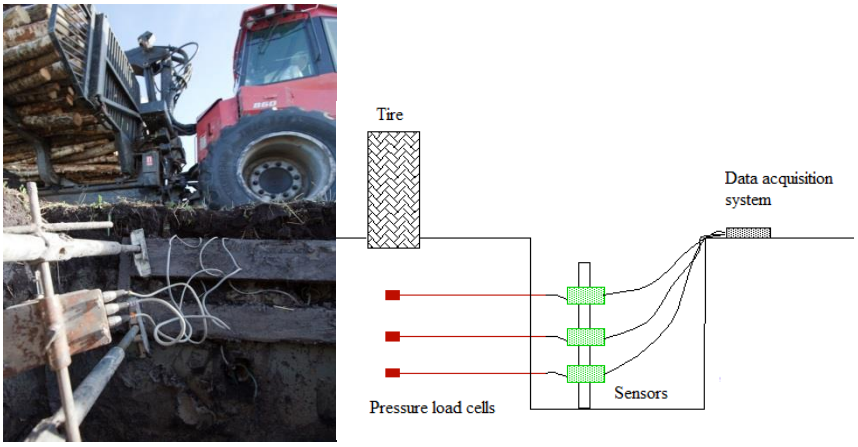

Figure 3 Pressure measurement

3.3 Soil moisture

Soil moisture content of the test track was measured at different spots on the day of the test as well as on the last day of test. Soil moisture content denotes the amount of water present in the soil, and is expressed as amount of water (in mm of water depth) present in a depth of 1 m of soil. There was no large difference in moisture content between the first and last day of test, but if different between various tracks. Figure 4 shows the average of moisture contents in different tracks on the first and last day of test.

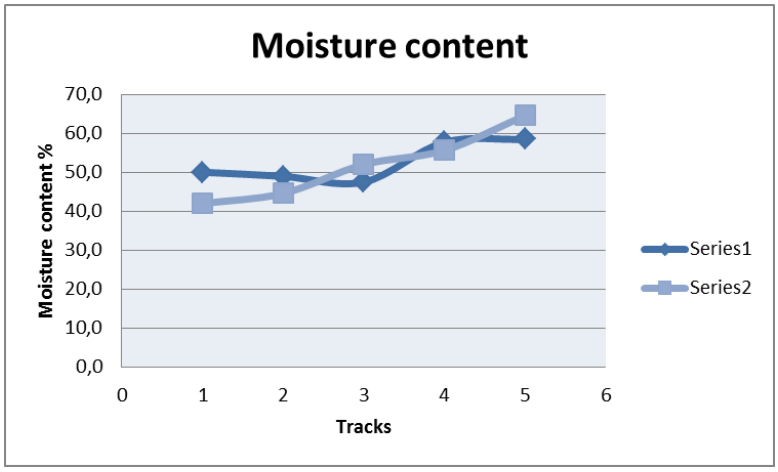

Figure 4 Soil moisture content

3.4 Soil penetration test

Penetration resistance test is vital in modelling tire-terrain interaction when it comes to WES based approach. Cone index of each track was obtained with the help of a cone penetrometer. An electron-cone penetrometer was used to measure the cone index before and after the vehicle pass. The vehicle at each track ran ten times at 3km/h in the same trial. Cone index measurements were taken at eight points in each track after each pass of the vehicle. For Rottne, cone index was only measured for straight tracks, but for Komatsu 860 with band

tracks, cone index value were measured for S-shaped track also. Cone index measurements were taken in an interval of 1 cm till 30 cm at each measuring point. The cone index value measured a 15 cm has the highest predictive power according to Saarilahti (Saarilahti, 2002). Due to this fact, the cone index value at 15 cm was taken in all the calculations. Figure 5 shows the penetration resistance measured after one vehicle pass of Rottne.

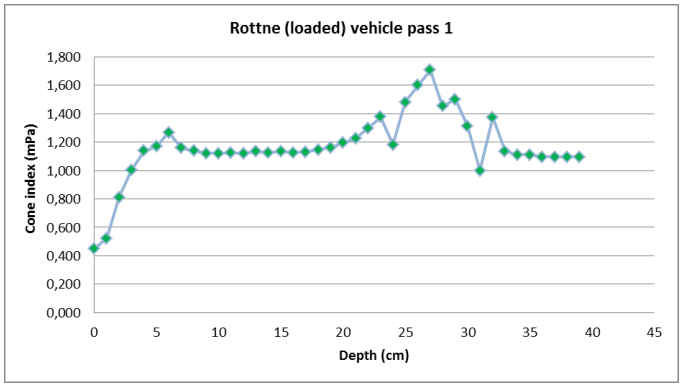

Figure 5 Average values of soil penetration test results at various depths

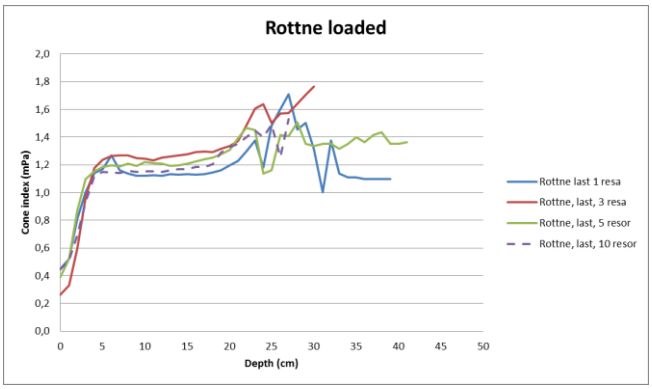

Figure 6 Soil penetration test after each pass of Rottne

Figure 6 shows the variation of cone index after first, third, fifth and 10th pass of loaded Rottne. From the diagram, it can be interpreted that the cone index almost remains a constant when measured in the depth ranging from 5 cm to 20 cm. In each case, the cone index display an irregular pattern after 20 cm. It is also interesting to note that the cone index after the 3rd pass is higher when compared to the cone index after the 10th pass.

3.5 Rut depth measurement

The rut depths after each vehicle pass were measured at ten points. Rut depths measurements were taken for both straight and S-shaped tracks. The machine configurations for which rut depth measurements were taken is given in **Table 2**. It can be inferred from Figure 7 that, for an unloaded Rottne, as the number of vehicle passes increases the rut depth also increases. Also, it has to be noted that the increase in rut depth is not severe as it was for the first three passes. The rut depth displays an increase when the same machine is under loaded condition.

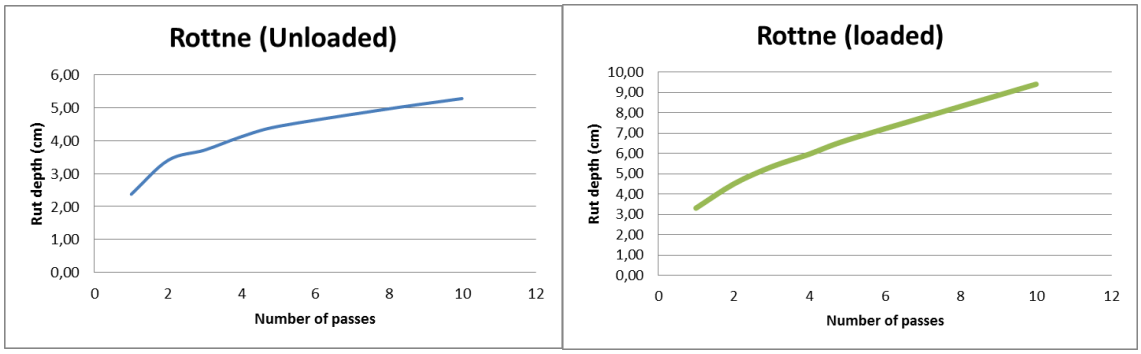

Figure 7 Rut depth measurements for unloaded and loaded conditions of Rottne

Figure 8 shows the rut depth comparison when Rottne maneuvers an S-shaped track. When the machine is taking an S-shaped track, there is considerable increase in rut depths when compared to a straight track. It can also be seen that the loaded machine produces more rut depth.

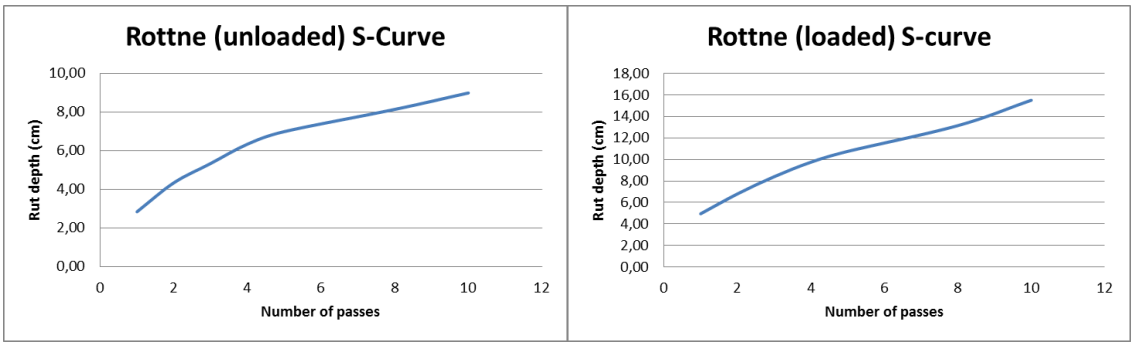

Figure 8 Rut depth measurements for unloaded and loaded conditions of Rottne in S-curve

3.6 Tire-soil contact area

Tire-soil contact area was measured for two machine configurations. 66 cm x 67 cm, was the measured area for Komatsu 860 (270 kPa) loaded and 60 cm x 55 cm was for Rottne F13s (450 kPa).

3.7 Forwarder running gear description

Both, Rottne and Komatsu employed Trelleborg 710/45-26.5 T428 163A8 forestry tire. Rottne was tested only at 450 kPa tire pressure level, while Komatsu was tested for three tire pressure levels 270 kPa, 450 kPa and 600 kPa. **Table 1** mentions the general forwarder parameters.

Table 1 Forwarder parameters

Symbol	Unit	Description	Value
h	m	Tire section height	0.333
Pi	kPa	Tire inflation levels	Rottne F 13s – 450 Komatsu 860 – 270, 450, 600
rc	m	Tire transversal radius	0.625
r1	m	Tire loaded radius	0.625
m	N/A	Number of axles	2 bogie axles
b	m	Tire width	0.71
d	m	Wheel diameter	1.34
PR	N/A	Ply rating	14-16

4 RUT DEPTH ANALYSIS

A detailed study of various rut depth models has been carried out here. New models developed to predict rut depth's is also included in this chapter.

4.1 Introduction

The wheel indentations caused by the forest machines while traversing through the terrain is called ruts. Wheel sinkage is different from rutting; wheel sinkage is measured when the wheel/vehicle is in static position, while rut depth is measured after the wheel has passed. The difference between sinkage and rut depths measurement is small (Affleck, July 2005). Rut depth measurements are one the best indicator to assess the impact of the forest machines on the forest ground. Rut depths are also caused by wheel slip. Rut depth dimensions are also affected by steering system as well as transmission systems (Edlund, et al., 2012). The influence of turning radius on rut depth has also been investigated by Liu, Howard, Anderson, & Ayers, 2009 (Liu, et al., 2009).

4.2 WES based rut depth models

Most of the WES based rut depth models are for single pass of a wheel. Here, the rut depth models suggested by Saarilahti (Saarilahti, 2002) are taken into account. Those models are applied to estimate the rut depth for the single vehicle pass of the forwarder or the rut depth after the 4^{th} wheel pass. The analysis was done for both Rottne and Komatsu for all the machine configurations as mentioned in **Table 1**.

Results of calculations with the available rut depth models to predict the rut depth after the first vehicle pass was done for both Rottne and Komatsu and is shown in Figure 2Figure 9 and Figure 10. The equations used for the analysis are presented in the Appendix A3. The machine configurations tested are described in **Table** 1.

Table 2 Machine configuration

Rottne	
Track	Machine Condition
1	Rottne Straight Unloaded 450 kPa
2	Rottne Straight Loaded 450 kPa
3	Rottne Loaded Bogie 450 kPa
4	Rottne S track unloaded 450 kPa
5	Rottne S track loaded 450 kPa
6	Rottne straight loaded 450 kPa
Komatsu	
Track	Machine Condition
1	Komatsu Straight loaded 450 kPa
2	Komatsu Straight loaded 600 kPa
3	Komatsu Straight unloaded 600 kPa
4	Komatsu Straight loaded 270 kPa
5	Komatsu S track unloaded 600 kPa
6	Komatsu S track loaded 600 kPa

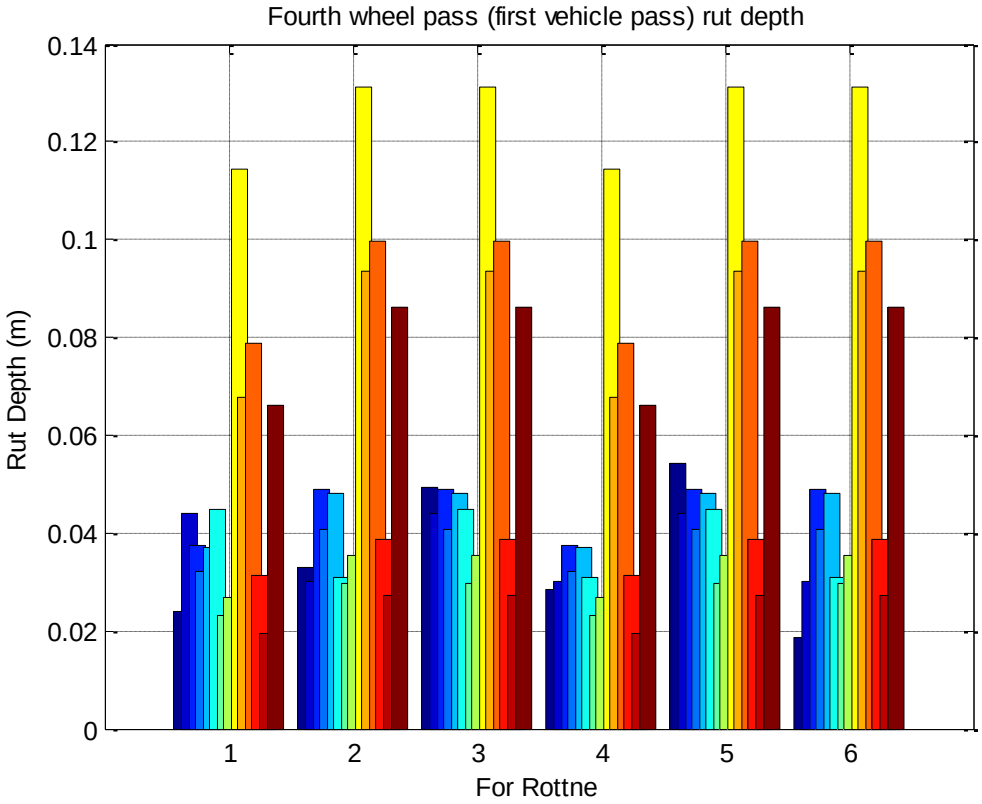

Figure 9 First vehicle pass rut depth for Rottne

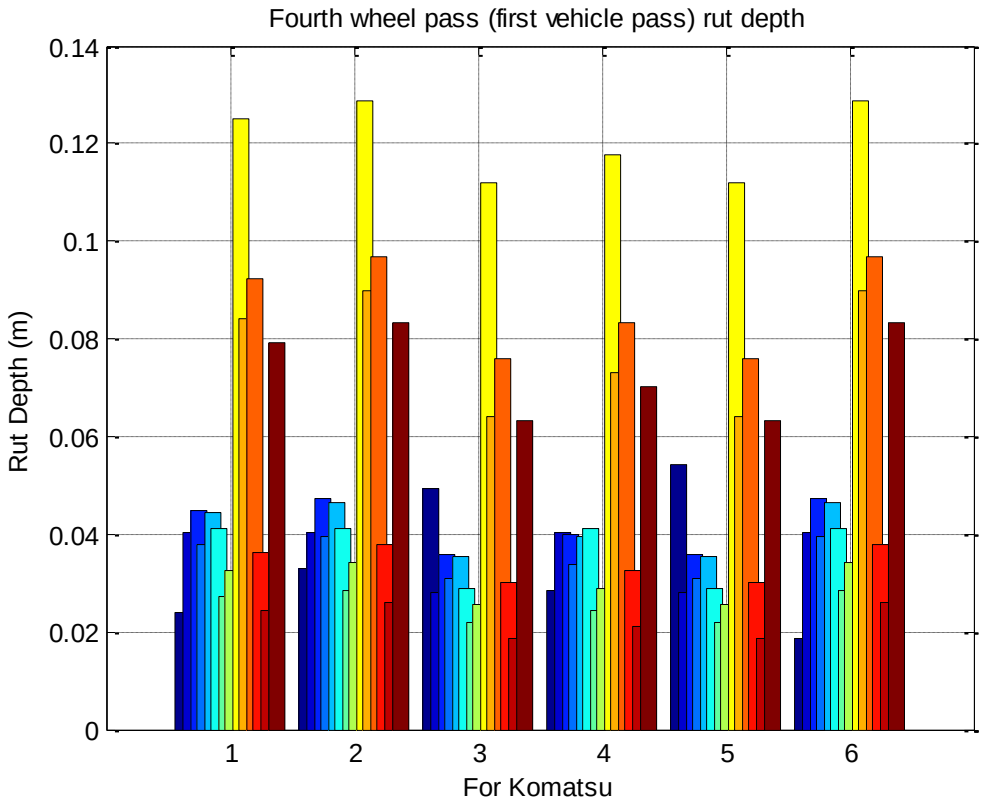

Figure 10 First vehicle pass rut depth for Komatsu

For straight track, Antilla 5 and Antilla 7 give good results for Rottne. Antilla 6 and Antilla 7 give good results for Komatsu straight driving condition also. The rut depth models available cannot be used for rut depth prediction for S shaped tracks; they can only be applied for straight tracks. In track 4 and 5 for Rottne, which are S shaped (slalom), Antilla model's 1,2 and 3 give quite satisfactory results. For S shaped tracks, the rut depth calculation has to take into account the turning radius as well as velocity for accurate prediction; this has been verified by the works done on military vehicles equipped with tires (Liu, et al., 2009).

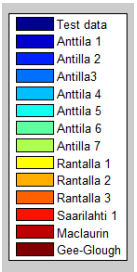

Figure 11 Rut depth model description

The equations used in the above mentioned models are derived for specific conditions; they are not designed to cater the needs of the specific conditions at Tierp. Such empirical equations can only be applied to conditions in which they were generated or more specifically, the results given by such equation are more suited to conditions in which they were developed. The coefficients used in such equations are fitted for the specific conditions, and the values of such coefficient's change as the test condition change. It is not

recommended to extrapolate such equations for cases where the test conditions are not in line with what it was when the equations were developed. In our case, the soil conditions in which the models were developed were similar, but not exactly. Taking that into account the rut depth models were used to see, how well it can predicted rutting.

Table 3 WES models description

Antilla 1	Antilla's (1998) model
Antilla2	Antilla's (1998) model
Antilla 3	Antilla's (1998) model
Antilla 4	Antilla's (1998) model
Antilla 5	Antilla's (1998) model
Antilla 6	Antilla's (1998) model
Antilla 7	Antilla's (1998) model
Rantala 1	Rantala's (2001) data for soft soils
Rantala 2	Rantala's (2001) data for soft soils
Rantala 3	Rantala's (2001) data for All soils
Saarilahti 1	Saarilahti et. al (1997)
Maclaurin	Maclaurin (1990)
GeeGlough	Gee-Glough (1985)

4.3 Refinement of WES based rut depth models

The existing WES based models analyzed is not designed for multipass or multiple wheel pass of vehicles. So the existing models have been fine tuned to take into account the vehicle pass and also few models have been proposed to take care of the same issue.

4.3.1 Non-linear regression analysis

To make the available models suitable for predicting the rut depth values in Tierp, non-linear regression analysis was carried out to find suitable coefficients for the models described in **Table 3**.By applying the newly derived coefficients to the existing models, the models can be used for rut depth prediction after the first vehicle pass for the conditions in Tierp. Both the left side and right side rut depths values of Rottne and Komatsu were used for non-linear regression analysis to improve the calculation. The new coefficient's obtained after the non-linear-regression analysis is shown in **Table 4**. The results of the non-liner regression analysis are shown in Figure 12.

Table 4 Regression analysis constants

Model Used	Coefficient (original)		Coefficient (new)		Mean Square Error
	a	b	a	b	
Maclaurin	0.224	1.25	0.6474	1.665	1.5 E-04
Antilla 1	0.003	0.910	0.0040	0.7552	1.2780 E-04
Antilla 2	0.248	NA	0.1900	NA	1.5 E-04
Antilla 3	0.003	0.380	0.0040	0.1991	1.5 E-04
Antilla 4	0.000	0.328	-0.0191	0.3953	1.5 E-04
Antilla 5	0.005	1.212	0.0054	1.0120	1.2780 E-04
Antilla 6	0.001	0.287	-0.0142	0.2950	1.5 E-04
Antilla 7	-0.001	0.248	-0.0142	0.2950	1.5 E-04
Rantala 1	0.059	0.490	-0.0191	0.3953	1.5 E-04
Rantala 2	0.989	1.23	0.8675	1.6165	1.5 E-04
Rantala 3	0.010	0.610	-0.0191	0.3953	1.5 E-04
Saarilahti	0.142	0.83	0.6474	1.6165	1.2780 E-04

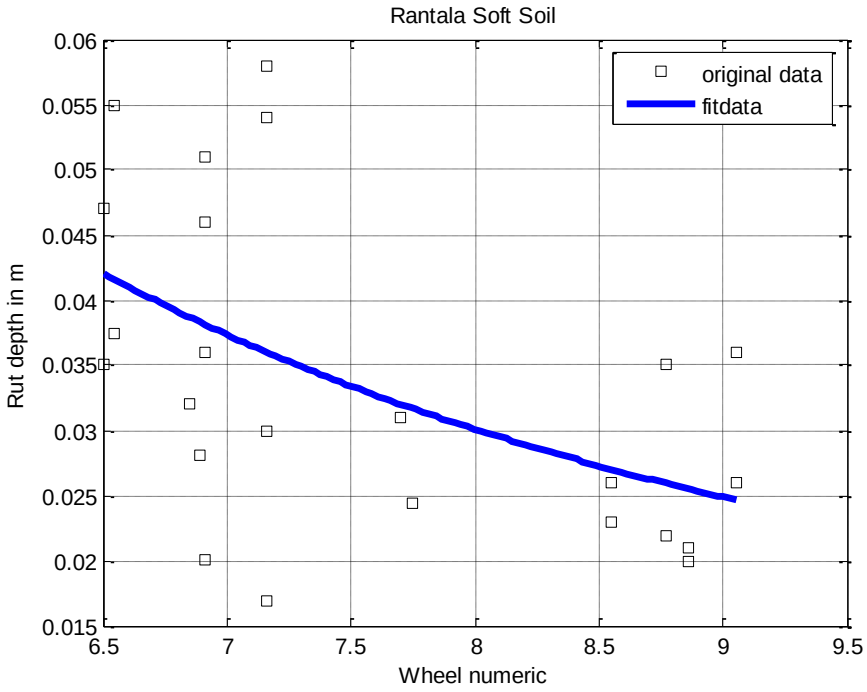

Figure 12 Regression analysis results best fitting curve

4.3.1.1 Analysis of variations of constants in WES equation

The constants in Antilla's Equation 1 were analyzed to see the effect when the cone Index value varies. The results of which are displayed in Figure 13. The range of cone index value evaluated was from 50 to 500 kPa. It can be seen that, the value of constant 'a' remains constant at 0.004, but, the value of 'b' is linearly increasing with cone index. From these two

graphs, the conclusion that can be derived is that, the constant 'b' is a parameter that depends on the cone index, which in-turn depends on the soil penetration resistance.

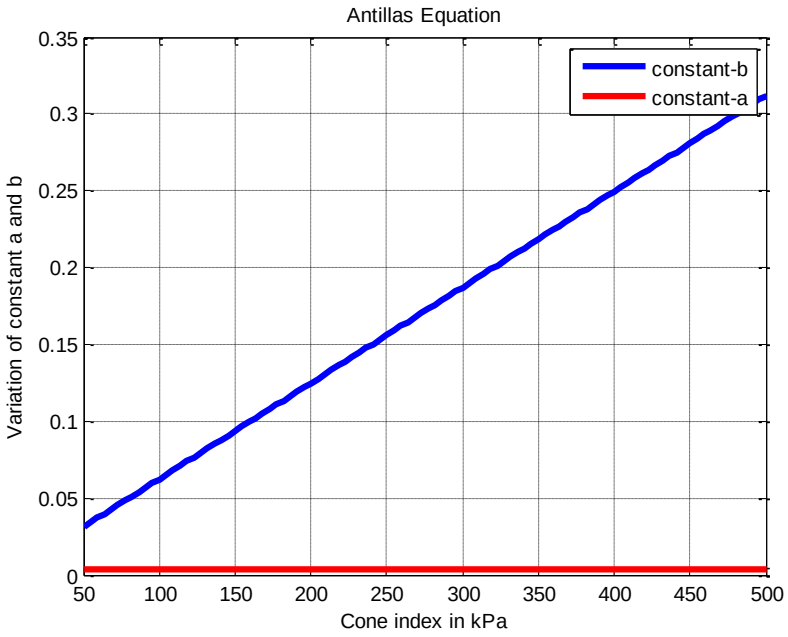

Figure 13 Variation of constants

4.3.2 Application of 'novel wheel mobility number'

The 'novel wheel mobility' number developed by Shawky Hegazy and Corina Sandu (Hegazy & Sandu, 2013) was introduced in the project to analyze its effect in predicting the rut depth. The model was applied to Antilla's equation 3, 4 and 5 replacing N_{CC}, N_{ci} and C_N. Non-linear regression analysis was carried out to find out the new coefficient when 'novel wheel mobility number' was applied. The proposed wheel mobility number is:

$$N_{HS} = \frac{CIbd}{W} k_{HS} \tag{9}$$

$$k_{HS} = \sqrt{\frac{h-\delta}{d}} = \sqrt{\frac{R1}{d}} \tag{10}$$

Where,

k_{HS} = proposed coefficient

R1= loaded height of the wheel

h=tire section height

δ = tire deflection

Antilla's equation3, 4 and 5 has been given below respectively.

$$z = a + \frac{b}{N} \tag{11}$$

Where,

z = rut depth

a,b= constants

N= wheel numeric

Table 5 Antilla's models original value of constants

	a	b	N
Model 1	0.003	0.380	N_{CC}
Model2	0.000	0.328	N_{CI}
Model3	0.005	01.212	C_N

Non-linear regression analysis was carried out to determine the best fitting coefficient for the Antilla's equation when the proposed wheel numeric is applied. The new coefficients are shown in **Table 6**.

Table 6 New coefficient's in the Antilla's model

	a	b	Mean Square Error
Model 1	0.004	0.1991	1.2780 E-04
Model 2	0.0054	0.2668	1.2780 E-04
Model 3	0.0054	0.2668	1.2780 E-04

The new coefficients and the new wheel numeric were applied to Antilla's equation, rut depth values were obtained from first vehicle pass for both Komatsu and Rottne, the results of which are shown in Figure 14 and Figure 15. It can be seen that the results for Komatsu are satisfactory, especially for the fourth track/machine configuration.

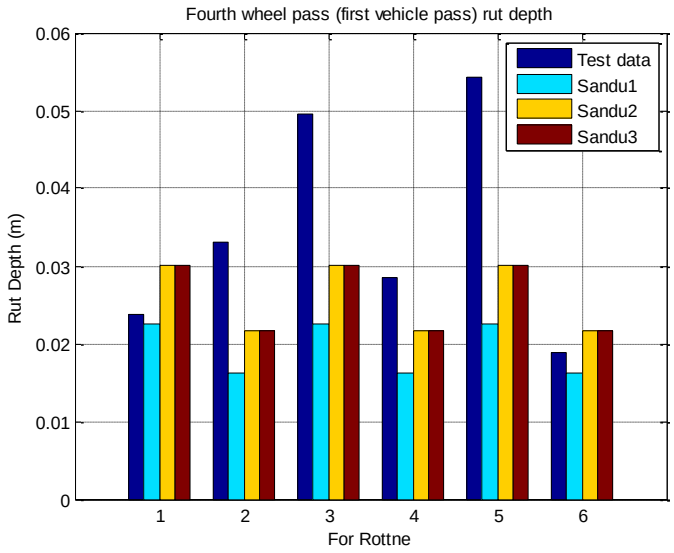

Figure 14 Comparison of rut depth with the new model for Rottne

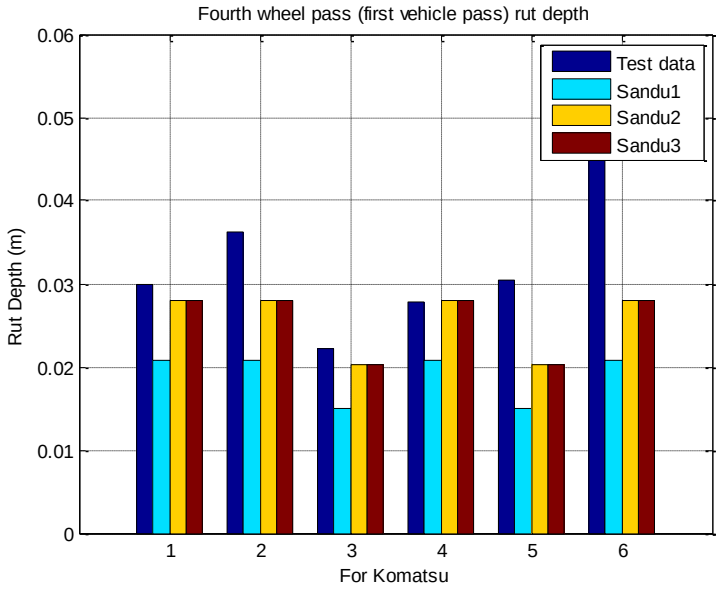

Figure 15 Comparison of rut depth with the new model for Komatsu

The mean square error values of the new equations are similar to the Antilla's 1 and 5^{th} model, as well as Saarilahti's equation, it can be concluded that these models could be used for estimating the rut depth after the first vehicle pass. It should always be kept in mind that the equation is empirical and cannot be extrapolated beyond the limits.

The new wheel mobility number has been applied into Antilla's equation 5 and variation of the constants with respect to cone index was studied. It is evident from Figure 16 and Figure 17 that the constants in the equation remain as such for the cone index values ranging from 1000 to 3000 kPa. But, it has been noticed that this value of constants will change for another range of cone index values. So, it can be inferred that the soil characteristics also have a bearing on the constants. Further detailed studies are needed to explore the relationships.

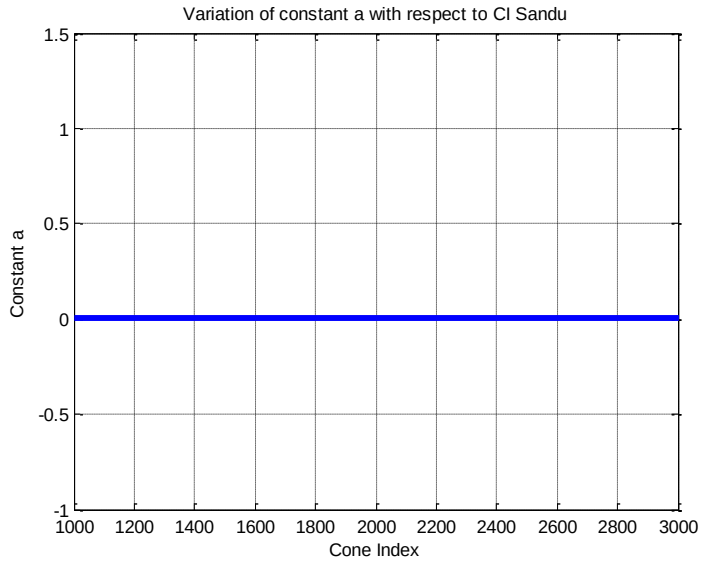

Figure 16 Variation of constant 'a'

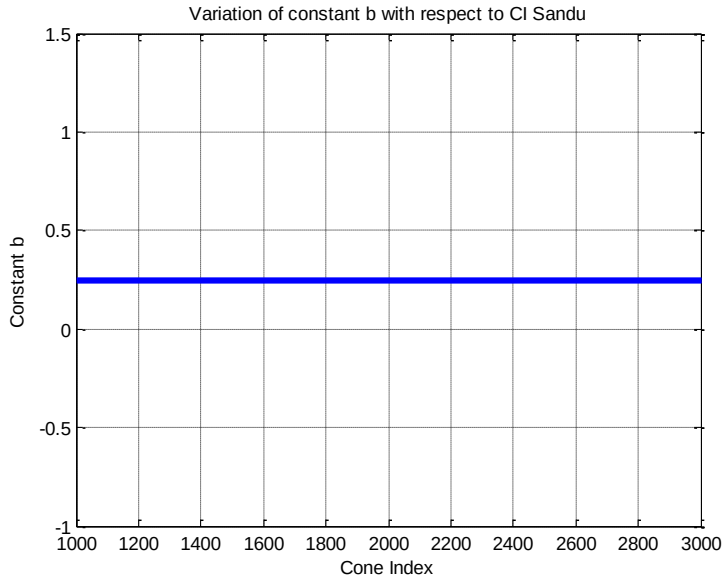

Figure 17 Variation of constant 'b'

4.3.3 Multi-pass rut depth models

When a wheel passes over a terrain, it creates the first rut; the following wheel passes over the same rut, and increases the rut depth at that particular point. The bearing capacity of the soil after the first wheel pass would increase and the consecutive rut depth will be small. In this thesis, wheel multi-pass is studied. Some of the examples of multi-pass rut depth created are by earth moving machines, agricultural, forestry and military vehicles.

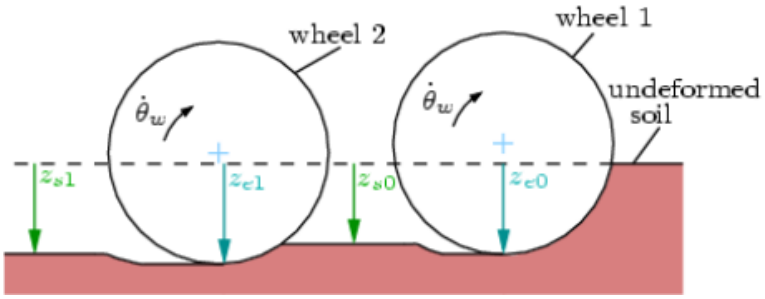

Figure 18 Wheel multi-pass

Scholander conducted repetitive plate loading tests on Swedish forest soil and found the general equation for settlement after n loading cycles (Saarilahti, 2002).

$$s_n = s_1 n^{1/a} \tag{12}$$

Where,

s_n = settlement after the nth loading cycle

s_1 = settlement after the 1st cycle

n= number of passes

a=repeatedness coefficient

The repeatedness coefficient is also called multi-pass coefficient. The multi-pass coefficient is 2-5 for wet and fine grained soils and is higher for soils that are drier and coarser.

Abebe introduced a multi-pass sinkage model for tractor. This model is similar to the model proposed by Scholander (Saarilahti, 2002).

$$z_n = z_1 n^{1/a} \tag{13}$$

Where,

Z_n= sinkage after pass n

Z_1= first pass sinkage

n= number of passes

a=multi-pass coefficient

Literature associated with multi-pass rut depth models is scarce when compared to single pass rut depth models. Here, Abebe's equation was used to estimate the rut depth after the multi-pass activity of the forwarder. Abebe's equation was developed to take into account the multi-

pass effect of a single wheel with a constant load, but in the case at Tierp; the forwarder wheels had different loads.

So, regression analysis was carried out to find out the multi-pass coefficient that could best describe the rut depths after the n number of vehicle passes. Regression analysis was carried out for all the track combinations for both Rottne and Komatsu. It was found that better results were obtained when regression analysis was carried out between the rut depth and the number of vehicle passes when compared to number of wheel passes, which is a multiple of four. The results of such analysis for both Rottne and Komatsu are shown in Figure 19 and Figure 20.

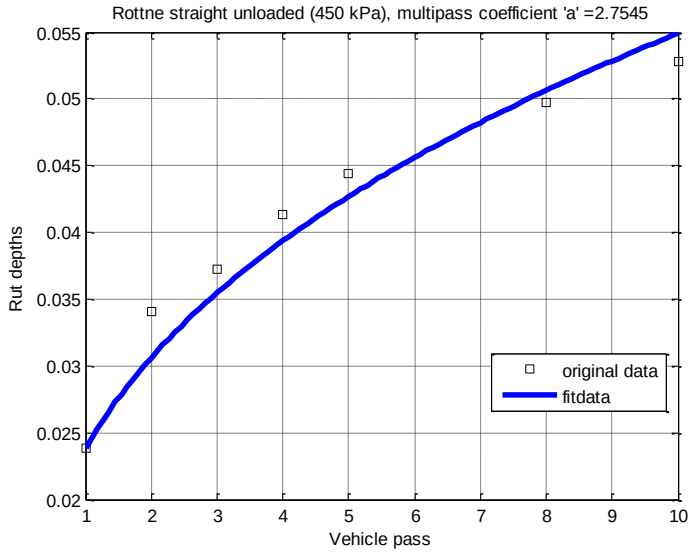

Figure 19 Regression analyses to estimate the multi-pas coefficient for Rottne

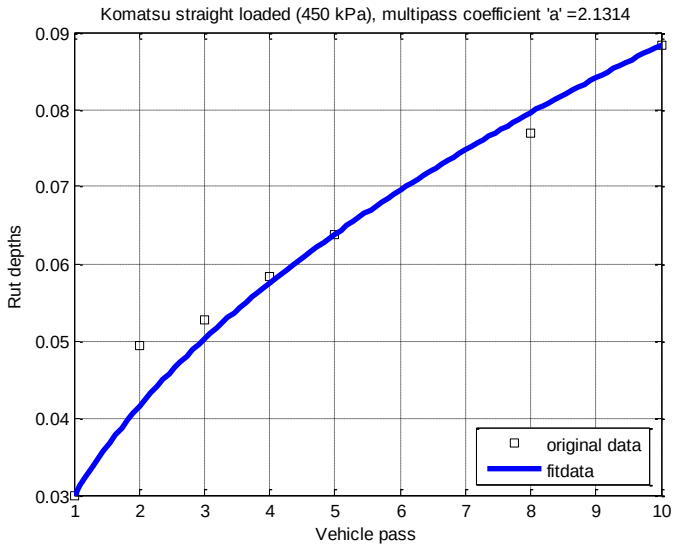

Figure 20 Regression analyses to estimate the multi-pas coefficient for Komatsu

For most cases, the values of multi-pass coefficient lies between 2 and 3, the same was mentioned in Saarilahti's report (Saarilahti, 2002). **Table 7** shows the multi-pass coefficient obtained for each vehicle setup mentioned in **Table 2** .

Table 7 Multi-pass coefficients estimated

Rottne	
Track	Multi-pass coefficient
1	2.75
2	2.24
3	2.06
4	1.93
5	2.53
6	1.9
Komatsu	
Track	Multi-pass coefficient
1	2.13
2	1.81
3	2.61
4	2.32
5	2.48
6	2.29

Multi-pass coefficient can be modelled by the equation

$$a = \frac{\ln(j) - \ln(i)}{\ln(z_j) - \ln(z_i)} \tag{14}$$

Where,

a= multi-pass coefficient

j,i= ordinary number of passes

It has been concluded in the previous thesis work on tire-soil interaction by Wijekoon (2012) that the multi-pass coefficients estimated through this equation is inferior to the regression analysis approach; much variation was observed while using this equation.

Figure 21 and Figure 22 shows the comparison between the rut depth predicted using Abebe's equation, with the estimated multi-pass coefficient, for Rottne and Komatsu versus the original test data. The coefficient of determination was found to be 95.3 % for Rottne and 96.4 % for Komatsu.

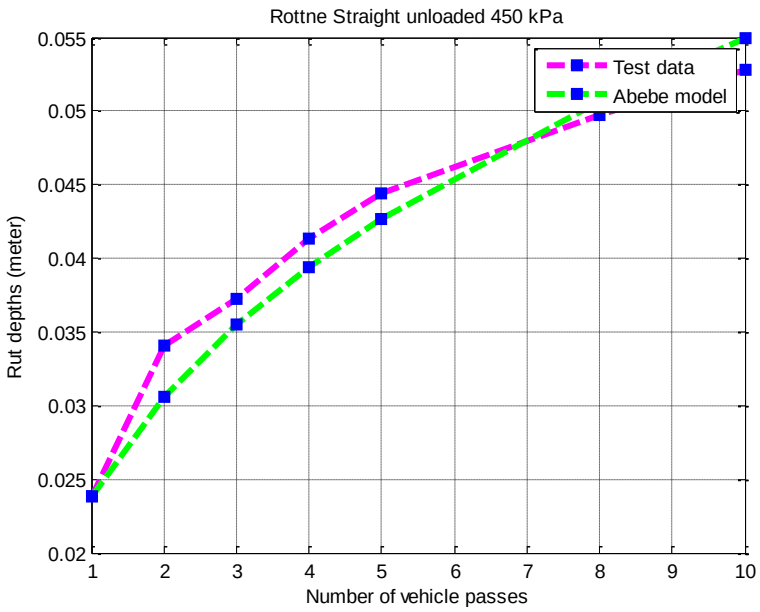

Figure 21 Predicted rut depth vs. measured rut depth for Rottne

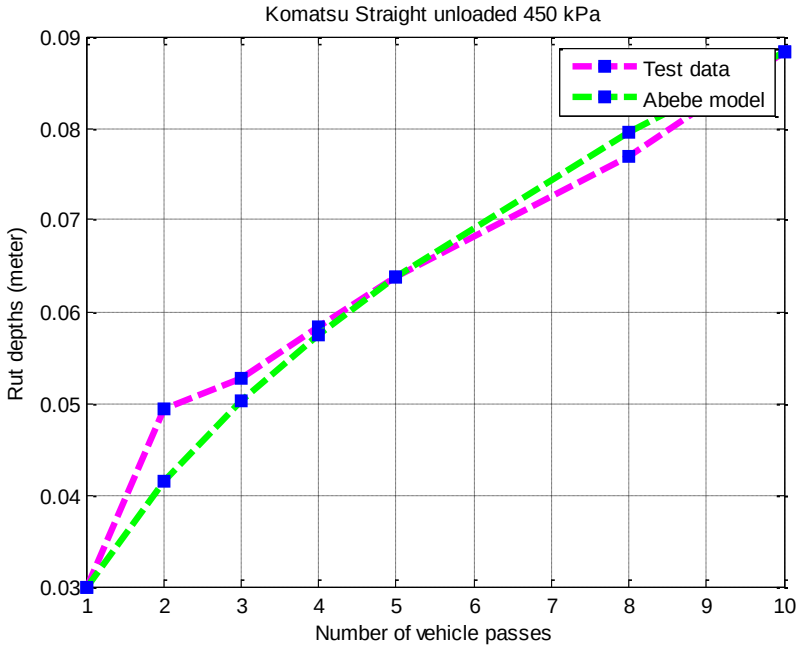

Figure 22 Predicted rut depth vs. measured rut depth for Komatsu

4.3.4 Rut depth estimation with changing Cone Index

In most of the models that deal with multi-pass rut depth analysis, the cone index used will be the one before the vehicle pass or an average cone index value. But, in reality, as each wheel passes a particular path or point in soil, the soil properties at that specific point changes or the cone index value varies (Akay, et al., 2006).

In the new model developed, the cone index after each wheel pass has been taken into account; this new cone index is then used to compute the rut depth caused by the successive wheels. Maclaurin's (1990) equation has been used to estimate the sinkage caused by each wheel.

Brixius has developed an equation to compute the cone index after pass as a function of cone index before pass and mobility number. This equation is applicable in areas where compactible soil exists (Akay, et al., 2006).

$$\frac{ACI}{BCI} = 1 + \left(1.8e^{-0.11B_n}\right) \tag{15}$$

$$B_n = \frac{CIbd}{W}\left(\frac{1+\left(\frac{5\delta}{h}\right)}{1+\left(\frac{3b}{d}\right)}\right) \tag{16}$$

Where,

ACI= cone index after pass

BCI= cone index before pass

B_n= mobility number

δ = tire deflection

h= tire section height

d= tire diameter

The rut depth created by each wheel was computed by substituting the cone index after each pass of the previous wheel, so each wheel encounters a new/different terrain, into the Maclaurin's equation.

$$z = d\left(\frac{0.224}{N_{CI}^{1.25}}\right) \tag{17}$$

Where,

Z= rut depth

d= wheel diameter

N_{CI}= Wheel numeric

The new method was tried for Rottne, the results of which are shown in Figure 23. Only straight tracks were considered in the analysis, because, the existing models cannot be used to estimate the rut depth for S shaped tracks. From Figure 23, it is evident that model can predict the rut depth well after one vehicle pass, even though not accurate. This model is designed to take into account the changing soil conditions, which is absent in the other WES based rut depth models.

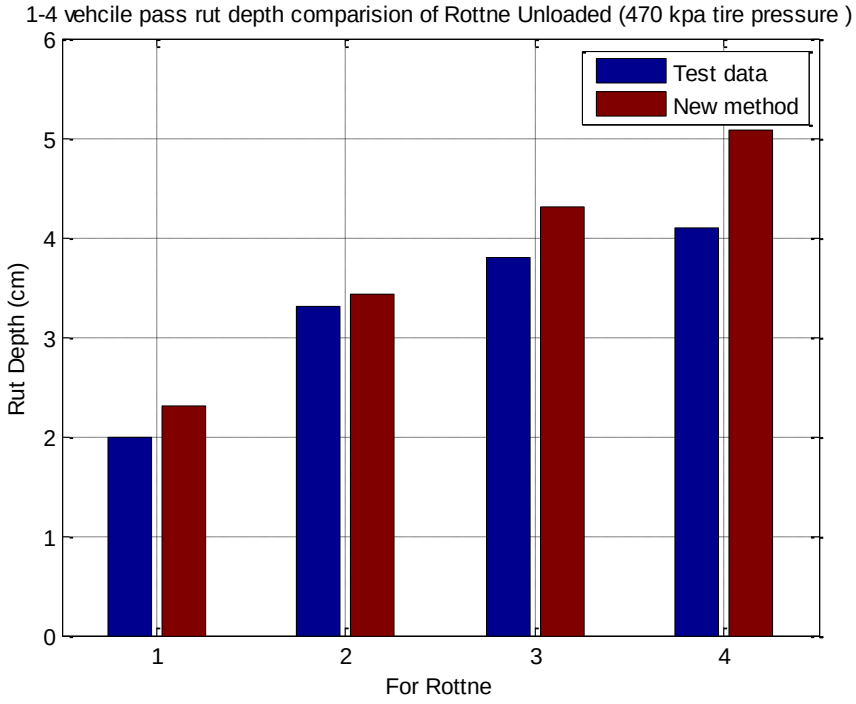

Figure 23 Rut depth comparisons with measured data

4.3.5 Rut depth estimation with Kharkhuta's model

Another model developed by Kharkhuta was studied to assess its ability to predict rut depths (Lyasko, 2010); this multipass model was studied because of its simplicity. The model is described by Equation 18.

$$Z_N = Z_1\left(\chi \log N + 1\right) \tag{18}$$

Where,

χ is the Kharkhuta's coefficient

The value of Kharkhuta's coefficient can be determined after field tests. The value used here is obtained from the work done by Lyasko (Lyasko, 2010).Analysis was done for both Rottne and Komatsu, but the results obtained were not satisfactory, it is evident from Figure 24 and Figure 25.

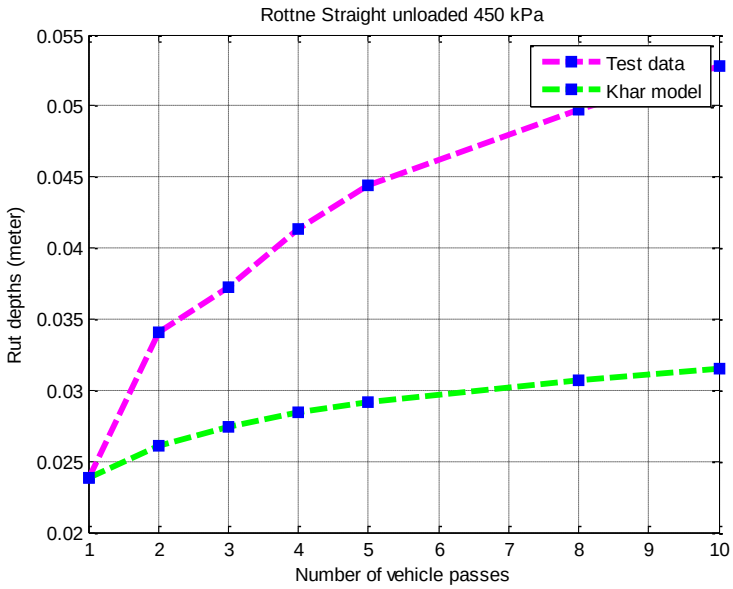

Figure 24 Measured rut depth vs predicted rut depth with Kharkhuta's model for Rottne

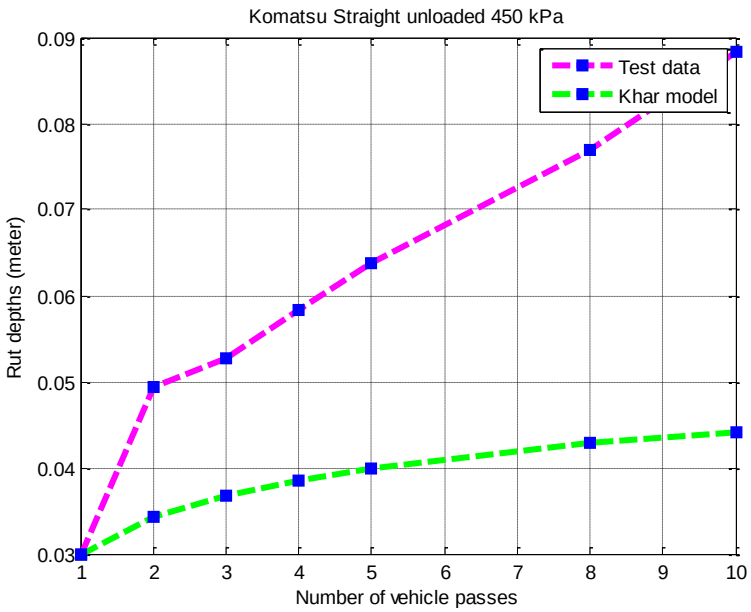

Figure 25 Measured rut depth vs predicted rut depth with Kharkhuta's model for Komatsu

4.3.6 Change in rut depth with cone index

The change in rut depth percentage as a function of change in cone index percentage after a number of specified passes was analyzed. Here, the change in rut depth percentage between the first and the tenth pass of the vehicle at a depth of 15 cm was compared with the difference in cone index percentage after the first pass and the tenth pass; as a result an empirical equation was derived. This method has been implemented for both Rottne and Komatsu.

For Rottne, loaded machine at 450 kPa was used and a fourth degree polynomial with a coefficient of determination 85% was derived.

$$y = -0.0083x^4 - 0.085x^3 + 3.229x^2 + 4.975x + 21.23 \quad (19)$$

For Komatsu, the equation was derived for a loaded machine with 450 kPa tire pressure; a fourth degree polynomial was derived with a coefficient of determination of 53%.

$$y = -0.004508x^4 - 0.1321x^3 + 0.3313x^2 + 23.98x + 287.2 \quad (20)$$

Where,

y= change in rut depth percentage

x= change in cone index percentage

The empirical equation so derived can be used to determine the change in rut depth percentage for the specific vehicles in the specific soil terrain at Tierp. More filed test needs to be done to determine the effectiveness of the equation.

4.3.7 Cone Index vs. Depth of measurement

In this section, the cone index variation at various depths of measurement after specific number of vehicle passes was analyzed. Empirical equations were derived for the evaluation of cone index at different depth, till 21 cm, after specific vehicle passes. Figure 26 show the variation of cone index with depth for Rottne and ProSilva.

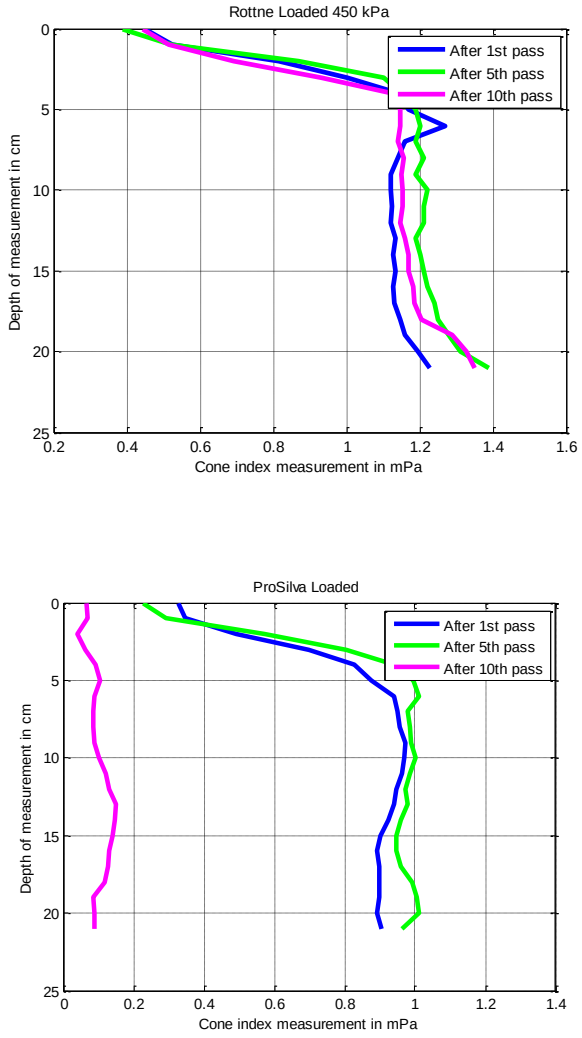

Figure 26 Variation of cone index with depth after specific number of vehicle passages

It can be seen from Figure 26 that the cone index value after the 10^{th} vehicle pass is comparatively less than the 5^{th} vehicle pass values, it was expected that the cone index should increase after each vehicle pass. Similar trend can be noticed in all the machines tested, cone index values after 10th pass is less when compared to other passes. The possible cause for this may be due to increase in moisture content during the 10^{th} pass or due to a reduction in bulk density. Empirical linear equations were derived for various machine configurations, as shown in **Table 8** along with their coefficient of determination, connecting cone index and depth of measurement, these equations can be used under specified conditions to determine the cone index by taking into account only the depth of measurement.

For Rottne loaded 450 kPa, Komatsu loaded 450 kPa, ProSilva loaded 450 kPa, equations were derived for cone index after 1^{st},5^{th} and 10^{th} pass based on the data availability. For Komatsu machine installed with the tracks ECO Track and Magnum, equations were derived for only cone index after 1^{st} and 10^{th} pass.

The equations are of the form:

$$y_n = a + bx \tag{21}$$

Where,

y= cone index

x= depth of measurement

n= number of vehicle pass (1, 5, 10)

Table 8 Coefficients of the empirical model

Rottne loaded 450 kPa			
n	a	b	R^2 (%)
1	0.86	0.014	38
5	0.85	0.02	51
10	0.78	0.02	61
Komatsu loaded 450 kPa			
1	0.81	0.02	42
5	0.64	0.03	72
10	0.74	0.024	64
ProSilva loaded			
1	0.64	0.018	38
5	0.66	0.021	39
10	0.07	0.002	32
Komatsu ECO Track			
1	0.83	0.0177	72
10	0.678	0.0225	78
Komatsu Magnum track			
1	0.75	0.032	43
10	0.76	0.026	49

It can be seen from **Table 8**, coefficient *a*, ranges from 0.6 to 0.9 and the coefficient *b* ranges from 0.01 to 0.03. This range represents a trend; results from more field test can be used to estimate the stability of this range. From Figure 26, it can be seen that the graph does not look linear; but linear equations were proposed to keep the analysis simple and to reduce the number of coefficients. A word of caution, more tests needs to be done to fix the suitability of the equation, various machine configurations has to be tested under various conditions so as to generalize and suggest a range of values for the coefficients in the equation.

5 PRESSURE MODELS

Various models to estimate the pressure in tire-soil interface has been examined in this chapter.

The tire-soil contact pressure depends on the type of tire, inflation pressure and the load acting on it. Top soil compaction is depended on the tire soil contact pressure (Botta, et al., 2008). It has been shown by Arvindsson & Keller, 2007 that the tire inflation pressure affects the top soil stresses, while, the load acting on the wheel influences the subsoil stresses. The soil-tire stress distribution increases with tire inflation pressure and the peak stress is higher than the tire inflation pressure (Schjønning , et al., 2007) .For simplification purposes, the average contact stresses can been taken as the tire inflation pressure (Plackett, 1984). But many works have reported the average stress to be higher as well as lower than the tire inflation pressure.

The mean ground contact pressure can be assumed as the inflation pressure when the recommended inflation pressure is used. The work of Arvindsson & Keller, 2007 confirmed that the maximum stress at 10 cm depth was higher than the infalation pressure.

The wheel arrangment also affect the tire-soil contact pressure. Dual wheels and tandem wheel stress distribution have been studied by Arvindsson & Keller, 2007. In the same work they also investigated the effect of tire inflation pressure on the soil stresses.

Various pressure models suggested by Saarilahti (Saarilahti, 2002) for forest machines are used to evaluate the tire-soil contact pressure of the machines Rottne F13s loaded with 450 kPa inflation pressure and Komatsu 860.3 loaded with 270 kPa inflation pressure. The average load of the fourth wheel on the right side of the machines is taken for calculation purposes. The pressure models used in the calculations are mentioned in the Appendix A6.

For the models; Swedish formula, Schwanghart (1991), Komandi(1990), Silverside and Sundberg (1989), Kemp (1990), Grecenko (1995), Krick (1969), Pillai and Fiedling (1986), Febo (1987) ,Söhne (1969), Diserns (2008) 1, Diserns (2008) 2, Keller (2005), Duttman (2012), Lyasko (1994), Diserns (2011) 1, Grecenko and Prikner (2013), Sharma and Pandey (1996) 1, Sharma and Pandey (1996) 2, Grecenko (1995) 1, Grecenko (1995) 2, Grecenko (1995) 3, Grecenko (1995) 4 and Grecenko (1995) 5, the contact pressure has been calculated by dividing the load with the contact area provided by various authors and obtained from Saarilahti's report (Saarilahti, 2002). The pressure values estimated from various models are compared with the pressure obtained by dividing the load on the wheels with the measured contact area as well as pressure measured at a depth of 15cm below the ground. The results of the analysis are shown in Figure 27.

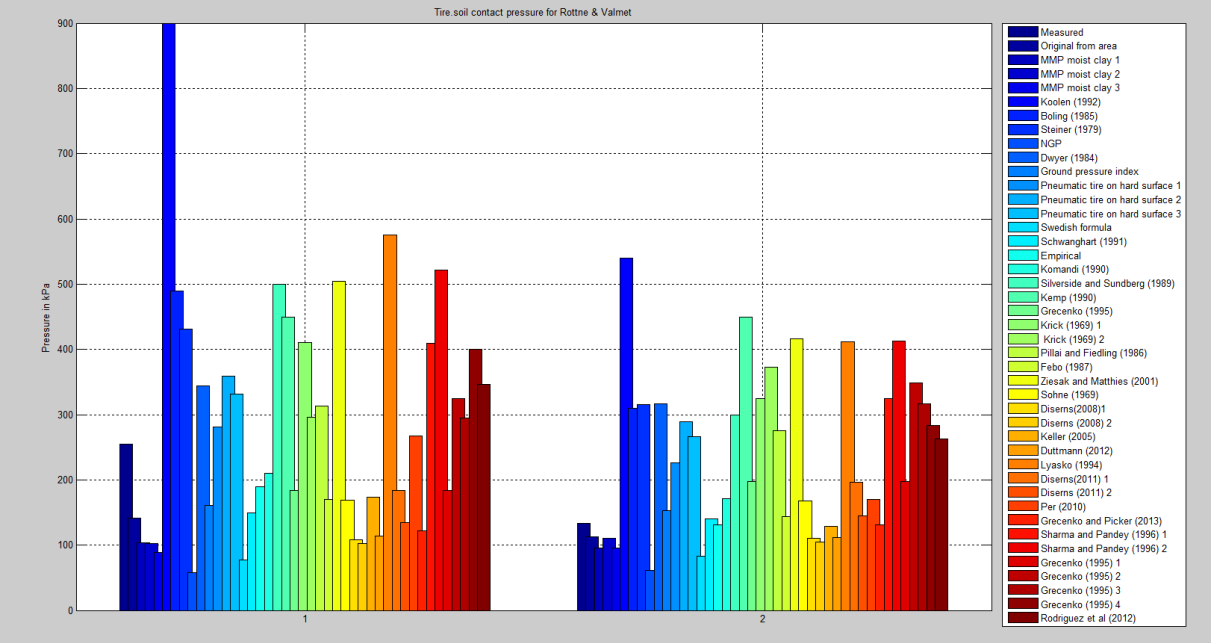

Figure 27 Tire-soil contact pressure comparisons for Rottne and Komatsu

All the models provide the pressure at the contact surface between the tire and the soil, so it seemed feasible to compare the pressure values obtained from various models with the pressure obtained by dividing the load by contact area. It is evident from the plots that most of the models do not predict the exact value, that is, the one obtained by dividing wheel load by contact area. It has to be noticed that the pressure obtained by dividing the load with the contact area is a simplified process, in reality, the soil pressure under a deformed tire is not uniform.

In case of Rottne, only, Schwanghart (1991) model (Schwanghart, 1991) is near to the pressure measured. For Komatsu, models like, MMP Moist clay 1, MMP Moist clay 2, Disern's (2008) 1, Disern's 2008 (2) (Diserns, 2008) and Duttmann (2012) (Duttmann, et al., 2012) provide values that are similar to the one obtained by obtained by dividing the load by contact area. As it is hard to estimate the exact value of the ground pressure due to the complex interaction between the soil and the tire, the models whose results are almost similar can be taken into account. Also, these models proposed here, can be taken to compare the tire-contact pressure of various machines or machine configurations.

But, from **Table 9**, it can be seen that the pressure at a depth of 15 cm is 255 kPa for Rottne and 133 kPa for Komatsu. The pressure at the contact surface between the tire and soil will definitely be more than 255 kPa and 133 kPa. Therefore, all the models that provide a value around 255 kPa can be considered. So, if the pressure at 15 cm depth is taken a yardstick to evaluate the pressure exerted by the tire, then for Rottne, only the model Per (2010) gives realistic result. But for Komatsu, Ground pressure index, Empirical, Keller (2005) and Disern's (2011) 2 gives nearby results. It has to be noted again that, these models are created for determining the surface pressure, even though they are considered for pressure estimation at 15 cm depth.

Table 9 Pressure values obtained from different models

Pressure models in kPa			
	Model	Rottne	Komatsu
1	Measured at 15 cm	255	133
2	Measured with contact area	141,2121	113,071
3	MMP Moist clay 1	104,1581	96,01613
4	MMP Moist clay 2	102,7476	110,2442
5	MMP Moist clay 3	89,19849	95,70653
6	Koolen (1992)	900	540
7	Boling (1985)	490	310
8	Steiner (1979)	431,618	314,91
9	NGP	57,4112	61,6
10	Dwyer (1984)	343,6524	316,7892
11	Ground pressure index	160,5798	152,5909
12	Pneumatic tire on hard surface 1	281,4245	226,5614
13	Pneumatic tire on hard surface 2	358,5026	288,6133
14	Pneumatic tire on hard surface 3	331,0877	266,5428
15	Swedish formula	76,86844	82,47686
16	Schwanghart (1990)	149,4342	140,6362
17	Empirical	189	131,4
18	Komandi (1990)	210,575	170,9031
19	Silverside and Sundberg (1989)	500	300
20	Kemp (1990)	450	450
21	Grecenko (1995)	184,342	197,7919
22	Krick (1969) 1	410,4923	325,1046
23	Krick (1969) 2	295,7585	372,9079
24	Pillai and Fiedling (1986)	313,6166	274,8352
25	Febo (1987)	170,1039	143,1681
26	Ziesak and Matthies (2001)	503,8587	416,2172
27	Söhne (1969)	169,4433	168,2188
28	Diserns (2008) 1	108,6815	110,8198
29	Diserns (2008) 2	103,0062	105,2105
30	Keller (2005)	173,0065	129,009
31	Duttmann (2012)	114,0139	111,7596
32	Lyasko (1994)	574,9605	411,5294
33	Diserns (2011) 1	183,518	196,9078
34	Diserns (2011) 2	134,6512	144,4756
35	Per (2010)	267,8	170,6
36	Grecenko (2014)	121,8328	130,7219
37	Sharma and Pandey (1996) 1	409,2652	324,1327
38	Sharma and Pandey (1996) 2	521,0926	412,6985
39	Grecenko (1995) 1	184,342	197,7919
40	Grecenko (1995) 2	324,6729	348,3614
41	Grecenko (1995) 3	295,1805	316,7172
42	Grecenko (1995) 4	400,1726	283,6072
43	Rodriguez et al (2012)	346,14	262,6

The Nominal Ground Pressure model is based on the assumption of fifteen percent sinkage (Saarilahti, 2002). The model is considered as a standard that is used in Nordic forest research. As expected this model gives very low ground pressure values when compared to other models. But the model is used an indicator of trafficability for wheeled as well as tracked vehicles (Saarilahti, 2002).

It can be seen from the work of Hetherington & White, (2002) that the MMP models do not represent actual ground pressure. It can work as an indicator of vehicle performance rather than a model to predict the actual contact pressure.

The model proposed by Komandi (1990) was developed for agricultural tires (Saarilahti, 2002). In the model proposed by Silverside and Sundberg (1989), it is assumed that ten percent wheel load is supported by side walls.

Whereas, Kemp (1990) assumed the sidewall support to be zero and proposed the inflation pressure to be equal to the ground pressure. Febo (1987) used wide agricultural tires to suggest the pressure model that is applicable to hard surface; the values predicted by Febo (1987) were very high.

The values predicted by Ziesak and Matthies (2001) were within a good range of the original values, Ziesak and Matthies (2001) model were developed to predict average contact pressure for forestry tires on hard surface. The model by Lyasko (Lyasko, 1994) gives good results; the model is based on a tests on rigid surface conducted with the help of a single-wheel tester. Diseren's (2008) model gives good results, this empirical model have been developed by testing twenty four different trailer tires, both cross-ply and radial were taken into account, in soils ranging from soft to hard.

The model proposed by Keller (2005) (Keller, 2005), is based on field experiments with tractors , trailers and harvesters in Sweden and Denmark for agricultural tires, this model also provide a good estimate of the contact pressure. The model given by Duttmann, et al., 2012 also provides results that are comparable, the eqution is based on field study conducted in clayey silt soil in German farm vehicles.

Diserens , et al., (2011) model was developed for traction tires for grasslands and open ground sites, harvesters and tractors were used for the experiment, the model provided good results. The model proposed by Per (2010) , predicted contact pressure with the help of tests done with radial tires in Sandy soil, even though the test conditions and tire type was different from what it was on the tested forwarders at Tierp, the model provided satisfactory results.

The contact area value for a rectangular patch provided by Sharma and Pandey (Sharma & Pandey, 1996) were used to obtain the contact pressure, the result was satisfactory when the contact area was used for a rectangular patch, but in reality, the conatct patch is not exactly rectangular, an elliptical patch provides a better estimate of the contact area (Wulfsohn & Upadhyaya, 1992). Grecenko's (1995) model (Grecenko, 1995), has been created for hard grounds, it returns satisfactory value of contact pressure in the calculations.

The work of Cirello, et al., (2009) show that the ground surface pressure will be in the range of 200 to 600 kPa, and that too for a tire with load ranging from 4 kN to 6 kN. From this result, it can be observed that all the models that provide a pressure value less than 200 kPa seems less realistic, but, this work was carried out for hard surface, so a complete rejection of the all the models that return values less that 200 kPa cannot be done unless or until an expiremtal analysis has been carried out similar to what Cirello, et al., (2009) has been done in soft soil.

Another interesting observation is that, the work done by Lamande´ & Schjønning, (2011) suggests a maximum surface pressure of 200 kPa for a 60 kN loaded wheel. Therefore, a model than can accurately predict the surface pressure is lacking. But experimental method followed by Cirello, et al., (2009) seems to be a good option to find accurate pressure, this approach can be used further to develop an empirical model.

Hetherington & White (2002), from their studies have shown that the surface pressure can be found by using a multipying factor with the pressure measured at a specified depth. But the uncertanity existing over such a factor acts a major source of error in determing the surface pressure.

The surface pressure value also depend on the type of soil, tyre inflation pressure and vehicle weight. Higher weight and higher inflation pressure would increase in the ground pressure level.

It has been mentioned by Wästerlund (Wästerlund, 1989), that trees standing near to the ruts whose soil layer is exposed to contact pressure of 60-90 kPa show reduced growth. Also spruce seedling demonstrates reduced growth when exposed to static load greater than 80 kPa. It is evident from the analysis above that the machines analyzed apply contact pressure greater that the threshold values mentioned by Wästerlund, this highlights the impact the machines can have on the forest floor.

6 Tire-Soil Contact Area

This chapter provides an insight into various models that are used to determine the contact - patch area between a tire and soil.

Tire soil contact area is a very important parameter in determining various aspects of vehicle mobility. The loaded area play an important role in determining the distribution of stresses at the soil surface, and also affects the stress in subsoil. The stresses in soil are directly dependent on stresses on the tire soil interface. To determine the stresses in the soil, the contact area has to be estimated accurately and the performance of soil compaction models are highly dependent on the contact area (Keller, 2005). So, accurate estimation of the tire-soil contact area play a prominent role in improving the stress propogation models.

The precise determination of contact area is necessary in the finite element analysis of tire-soil interaction (Yong, et al., 1984). Contact area comes into picture when determing the surface pressures (Döll, 2001) as well as when estimating the soil compaction (Defossez & Richard, 2002) .

The contact area depends on factors like plasticity and elsticity of both tire and ground. It has been mentioned by Diserns, et al., 2011 about the dependence of the contact area in farmlands on the forces acting on the wheels, namely, traction force, bracking force and rolling resistance. As the surface gets harder, for a given load and inflation pressure, the contact area increases (Diserns, 2008). For bigger tires, the contact area increase with the wheel load.

The tire inflation pressure influences the tire foot-print area as can be seen from the work of Schjønning , et al., 2007. The contact area doubles when reducing the inflation pressure. If the recommeded inflation pressure is used, then the contact area will be an intermediate value (Schjønning , et al., 2007).

The contact area between a pneumatic tire and a hard surface can be considered as a circle, if the tire has high inflation pressure and if it is of cross-ply type. As the tire pressure reduces the contact area transforms to an elliptical shape, similar shape can be seen on softer ground also.

Various models associated with calculating the contact area the tire soil interface has been done, the models are described in Appendix A5. The tire-soil contact area estimation has been done for Rottne F13s loaded with 450 kPa inflation pressure and Komatsu 860 loaded with 270 kPa inflation pressure as the measured tire-soil contact imprint area is only available for them. The results of the estimated contacted area with different models is shown in Figure 28. The model, Per Schjønning (2007), is not applicable to Komatsu; being an empirical model it does not satisfy the conditions under which Komatsu was tested.

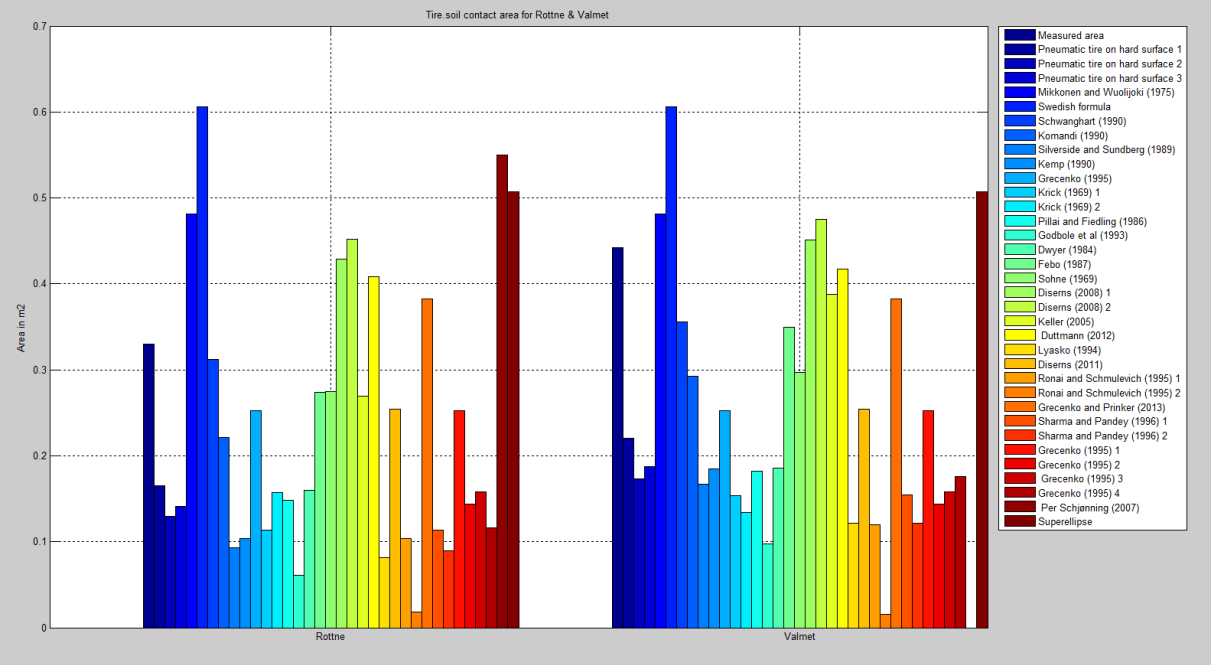

Figure 28 Contact area comparisons

The measured contact area for both the machines has been obtained by multiplying the length and breadth of the measured footprint, but in reality, the actual contact area is not rectangular all the time. The tire-soil contact dimensions measured just gives the rough length and breadth. The last wheel on the right side of both machines has been taken into account. The contact areas of both Rottne and Komatsu obtained through different models are compared with the measured values in **Table 10**. Models proposed by Saarilahti in his report (Saarilahti, 2002) is used, also models developed by other researchers in the field has also been used.

Due to the complex behavior of tire and soil interaction, it is hard to estimate the exact value of the contact area; those models that provide contact areas that are similar can be used for future purposes, outliers can be omitted.

All these models are good to compare two machines or machine configurations. The empirical models are only applicable to the conditions in which they were derived, it is not always advisable to extrapolate them to other regimes, but for comparison purposes it can be used, even though the results generated may not be accurate.

Out of all the models explored, some of them provide results that are satisfactory. In the case of Rottne, models Schwanghart (1990), Grecenko and Prinker (2014) provide good results. When it comes to Komatsu, Disern's (2008) 1, Disern's (2008) 2 and Duttmann (2012) models provide satisfactory results.

Table 10 Area values obtained from different models

	Model	Rottne contact Area in (m^2)	Komatsu contact Area in (m^2)
1	Measured area	0,33	0,4422
2	Pneumatic tire on hard surface 1	0,165586132	0,220690713
3	Pneumatic tire on hard surface 2	0,129985114	0,17324221
4	Pneumatic tire on hard surface 3	0,140748213	0,187587106
5	Mikkonen and Wuolijki (1975)	0,48125	0,48125
6	Swedish formula	0,606230625	0,606230625
7	Schwanghart (1990)	0,311842879	0,35552717
8	Komandi (1990)	0,221298855	0,292563381
9	Silverside and Sundberg (1989)	0,0932	0,166666667
10	Kemp (1990)	0,103555556	0,185185185
11	Grecenko (1995)	0,252791	0,252791
12	Krick (1969) 1	0,113522216	0,153796667
13	Krick (1969) 2	0,15756098	0,134081378
14	Pillai and Fiedling (1986)	0,148589077	0,181927183
15	Godbole et al	0,061377459	0,097147325
16	Dwyer (1984)	0,159680847	0,185859969
17	Febo (1987)	0,27395024	0,349239891
18	Söhne (1969)	0,275018303	0,297231969
19	Diserns (2008) 1	0,42877567	0,45118273
20	Diserns (2008) 2	0,4523999	0,47523786
21	Keller (2005)	0,269354	0,38757
22	Duttmann (2013)	0,408722005	0,416966511
23	Lyasko (1994)	0,08104905	0,121498009
24	Diserns (2011)	0,25392598	0,25392598
25	Ronai and Schmuelvich (1995) 1	0,10402538	0,11957708
26	Ronai and Schmuelvich (1995) 2	0,018184887	0,015543568
27	Grecenko and Prinker (2014)	0,382491477	0,382491477
28	Sharma and Pandey (1996) 1	0,113862613	0,154257827
29	Sharma and Pandey (1996) 2	0,089427487	0,121153814
30	Grecenko (1995) 1	0,252791	0,252791
31	Grecenko (1995) 2	0,143529087	0,143529087
32	Grecenko (1995) 3	0,157869531	0,157869531
33	Grecenko (1995) 4	0,116449738	0,176300201
34	Per Schjønning (2007)	0,55	NA
35	Superellipse	0,5072	0,5072

The Schwanghart (1991) model (Schwanghart, 1991) is based on tests done with four different tires at different inflation pressure and different loads in a soil bin filled with sandy loam, the results are more close to area measured in Rottne, the variations are due to the inherent empirical modelling characteristics.

The area predicted by Grecenko and Prikner (2013) model (Grecenko & Prikner, 2013) is comparatively away from the original area than Schwanghart model. Here, pressure plates in soil containers were used for testing compaction capacity of soil, Suchdol loam was used in the test.

The Disern's (2008) model (Diserns, 2008) is based on test done on soft to hard soils with trailer tires, by applying various loads and inflation pressures. The tires that were taken into account include Cross-ply farming tires, Radial low size tires and Radial terra tires. This work is more reliable in semi-firm to firm soil types.

The Duttmann (2012) model (Duttmann, et al., 2012) is based on test carried out during silage maize harvest in Germany during the Autumn of 2008. The soil type was mainly clayey silt and machines tested include a Forage harvester, a tractor and a trailer (tandem axle).

6.1 Super ellipse as tire soil contact area

If the tire pressure is low or the softer the ground, the shape of the contact area is elliptical (Hallonborg, 1996). For vehicles traversing in forestry terrain the contact area is not symmetric about its transverse axis. In such cases, each quadrant of the elliptical contact area produces different shapes or its own elliptical shape. Mathematical equations for deriving the contact areas in such cases are intricate. The approach of modelling the tire soil contact area as super ellipse was introduced by Hallonborg, 1996. The equation of the super ellipse in orthogonal coordinate system is:

$$\frac{x^n}{a^n} + \frac{y^n}{b^n} = 1 \tag{22}$$

where: n determine the shape of the ellipse, a and b are the half axes of the super ellipse. When $n = 2$, the curve is an ellipse. For $n=2$, when $a=b$, the curve becomes a circle. The curve changes to a rectangle lying on a side as n tends to ∞ (Hallonborg, 1996).

The tire soil contact area can be obtained by taking the sum of the areas in each of the four quadrants; the area of one quadrant is given by:

$$A_{quadrant} = b\int_0^a \left(1 - \frac{x^n}{a^n}\right)^{1/n} dx \tag{23}$$

$$n = 2.10\left(w_{tyre} d_{tyre}\right)^2 + 2 \quad (24)$$

Where,

$a = w_{tyre}$ =tire width in m

b = length of contact area in m

d_{tyre} = tire diameter in m

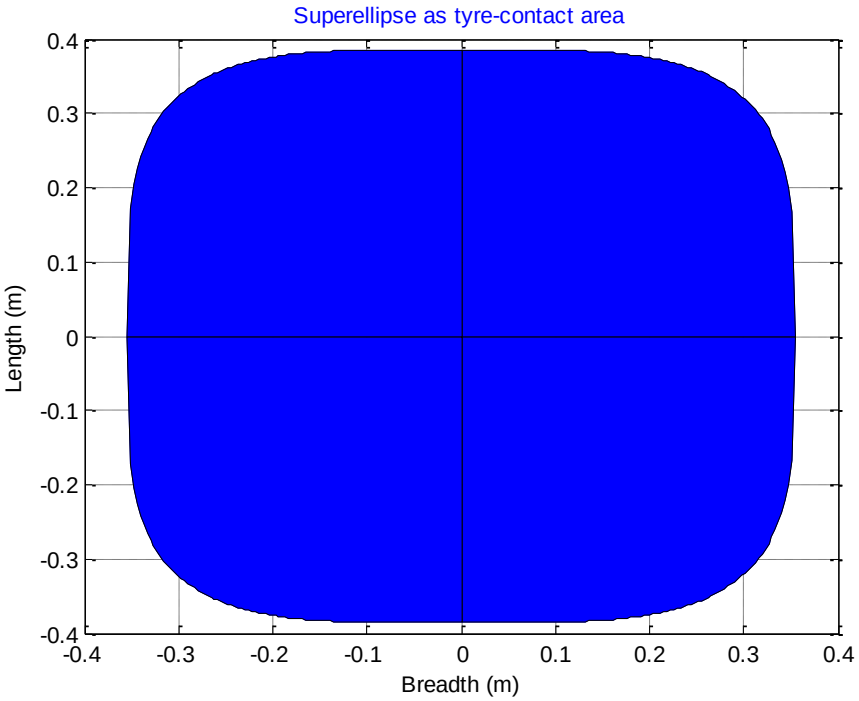

Figure 29 Superellipse as tire-soil contact area

Super ellipse concept was used to obtain the tire-soil contact area of both the forwarders, the results of which is mentioned in **Table 10** and shown in Figure 29. From the works of Hallonborg, 1996 and Keller, 2005, the super ellipse model can be considered to provide an accurate and reliable estimate of the conatct area. Super ellipse model has been tested many times and is accepted as a model that gives accurate values for various tires; it is evident from the test carried out by Schjønning , et al., 2007. So, the super ellipse model can be considered to be more relaibale than the other models.

7 Mobility Models

Mobility models are scrutinized here in order to get an overall idea about their feasibility.

The mobility models or mobility parameters can be used to assess the vehicle mobility. There are different mobility models proposed by different authors. The mobility numbers investigated in this project include, thrust coefficient, rolling resistance coefficient and drawbar pull coefficient. These variables could give an idea about the performance of the vehicle in a specific terrain.

Thrust coefficient gives an idea about gross traction, drawbar pull deals with net traction and finally rolling resistance coefficient gives a picture about the resistance encountered by the wheels of the vehicle.

Different models dealing with mobility number estimation are available; the models used in the project include the ones suggested by Saarilahti (Saarilahti, 2002). The models used include Turnage(WESFIELD), Turnage(WESLAB), Wismer&Luth, N.I.A.E models, Brixius, Ashmore et al.,Rummer and Ashmore, Maclaurin, Sharma and Pandey, McAllister and finally the model suggested by Bruce Maclaurin (Maclaurin, 2013). The equations used are attached in Appendix A4. The calculation is based on the average loads on the front wheels. The results of the analysis are shown in **Table 11**.

Table 11 Mobility parameters for Rottne

Rottne straight loaded 450 kPa			
Mobility Models	μ_P	μ_R	μ_T
Turnage (1972b), WESFIELD	0,081637	0,152766	NA
Turnage (1972a), WESLAB	0,298868	0,112109	NA
Wismer and Luth (1973)	0,211762	0,149543	0,361305
N.I.A.E Models	0,450022	0,924718	NA
Brixiuis (1987)	0,111106	0,186453	0,333558
Ashmore et al (1987)	0,633281	0,034753	NA
Rummer and Ashmore (1985)	NA	0,228545	NA
Maclaurin (1990)	0,282501	0,123	NA
Maclaurin (1990_rounded wheel numeric/new)	0,263134	0,128837	NA
Sharma and Pandey (1998)	0,055395	NA	0,113417
McAllister	NA	0,12958	NA
Bruce Maclaurin (2013)	NA	0,139589	NA

Table 12 Mobility parameters for Komatsu

Komatsu straight loaded 600 kPa			
Mobility Models	μ_P	μ_R	μ_T
Turnage (1972b), WESFIELD	0,515765	0,083871	NA
Turnage (1972a), WESLAB	0,558379	0,083871	NA
Wismer and Luth (1973)	0,562545	0,0775	0,640045
N.I.A.E Models	0,493417	1,481774	NA
Brixiuis (1987)	0,433011	0,079985	0,548996
Ashmore et al (1987)	0,136424	0,16677	NA
Rummer and Ashmore (1985)	NA	0,070659	NA
Maclaurin (1990)	0,44321	0,081175	NA
Maclaurin (1990_rounded wheel numeric/ new)	0,459883	0,077412	NA
Sharma and Pandey (1998)	0,089306	Na	0,167311
McAllister	NA	0,099758	NA
Bruce Maclaurin ((2013)	NA	0,08273	NA

The thrust coefficients were only available for few models. Also, a comparison of rolling resistance coefficient and drawbar pull for Rottne straight loaded 450 kPa inflation pressures with cone Index have been done. The results of which are shown in Figure 30.

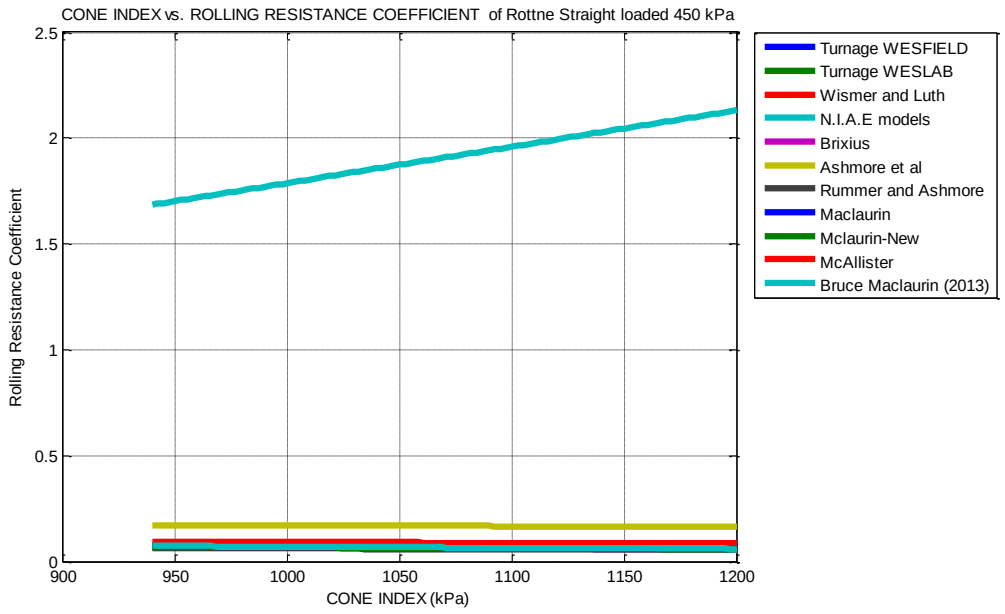

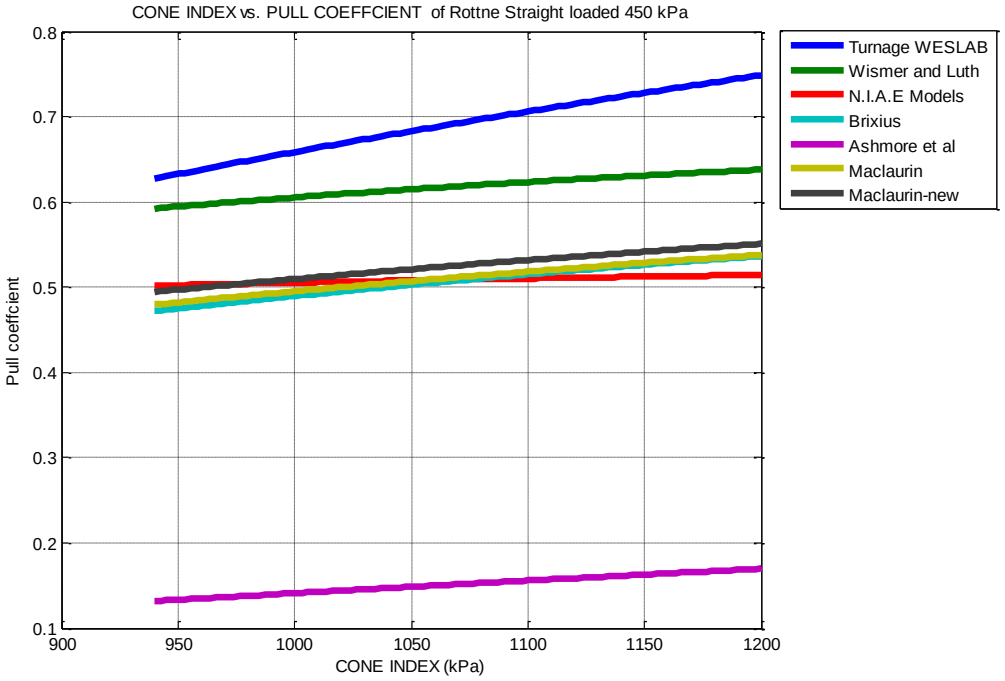

Figure 30 Evaluation of rolling resistance coefficient and pull coefficient with changing cone index

It is evident from the figure that drawbar pull coefficient increases as the cone index increases and from the figure it can be inferred that the rolling resistance coefficient decreases as cone index increases.

The range of cone index that was used for calculation was from 940 kPa to 1200 kPa, all the models gave good results in this range. For rolling resistance coefficient, Brixius, Turnage

WESFIELD, Maclaurin, Wismer and Luth, McAllister,Bruce Maclaurin and Turnage WESLAB gives similar results for 1050 kPa to 1200 kPa. Regarding drawbar pull coefficient, Turnage WESLAB, Maclaurin and Maclaurin New provide similar results in the cone index range specified.

To get a more realistic view in the forest terrain, the cone index range was changed from 200 kPa to 1160 kPa , when such a change is done, only few models give realistic values, this is done only for Rottne straight loaded with 450 kPa inflation pressure. Also, Saarilahti's report (Saarilahti, 2002) provide a list of cone index values which shows the start of cone index values from where heavy vehicle mobility starts, and it also mentions the same range of cone index's as used here. It can be inferred that the other models that gave unusual values were designed not to predict mobility parameters in this regime. The results of such an analysis is shown in Figure 31.

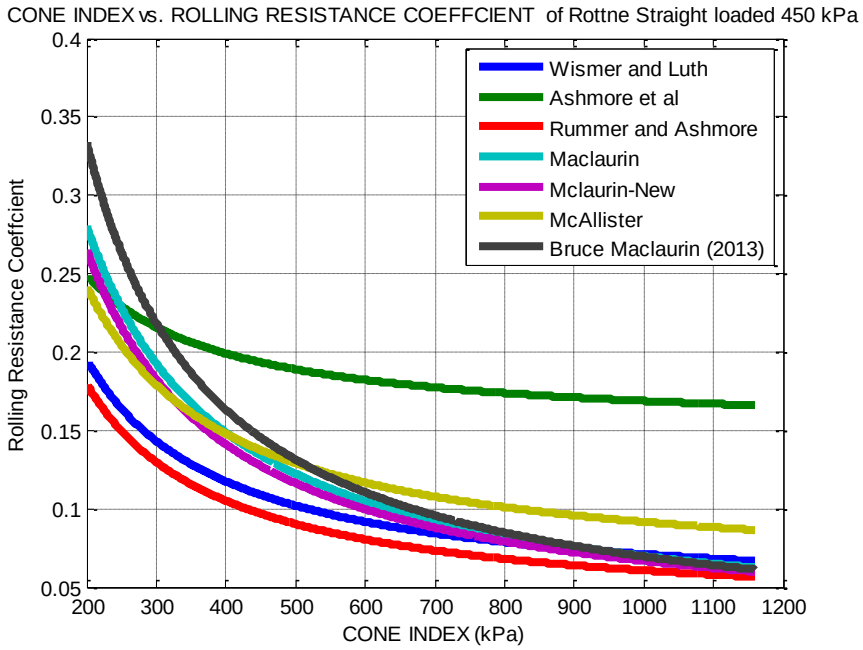

Figure 31 Rolling resistance coefficient

From Figure 31, it can be seen that models, Wismer and Luth, Bruce Maclaurin, Maclaurin New, McAllister and Maclaurin, gives same range of results in the cone index range 700 kPa to 1160 kPa. Wismer and Luth, Maclaurin New and Maclaurin models exhibit such a trend right from 200 kPa.

According to Saarilahti's report (Saarilahti, 2002), rolling resistance is inversely proportional to soil bearing capacity. A high value of rolling resistance coefficient indicates poor trafficability and mobility in the specific terrain. It is always advisable to have a rolling resistance coefficient below 0.2. Regarding the drawbar pull coefficient, it is recommended to

have a pull coefficient value above 0.25; too low values necessitate an increase in slip to produce more pull (Saarilahti, 2002).

It has to be noted that all the models used are empirical models that are developed under specific conditions with certain vehicle type and soil conditions. These models could be used for comparative purposes between different machines.

7.1 Change of soil density and cohesion due to multi-pass

After each wheel passes, the following wheels experience a new and more compacted soil. The change of soil density and cohesion due to multi-pass effect has been investigated and plotted as shown in Figure 32.

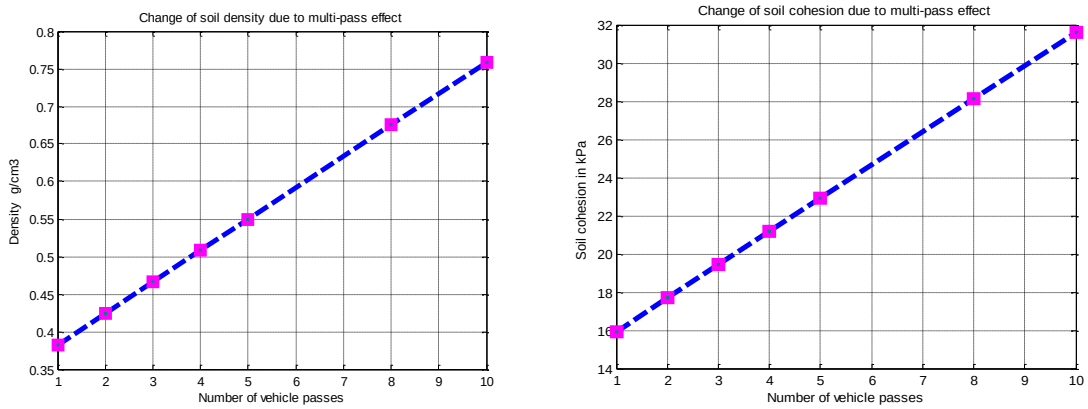

Figure 32 Change of soil density and soil-cohesion due to multipass

It is evident from Figure 32 that the soil density and cohesion values increases with multi pass. This increase in soil density implies an increase in soil compaction. Soil compaction data can be used to predict the impacts caused by the loads imposed by tires on soils; such an analysis can be used to estimate the degree of compaction due to vehicle pass. The soil density of peat soil used in calculations has been obtained from the work done by K.Berglund and Ö.Berglund (Berglund & Berglund, 2008).

$$\gamma_{sn} = \gamma_s \left[1 + \left(1 - e^{\frac{-s_0}{k_1}} \right) k_2 + k_3 n_p \right] \tag{25}$$

$$c_n = c \left[1 + \left(1 - e^{\frac{-s_0}{k_1}} \right) k_2 + k_3 n_p \right] \tag{26}$$

Where,

γ_{sn} = soil density after nth pass

γ_s = undisturbed soil density

s_0 = wheel slip

k_1, k_2, k_3 = fitting constants

n_p = number of wheel passes

c_n = soil cohesion after nth pass

c = soil cohesion of undisturbed soil

It has to be noted that the constants in the equation has been obtained by C.Sandu (Sandu & Senatore, 2011) through extrapolation of data from the tests done by Holm (Holm, 1969). In the test's conducted by Holm (Holm, 1969), tractor tires were tested in a soil bin filled with loam soil at different loads and inflation pressures and different axle configurations in various moisture settings. To estimate the accurate values of the constants, tests have to be done on the specified forest soil.

It will be good if we could connect density and cohesion with cone index; this approach will aid in connecting various terramechanics parameters only to cone index.

8 TESTING WITH ROOTS

Root's tested in laboratory are analyzed and various root reinforcement models are tested for its applicability. The effect of roots on rut depth is also looked up in this section.

8.1 Laboratory root test's

Roots play a vital role in stabilizing slopes by improving the shear resistance of soil; roots of trees and woody shrubs support slopes subjected to erosion or slippage. The number of roots, their directional distribution and their tensile strength affects the soil shear strength. Tensile strength is considered as the major contributor to soil shear resistance. The tensile strength also have a bearing on the plant anchorage; the roots in tensions offer approximately 60 % resistance to overturning due to a storm (Genet, et al., 2007).

It is interesting to note that the root strength is connected to factors like local environment, species, season and root diameter (Gray & Sotir, 1996). Lindström & Rune (1999) have found that the resistance to tensile failure of roots depend on the mode of planting; naturally regenerated pine had strogner roots when compared to planted pines. The time of the year also affects the root tensile strength; roots are stronger in winter than in summer due to decreased water content (Genet, et al., 2007). The experements carried out by Genet, et al., (2007) revelaed that the root tensile strength increase with a decrease in root diameter; the same work revealed the influence of cellulose content on root tensile strength.

Roots and small branches were obtained from Pine trees in the surroundings of the Machine design department at KTH Royal Institute of Technology, Stockholm. This was done to simulate the effect of tree roots in shear resistance. Root fibers increase the shear resistance of the soil by transferring the shear stresses developed in soil to tensile strength in the root fibers. The roots deform when shearing occur; as a result the fiber elongates and mobilizes the tensile strength.

The branches are similar in size to the tree roots; so it was also taken into consideration. Six sets of branches were obtained, two of them from a tree that is unidentified. The leaves/thorns in them were removed; it was ensured that too much bark was not removed. Pollen & Simon (2007) and Hudek, et al., (2010) mentioned that roots with bark will affect the shear resistance.

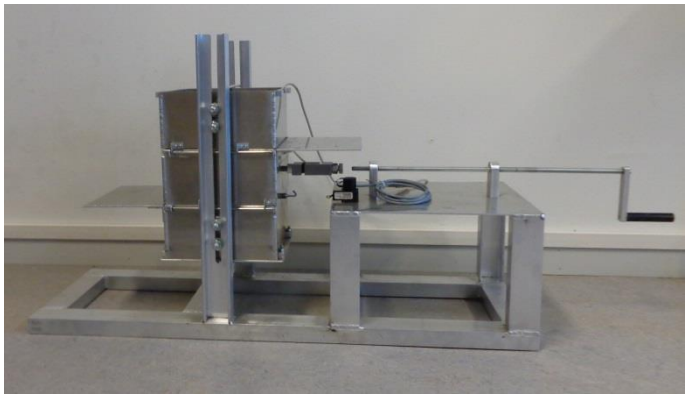

Figure 33 Root testing machine

Next, the shear test apparatus designed by Pirnazarov, et al.,(2013) as shown in Figure 33 were used to estimate the shear strength of the soil with various root and branch architecture and numbers. It was planned to test roots with two ends free, one end fixed other free and two ends fixed as well as horizontal and vertical arrangement, but due to time constraints roots with both ends free was only tested. The soil type is unidentified, it is assumed to be sandy loam; it was obtained from the premises of the machine design department at KTH. The figures of various root configurations in detail can be found in the Appendix B.

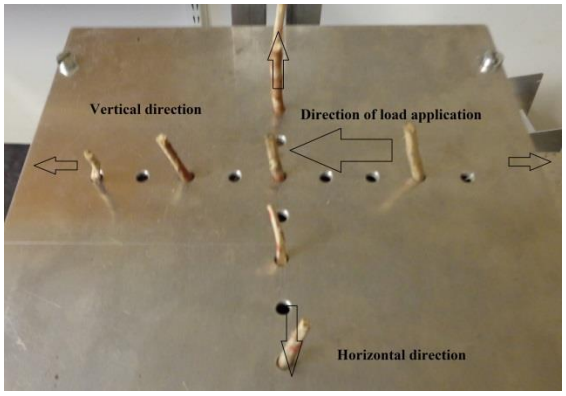

Figure 34 Root arrangement

Before testing the root systems, the friction force in the apparatus was estimated by testing it without load, and the average of the recorded frictional force was used further

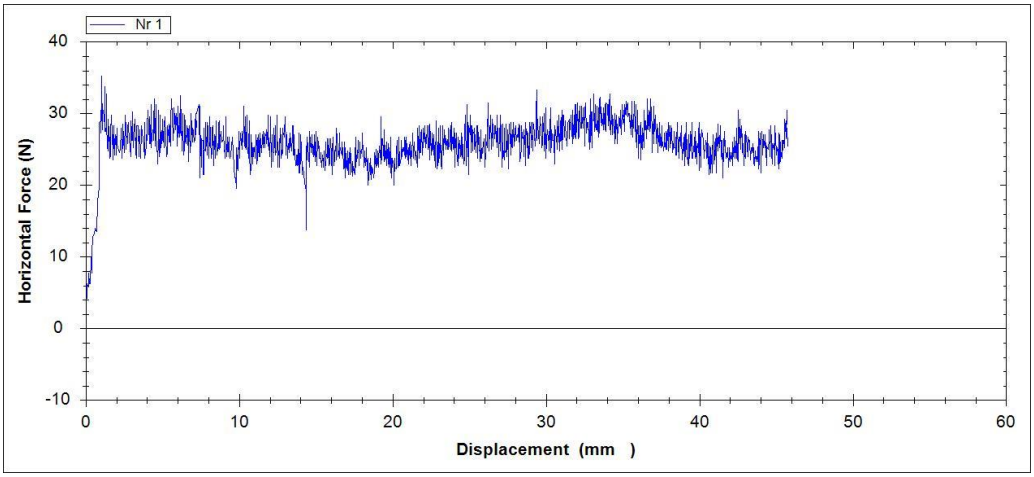

Figure 35 Frictional force on the test apparatus

First, the soil without roots was tested in in unidentified sandy soil. Initially, the root/branches was placed in the shear box apparatus designed by Pirnazarov, et al., (2013), next it was filled with soil and properly distributed. Proper connection with load cells that measure the shear force and horizontal displacement was ensured.

Tests were done four times for a particular configuration. After the first test, the soil condition is left as such, then the shear box was bought to the initial position and again load was applied, similar tests were done for three more times. More details about the test rig can be found in the works of Pirnazarov, et al., (2013).

It was observed that during the first pass, after a particular displacement of 15 mm, as shown in Figure 36, the shear force was linearly increasing, but not at a high rate as before, this is due to the loss of cohesion property after the particular displacement. During the rest of the test, the shear force values were less compared to the first pass. It can be inferred that, the first pass of the wheel experiences maximum shear resistance in the particular soil with such a root system.; such a concept is substantiated by the works of Holm, 1969., Abebe, et al., 1989 and Sandu & Senatore, 2011.

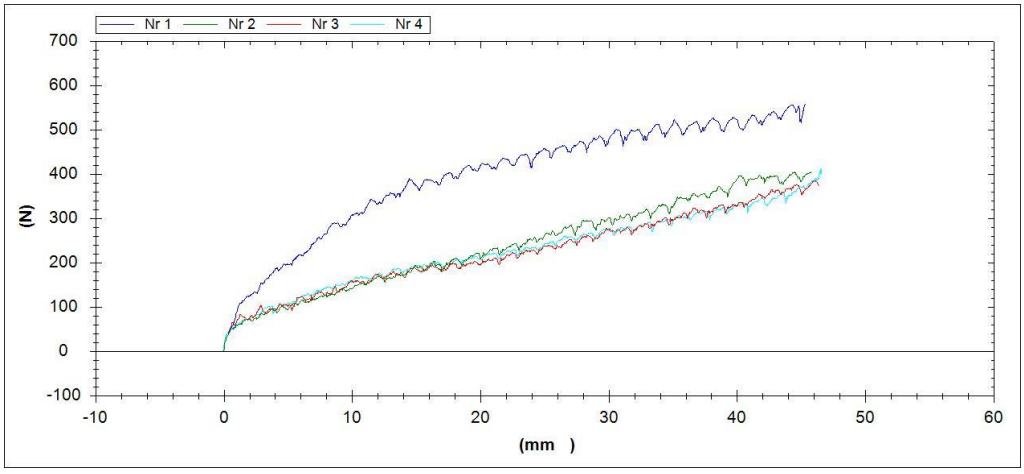

Figure 36 Shear resistance of the soil without roots/branches

Similar results were obtained for test's done with one branch with both ends free, here, the shear resistance was maximum for the first pass and it decreased for the consecutive passes.

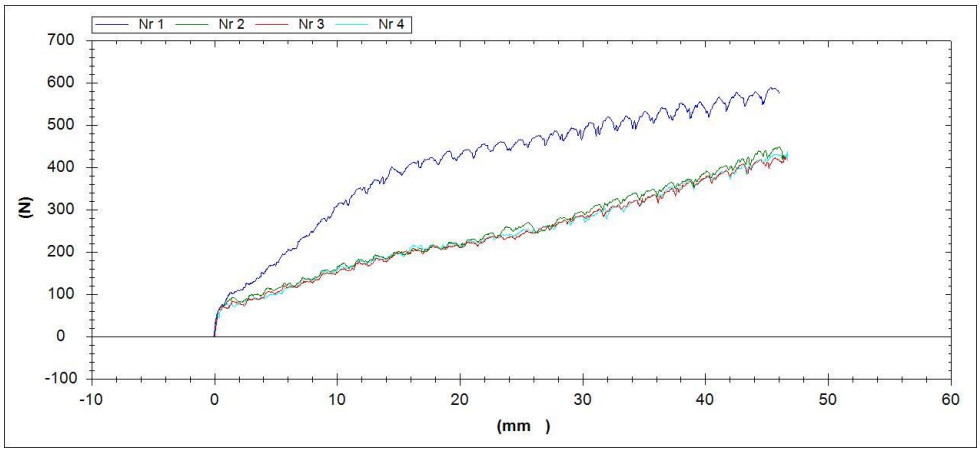

Figure 37 Shear resistance of soil with one branch

Next test were done for branches with both ends free, the number of branches used were 2, arranged horizontally. The shear force during the first go with two branches (or first test) was similar to the first test result as shown in Figure 37 of test with one branch, theoretically, when the number of roots increase the shear force must increase according to Equation 27, if the roots are identical, the shear force must be twice, which is not the case. This shows the variation between the theoretical and original test data, but it has to be noted that the equation is exclusively for roots.

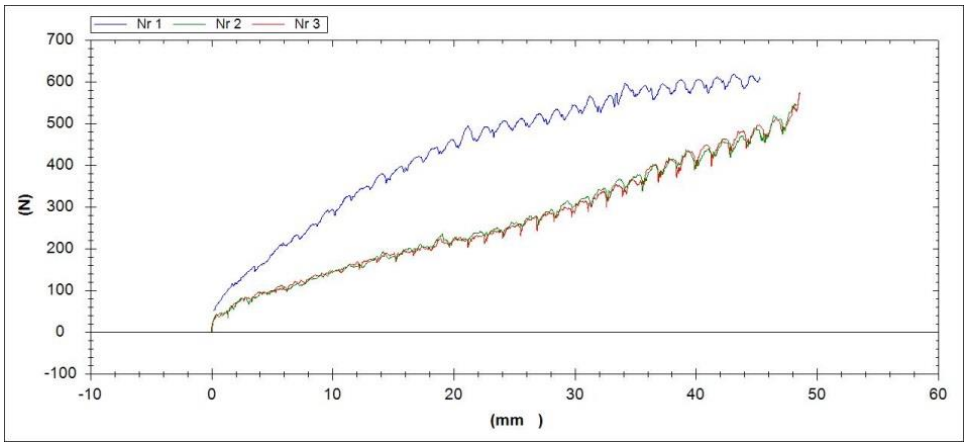

Figure 38 Shear resistances of 2 root branches in horizontal position

$$t_r = \sum\left(\frac{T_i n_i a_i}{A}\right) \tag{27}$$

Where,

t_r = mobilized tensile force of roots per unit area

T_i = ultimate tensile strength of roots

n_i = number of roots

a_i = mean cross sectional area of the roots

A = area of the shear plane

Next four branches were arranged in horizontal orientation, Figure 39 shows the results obtained; the first pass produced the maximum shear force, further passes produced low shear force values compared to the first pass.

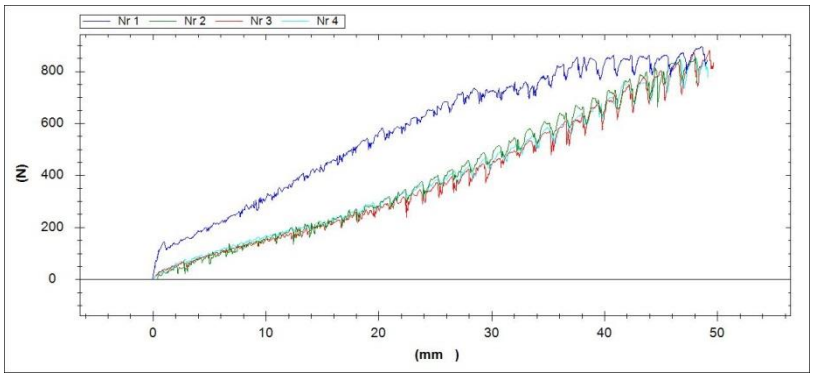

Figure 39 Shear resistances of 4 branches in horizontal position

The other set of tests include, arranging two roots in vertical direction with both ends free. The results were similar to normal test, wherein, the first test produced maximum shear force.

During the next test, where four roots were arranged in vertical direction with both ends free, the shear resistance of first pass was high compared to all other tests mentioned above. The possible explanation for this behavior is, the movable middle box had contact with the first root in vertical orientation, this root –tire interaction increased the shear force. When the tire is not in contact with the roots, that is, when the roots are at a certain depth below the soil tire interface, the shear resistance offered is not high as when they are in contact with the tire.

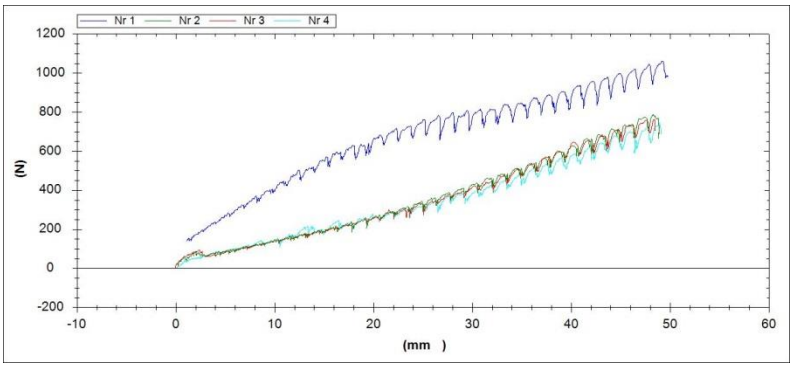

Figure 40 Test results with four branches in vertical orientation

A new series of test was done again; the soil cohesion and internal angle of soil friction was obtained with the available apparatus designed by Pirnazarov, et al., (2013), but the direct

shear test method was a crude one and did not follow the ASTM D3080 shear test standard. Here, fresh soil was obtained from the premises of KTH Machine design department, the soil type was not identified, but its texture represented the forest soil.

The data's of the experiments were saved and then it was used to compare with analytical models. The first test average shear force was compared to the ones calculated theoretically. All the calculations were done in Matlab

During the second series of test with new soil, one additional test was done for the 1st go of the machine to obtain more data values. When one root was tested in the new soil type, it displayed behavior that is completely different from what was seen in the previous tests. Here after a particular value of shear displacement, the shear force of the consecutive passes displayed a rise as shown in Figure 41.

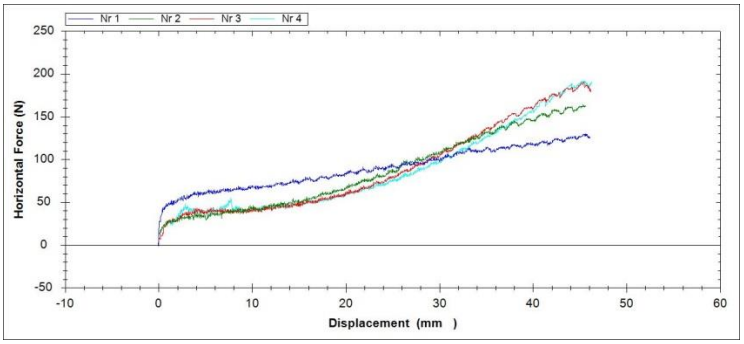

Figure 41 Test results with one root tested in new soil type

Similar results were obtained for tests with 2, 4 and 8 number of roots, for both vertical and horizontal orientation. It was observed that the maximum shear force from the new soil type is low compared to the sandy soil. Even with eight roots, the new soil shear resistance could not match the one offered by sandy textured soil. This shows the contribution from soil type and roots on the shear resistance.

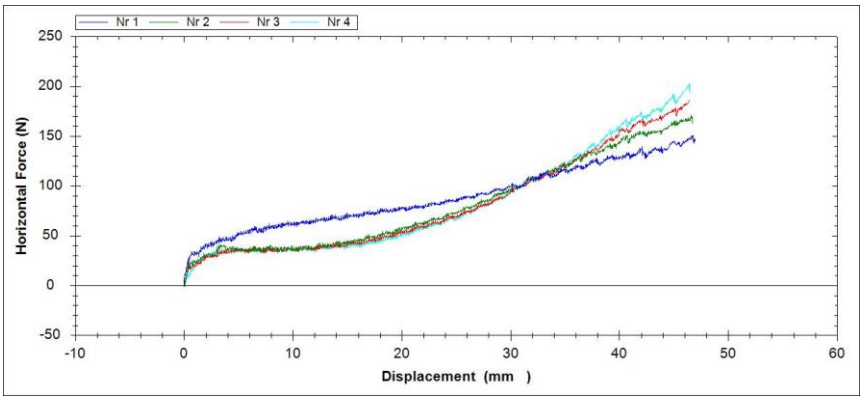

Figure 42 Results with 4 roots in horizontal position in new soil type

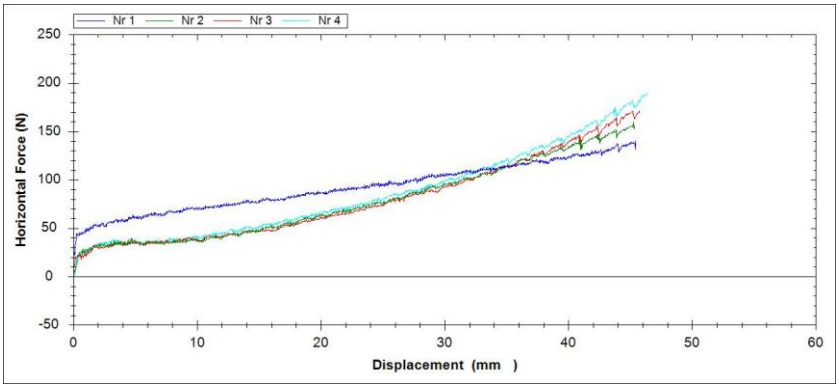

Figure 43 Results with 4 roots in vertical position in new soil type

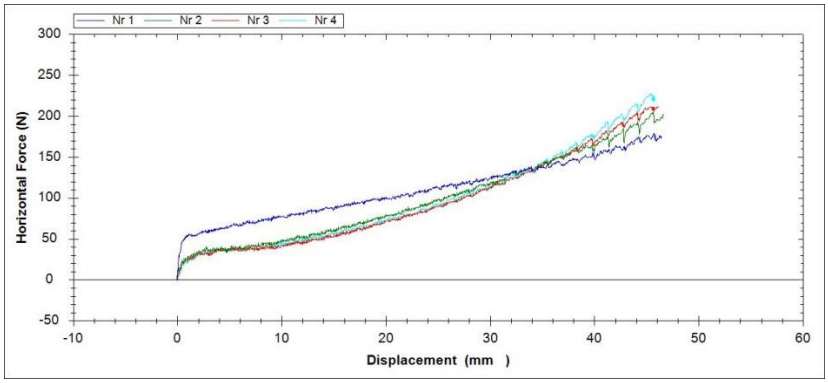

Figure 44 Results with 8 roots tested in new soil type

Also, a test was done to get an idea about the compaction the forest soil encounters, during loading. For this test, an aluminum plate was kept in the apparatus mentioned before and then filled with soil as usual. After that load was applied to estimate the resistance offered to compaction. From the test, it was observed that, after a particular displacement, a peak in resistance was observed as seen in Figure 45, this is assumed to be due to the aluminum plate interfering with soil particles and as a result offering high resistance; once that obstacle is overcame, the trend became normal. Otherwise, an almost linear rise in resistance is observed.

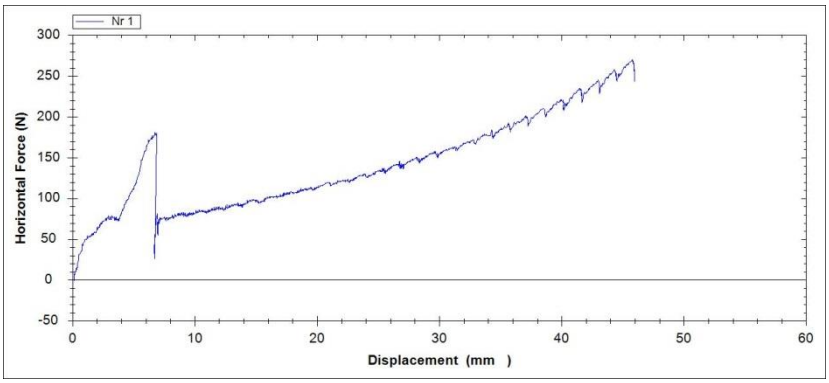

Figure 45 Compaction test results with aluminum plate

From Figure 46, it can be seen that when then number of roots are two, vertical arrangement offer more shear resistance, but when the number of roots are four, horizontal arrangement

offer more resistance. Also, when the arrangement is horizontal, four roots offer more resistance than 2 roots as seen in Figure 47. But when the arrangement is vertical, two roots offer more resistance than 4; it is evident from Figure 48. This demonstrates the complex behavior of soil-root interaction.

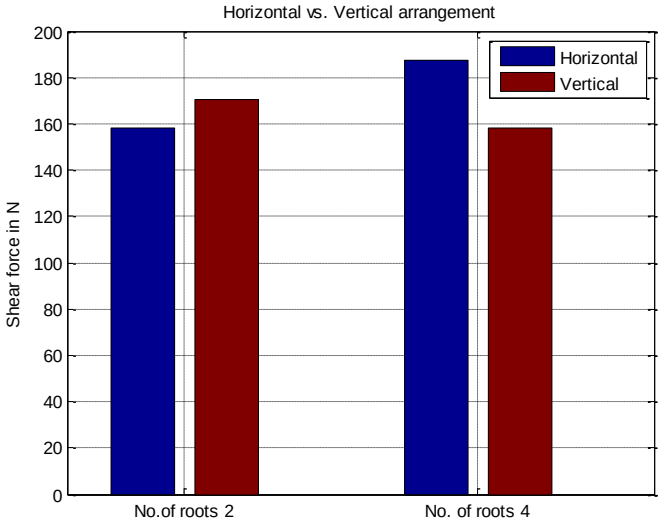

Figure 46 Root orientation comparisons

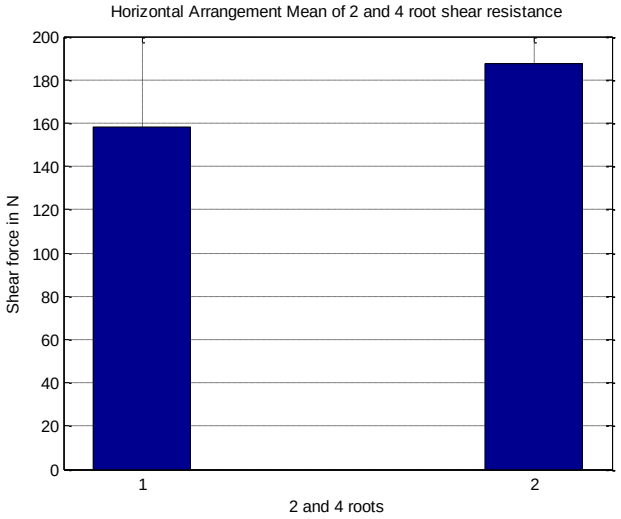

Figure 47 Horizontal arrangement shear strength comparison

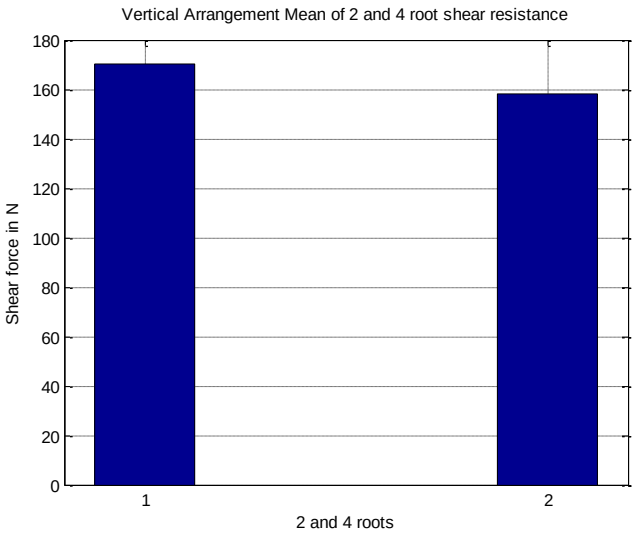

Figure 48 Vertical arrangement shear strength comparison

8.2 Root reinforcement analysis

The root reinforcement to the soil, as mentioned before, has been analyzed through lab tests. In this section, theoretical models available are utilized to estimate the reinforcement provided by roots to the soil. The models used include; perpendicular root model developed and tested by Wu (1976) and Waldron (1977), the model proposed by Abe & Ziemer, (1991) and the root stretch model developed by Gray & Barker (2013); these models are widely used to quantify the root reinforcement.

In the perpendicular root model, the shear stress is magnified by a horizontal element of the tensile stress (T_n), as shown in the Figure 49. This model assumes that the roots are well anchored and do not out when a tensile force is applied; this model is more suitable when the roots are in the 'fiber break mode' (Gray & Barker, 2013).

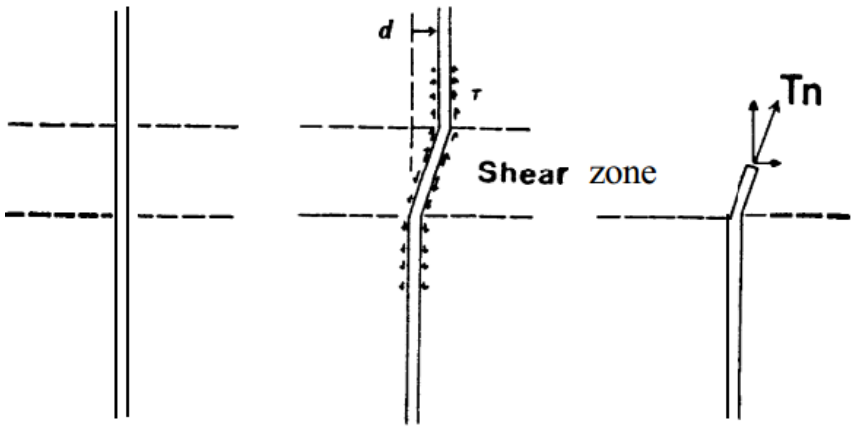

Figure 49 Perpendicular root reinforcement model

The total shear strength of the soil and roots can be calculated with the equation:

$$S_{sr} = c + \sigma \tan\phi + S_r \tag{28}$$

$$S_r = 1.2 T_r RAR \tag{29}$$

$$T_r = \alpha D^{-\beta} \tag{30}$$

Where,

S_{cr} = total shear strength of the soil and roots

c=soil cohesion value

σ = normal stress acting on the soil

ϕ =soil internal friction angle

S_r = increased shear resistance provided by the roots

T_r = Root tensile strength

RAR = Root area ratio

α, β = empirical value depending on species

Here two sets of α, β have been investigated, the first one, 23.40 and -0.87, proposed by Andre, et al., 2011 and 12.42 and -0.69, proposed by Hudek, et al., 2011.

As mentioned before, another model proposed by Abe & Ziemer, 1991 was also studied to assess the shear strength prediction capability. According to Abe & Ziemer, 1991, the extra reinforcement provided by roots come from its tensile stress and shear strength applied to a root by earth pressure. The model proposed by them is given as:

$$S_{sr} = c + \sigma \tan\phi + AS \tag{31}$$

$$AS = \left\{\left[\left(1 + B^2 b^2 e^{-2bx}\right)^{1/2} - 1\right] Ea_r\right\}\left(\cos\beta \tan\phi + \sin\beta\right) + EIb^3 B \tag{32}$$

Where,

AS= reinforcement provided by roots in Pa

B= one half of shear displacement in m

b= best fitting parameter

x= half length of the root in m

E=Young's modulus of the root in Pa

a_r = cross sectional area of the root in m^2

I= section modulus of the root in m^3

β = $\tan^{-1}$(Bb)

In the experiments carried out, it was noticed that the roots didn't break after the test. So, it is more feasible to apply the 'fiber stretch mode' analysis to estimate the reinforcement provided by the roots. The mobilized tensile strength will depend on the amount of fiber elongation and fiber tensile modulus when the fiber lacks enough elongation and strain compatibility issues forestall mobilization of root tensile strength (Gray & Barker, 2013). The extra reinforcement provided by roots to the shear strength of soil is given by Equation 33:

$$\Delta S = k\beta\left(\frac{A_R}{A}\right)\left[\sin\theta + \cos\theta.\tan\phi\right] \tag{33}$$

$$k = \sqrt{\frac{4z\tau_b E_R}{D}} \tag{34}$$

$$\beta = \sqrt{\sec\theta - 1} \tag{35}$$

$$\tau_b = h\gamma\left(1 - \sin\phi\right) f \tan\phi \tag{36}$$

$$\theta = \tan^{-1}(\frac{x}{z}) \quad (37)$$

Where,

ΔS = extra reinforcement provided by roots

A_R = cross sectional area of root

A = cross sectional area of the soil profile

θ = angle of shear distortion

x = shear displacement of roots

z = shear zone thickness

h = depth below the ground surface

γ = soil density

f = coefficient of friction between soil and roots

ϕ = internal friction angle of the soil

D = root diameter

E_R = fiber tensile modulus

The results of analysis to estimate the shear strength of soil with roots using the perpendicular root model and model proposed by Abe & Ziemer (1991) and the 'fiber stretch mode' with cohesion and friction angle value obtained from tests did not yield realistic results as seen in Appendix E; it was expected that the perpendicular model would not give proper results as the roots did not break. **Table 13** compares the result obtained using the root stretch mode analysis and the test data. Analysis for 1 root (1R), 2 root horizontal(2R_H) , 2 root vertical (2R_V) , 4 root horizontal (4R_H) , 4 root vertical (4R_V) and 8 roots (8R) arranged in vertical and horizontal orientation has been done.

It can be seen from **Table 13** that the root stretch model provides results that are similar to the test data, even though not accurate. The fiber tensile modulus was for general pine roots and not for the exact species; the value varies for each species in the pine family. The shear displacement of roots used was also an assumed one; the actual value was not measured. The coefficient of friction used was a general value obtained from (Gray & Barker, (2013). It is believed that these reasons caused a variation between the results.

The perpendicular model overestimates the reinforcement; it is mainly due to the assumption that the full tensile strength will be mobilized when soil shears and all the roots break simultaneously (Wu, 1976). This case of over estimation has been reported by Waldron & Dakessian, 1981 as well as Pollen & Simon, 2007. Pollen & Simon (2005) and Docker & Hubble (2008) noticed that the overestimation depends from species to species. Also it can been seen from the above table the model cannot distinguish between horizontal and vertical

orientation, as it gives the same value for both the cases of 2 roots and 4 roots in horizontal and vertical arrangement.

New cohesion and friction angle values were obtained by doing tests in the available machine as mentioned before, friction angle was estimated to be 48.79 degrees and cohesion was 1134 Pa. With the new cohesion and internal friction angle calculations were done, but it yielded results similar to the one obtained using the one retrieved from Wong's (Wong, 2010) literature. It has to be noted that the method employed to obtain the cohesion and internal friction angle did not follow the shear testing standard; but it was adopted to get an idea about where the values would lie.

Table 13 Shear strength of soil with roots in kPa: Test data vs. root reinforcement models

Arrangement	1R	2R_H	4R_H	2R_V	4R_V	8R
Test	0.8	1.9	2.8	2.12	2.72	1.10
Root-stretch	1.891	1.892	1.901	1.892	1.907	1.905
Abe & Ziemer	8.9	1.3	21.8	11.3	21.8	NA

In the perpendicualr model, the value of cohesion and friction angle significantly influences the results.So when the model is used in situations where the roots break, it should be ensured that the cohesiona dn friction angle values used should be obtained from laboratory tests.

Abe and Ziemer equation was used, but 'b', value obtained through equation proposed Abe & Ziemer, (1991) didn't yield realistic results, so the values obtained from the tests by Abe & Ziemer, (1991) was used. The same value has been used for all the root diameters, even though the value changes according to the empirical equation proposed in the literature.

From the analysis it was found that, the test data results and analytical results didn't match well. The value of cohesion and internal friction angle of the soil was not known accurately. It was noticed that the when the value of cohesion and friction angle was changed, it affected the test results significantly. Also it can been seen from the above table the model cannot distinguish between horizontal and vertical orientation, as it gives the same value for both the cases of 2 roots and 4 roots in horizontal and vertical arrangement.

But it is evident that the Root stretch mode provides results that are more realistic and comparabe with the test data as compared to the Abe and Ziemer model. It can therefore be conluded that the root stretch model provides good estimate when the root does not break. As a suggestion, it is prescribed to do more test with roots and obtain a coeffcient describing the diffrence between the two orientations and apply it to a thoeretical model that could predict the results well.

8.3 Rut depth comparison with and without roots

The rut depth produced by one vehicle pass of Rottne loaded with 450 kPa estimated from various WES models has been compared with the rut depth estimated by the same WES models when root reinforcement also comes into effect. The constants used in all the WES models are obtained from non-linear regression analysis as mentioned in section 4.3.1.

In this method, new cone index when roots are present has been obtained, and this value has been applied in the WES models to estimate the rut depth with roots. As expected all the models returned low value of rut depth when roots are taken into account. The WES models used includes the ones proposed by, Maclaurin, Antilla, Saarilahti and Rantala.

The root present was assumed to be of Casuarina glauca and the corresponding extra reinforcement provided by roots has been estimated from:

$$\Delta S = 61.16 \times RAR - 0.90 \tag{38}$$

Where,

ΔS = extra reinforcement by roots

RAR = root area ratio

The resistive force acting on a penetrating cone can be obtained from Equation 39 (Baladi & Rohani, 1981) and Figure 50.

$$F_Z = \int_0^L (\sigma \tan\phi + \tau) 2\Pi \eta \tan\alpha \, d\eta \tag{39}$$

$$CI = \frac{4F_Z}{\Pi D^2} \tag{40}$$

Where,

F_z =cone resistive force

σ = normal stress

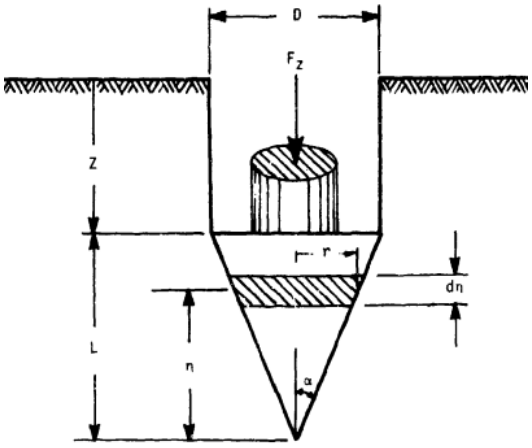

Figure 50 Cone penetrometer

The existing value of τ without roots was obtained, then the extra reinforcement due to roots was added and the new Cone index was obtained. This value of cone index was used in estimating the rut depth wit roots. The result of the analysis is shown in Figure 51, x-axis implies various WES models.

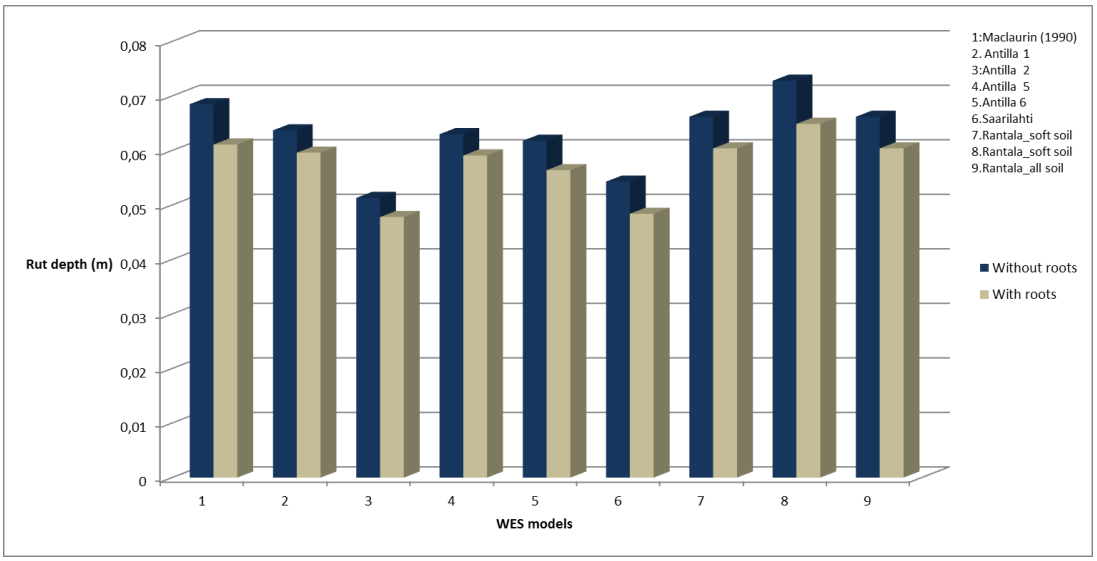

Figure 51 Rut depths with and without roots

8.4 Analysis of test data from lab root test

The test data from the lab test of the soil, newly collected, with roots have been analyzed. In the light of non-compatibility of available root reinforcement models, curve fitting approach with least squares method has been adopted to derive empirical equations for the corresponding tests. The results of the test data has been presented in Figure 52. A linear equation has been derived.

$$y = a + bx \tag{41}$$

Where,

y= shear resistance in N

x= displacement

a and b = empirical constants

Table 14 Coefficients of the empirical relation

Configuration	a	b	R^2 (%)
1 root	84.6	25.5	92
2 root horizontal	279.6	4.34	95
4 root horizontal	17.98	8.5	99
2 root vertical	343.8	4.34	86
4 root vertical	406	5.83	90
8 roots	127.2	2.761	75

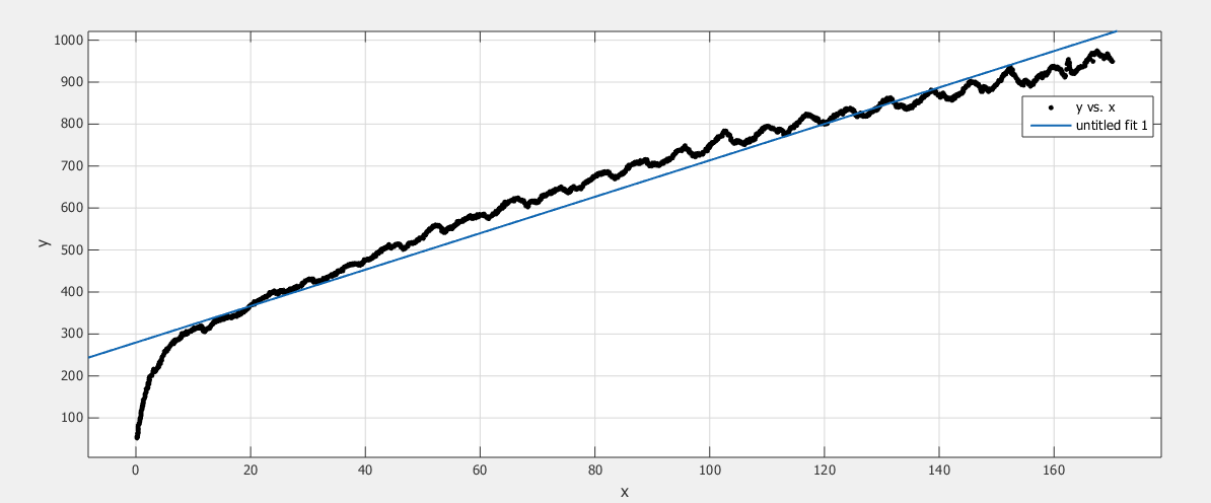

Figure 52 Diagram depicting the displacement vs. shear resistance of 2- root horizontal arrangement

8.5 Modelling roots as circular plate under elastic foundation and as plate under semi-infinite solid.

The roots systems due to its large density, is modelled as a circular plate under elastic foundation. In an ideal case the tire soil contact area can be assumed as circular, this is taken care by assuming roots as circular plate under an elastic foundation of soil.

Another modelling approach that was followed was modelling roots as rectangular plate under semi-infinite solid. Also, roots are considered as rectangular plate under a semi-infinite solid of soil.

Maximum deflection for circular plate under elastic foundation is given by Equation 42 (Timoshenko & Krieger, 1959).

(42)

$$w_{\max} = \frac{Pl^2}{8D} \tag{43}$$

$$l = \left(\frac{D}{k}\right)^{\frac{1}{4}} \tag{44}$$

$$D = \frac{Eh^3}{12(1-\nu^2)} \tag{45}$$

Where,

E = Young's modulus of pine root

ν = Poisson's ratio of pine root

k = modulus of subgrade reaction

Maximum deflection under semi-infinite solid:

$$D = \frac{Eh^3}{12(1-\nu^2)} \tag{46}$$

$$w_{\max} = \frac{0.192Pl_0^{\,2}}{D} \tag{47}$$

$$l_0 = \left(\frac{D}{k}\right)^{\frac{1}{4}}\left(\frac{1}{1.24}\right) \tag{48}$$

The rut depth due to various loads when roots are present in the above configuration is shown in Figure 53. The maximum deflection of the center part of the plates is considered as the maximum rut depth that could be produced when a wheel passes over such a material.

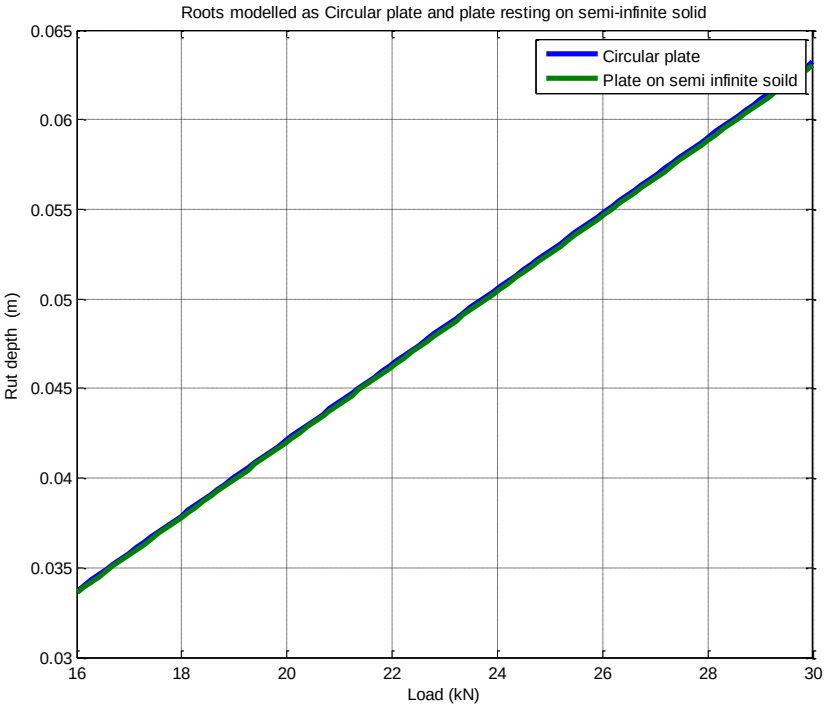

Figure 53 Load vs. Rut depth

It can be seen from the figure that, there is not much difference in the rut depth predicted by the two root configuration. More studies into the root configurations needs to be carried out to find a good model to simulate the effects of root or how roots can be modelled; FEM can be employed to delve more into studying the effects when roots are modelled as circular plate under elastic foundation and as plate under semi-infinite solid. Phenomenon's like cracking and sliding of roots can be studied with the help of DEM.

9 Slip Sinkage Effect

The effect of slip on the sinkage is dealt in this chapter. Sinkage at various slip levels has been studied here.

The increase in sinkage and motion resistance due to slip if referred as slip-sinkage effect. The influence slip-sinkage effect on vehicle sinkage and motion resistance is gaining momentum; before, much publication did not take into account this effect (Lyasko, 2009). Slip sinkage effect on wheel sinkage due to a single wheel has been studied here; the work of Lyasko (Lyasko, 2009) is the main inspiration. The necessity of predicting the accurate value of sinkage has been highlighted in the work of Lyasko (Lyasko, 2009). Works of Lyasko shows that for slip range from 0 to 33 % the sinkage increase monotonically and for 33% slip the increase is about 60%.

Lyasko, found the analytical Equation 49, between the sinkage and the slip of the wheel.

$$z = K_{SS} z_0 \tag{49}$$

$$K_{SS} = \frac{1+i}{1-0.5i} \tag{50}$$

Where,

z = sinkage due to slip

z_0 = static sinkage

i = slip

In the original work, Lyasko (2009), the static sinkage of the wheel has been obtained using the Nernstein-Goriatchkin equation with the help of test data, the detailed method can be found in Lyasko, 2009.

Here, in the thesis, the slip and sinkage affecting one wheel on the first axle is taken into account. Because, as mentioned by Abebe, et al., 1989 and Sandu & Senatore 2011, passes one to three of a single wheel produces the maximum sinkage or rut depth.

WES based approach and Bekker based approach has been tried on the slip sinkage effect. On analysis of both the models with respect to slip sinkage, it has been found that the sinkage increases as slip increases. But both models gave almost the same results for sinkage values as seen in Figure 54. Such an approach can be used to estimate the intesity of sinkage due to slippage and fine tune the slip values. It will be good to do a real field test to evaluate which model gives results that are same as tets results, to be more precise with the models.

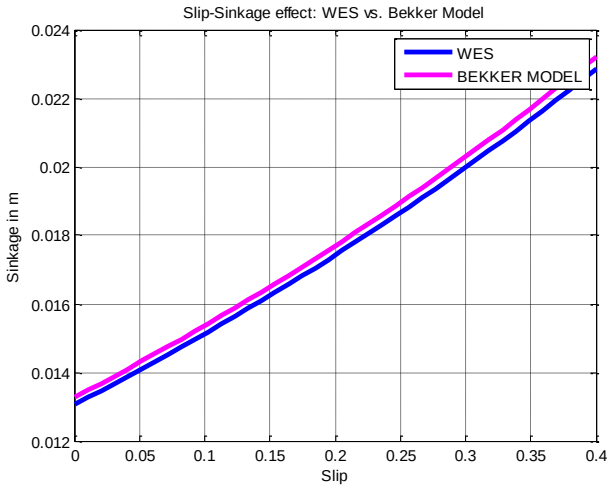

Figure 54 Slip-Sinkage effect

The static sinkage has been obtained using WES and Bekker based equation as described below.

$$z_0 = d\left(\frac{0.224}{N_{CI}^{1.25}}\right) \tag{51}$$

Bekker model:

$$z_0 = \begin{Bmatrix} \left(\frac{p_w}{k_c/l_t + k_\phi}\right)^{1/n} (if = l_t < b) \\ \left(\frac{p_w}{k_c/\mathrm{b} + k_\phi}\right)^{1/n} (if = l_t \geq b) \end{Bmatrix} \tag{52}$$

$$l_t = \left(\frac{D}{k}\right)^{\frac{1}{4}}\left(\frac{1}{1.24}\right) \tag{53}$$

Where,

p_w = wheel pressure

l_t = length of wheel flat section

b = wheel width

δ_t = wheel deflection

9.1 Estimating rut depth based on single wheel test

Another approach that has been tried is to utilize the result from a single wheel test and utilize it for multi-pass rut depth prediction; the analysis was carried out for Komatsu and the results were compared to test data.

Here, the maximum load acting on any wheel of the vehicle is taken into account, and then this load is applied into Maclaurin (1990) WES model by taking into account the slip acting on that wheel. The importance of slip-sinkage is explained in the above section, and it simulates the real tire-soil interaction situation.

The wheel with maximum load acting will produce the highest sinkage in static condition, and this sinkage can be taken as a yardstick to evaluate various vehicles. Here, the result of such an analysis for the entire vehicle configuration, as described in **Table 2**, has been done. The results of which are shown in Figure 55, except for S-shaped curves, the results are fairly matching to the test data.

To evaluate the model's validity further, the same analysis has been applied to S curves also, but with the difference that the rut depth values at the straight portion was only taken into account and compared to WES models as seen in Figure 56. It can therefore be seen from the results that the new approach could predict the rut depth with reasonably good accuracy.

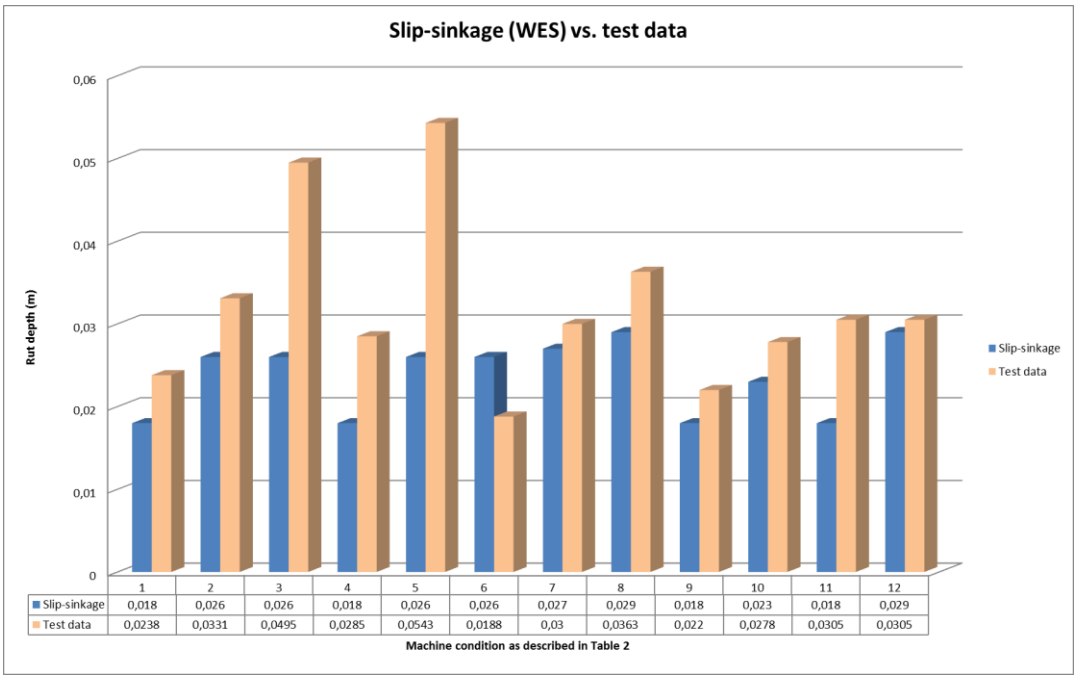

	1	2	3	4	5	6	7	8	9	10	11	12
Slip-sinkage	0,018	0,026	0,026	0,018	0,026	0,026	0,027	0,029	0,018	0,023	0,018	0,029
Test data	0,0238	0,0331	0,0495	0,0285	0,0543	0,0188	0,03	0,0363	0,022	0,0278	0,0305	0,0305

Figure 55 Calculated rut depths vs. Test data (conditions 4, 5 11 and 12 are S-shaped tracks)

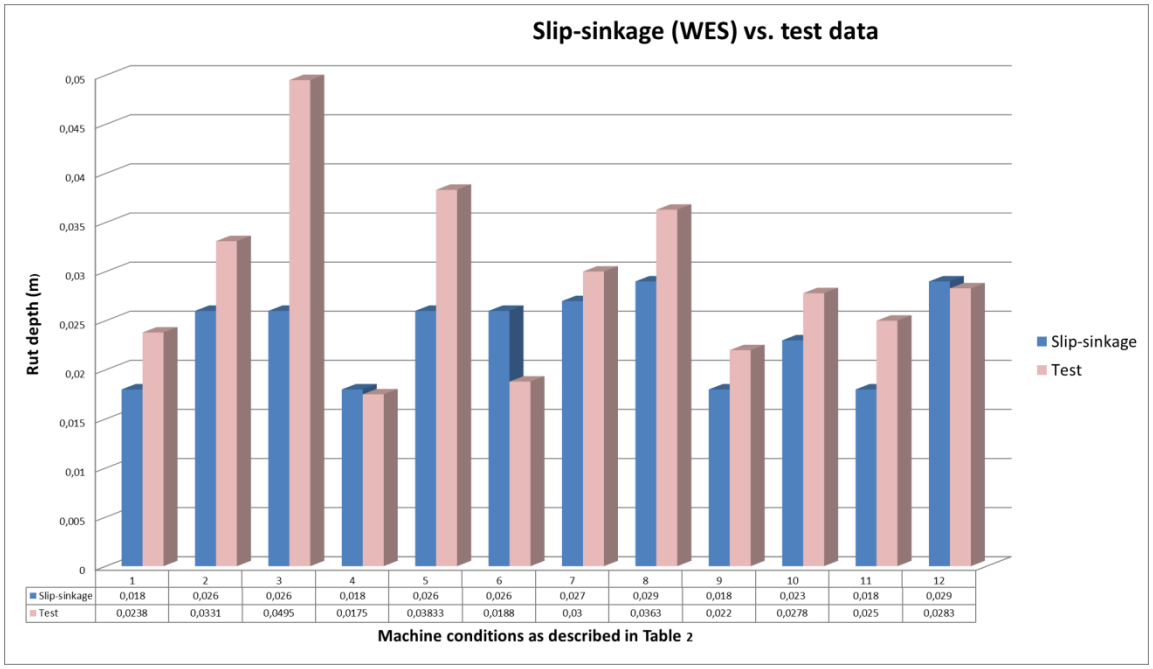

Figure 56 Calculated rut depth vs Test data (straight line portion of S-curve considered)

10 Co-relating WES and Bevameter models

A small step towards co-relating WES and Bekker based models has been carried out here. A new set of equations has been derived and available relations are also evaluated in this section.

Both the WES and Bevameter models, as explained before, have different input variables. For Nordic forests, it has been proposed by Saarilahti, that WES models could provide suitable results. The multibody simulation software MSC Adams uses Bekker based Bevameter approach to solve tire - soft soil interaction analysis. Also, many studies have been done with the aid of Bevameter data's. But the number of variables in the Bekker based model is many, when compared to WES models.

In this section, a study to co-relate both WES and Bekker based model is carried out. Two models have been derived to connect Cone index and Bekker constants. The models proposed below is applicable for a single wheel for one pass, as the 1st pass produce the maximum impact to the ground or rut depth.

The first model, it is applicable to sandy silt soils, the parameter 'n', dimensionless exponent of load-sinkage curve, is taken as one. At the end of the analysis, it has been verified that the estimated Bekker's cohesive and friction moduli of soil deformation of load-sinkage curve, $k_c$and k_φ, from the cone index value gives back the same value on 'n'. The explanation is given below:

According to Kalugin and Poletaev (Lyasko, 2010), the sinkage of the first wheel is:

$$z_1 = \left[\frac{3W}{2Bk_\phi \sqrt{D}} \right]^{\frac{2}{3}} \tag{54}$$

Rearranging Equation 54

$$k_\phi = \frac{3W}{(2B\sqrt{D})\,z_1^{1.6}} \tag{55}$$

Equation 56 gives the WES based sinkage model which can be applied to Equation 55, this will result in connecting k_ϕ with cone index.

$$z_1 = 0.010 + \frac{0.610}{N_{CI}} \tag{56}$$

According to Garbari (Lyasko, 2010), the motion resistance of the first wheel is given by:

$$MR = \frac{kBz_1^{\,2}}{2} \tag{57}$$

Motion resistance can also be written as:

$$MR = \mu_R W \tag{58}$$

The motion resistance coefficient can be expressed in terms of Cone index as proposed by Ashmore et al (1987), also the sinkage can be calculated using the relation proposed by Rantala (2001) as given by Equation 56. Equation 59 express motion resistance in terms of wheel numeric N_{CC}.

$$\mu_R = \left(0.380 - 0.50\right)\left(\frac{W}{W_r}\right) + \frac{0.21}{N_{CC}} + 0.21 \tag{59}$$

$$N_{CC} = \frac{CIbd}{W}\sqrt{\frac{\delta}{h}} \tag{60}$$

Equating Equation 57 and Equation 58, and on rearranging gives Equation (61);

$$\therefore k = \frac{2\mu_R W}{Bz_1^{\,2}} \tag{61}$$

Where, μ_R is a function of cone index as seen from Equation (59) :

Also,

$$k = \frac{k_c}{B} + k_\phi \tag{62}$$

$$\therefore k_c = \left(k - k_\varphi\right)B \tag{63}$$

And finally, applying Equation 55 and Equation 61 into Equation 63 results in connecting k_c with cone index. In a nutshell, the relations can be described as shown below:

$$n = 1 \tag{64}$$

$$k_\phi = \frac{3W}{2B\sqrt{D}z_1^{\,1.6}} \tag{65}$$

$$k_c = \left(\frac{3W}{2B\sqrt{D} z_1^{1.6}} - \frac{2\mu_R W}{B z_1^{2}} \right) B \tag{66}$$

In the second model, an empirical model connecting k_c and k_φ, has been obtained. Then the equation connecting Cone index and k_φ obtained from the previous model has been used. By combining both the models, the value of k_c, has been obtained. This model is applicable to all soils, but, it has to be noted that this model is an empirical model and can be applied to soil conditions at Tierp, where the data's were obtained, but not extrapolated to other conditions.

The empirical relation connecting k_c and k_φ, is:

$$k_c = \left(7.6 \times 10^{-5}\right) k_\phi^{\,2} - \left(0.032\right) k_\phi + 122.6 \tag{67}$$

From the Equation 55, we know;

$$k_\phi = \frac{3W}{(2B\sqrt{D})\, z_1^{1.6}} \tag{68}$$

The value of 'n' is estimated using the equation:

$$z = \left[\frac{3W}{(3-n)(k_c + Bk_\phi)\sqrt{D}} \right]^{\frac{2}{2n+1}} \tag{69}$$

It has to be noted the equations so derived, from both the models, have not been verified. It is highly suggested to tests with soils to determine the capability of the equation. A specified amount of load has to be applied in single wheel tester and simulate a single wheel pass. Specified sample of soil has to be collected, and its cone index has to me measured. The same sample of soil has to undergo a Bevameter test to determine the Bekker constants. After that all the values obtained should be used to evaluate the equations.

Another approach done to co-relate both WES and Bekker models were to compare the ratio of rut depths given by WES and Bekker models. Two approaches were invested as part this procedure.

In the first approach, the equation connecting Cone index to Bekker parameters, as proposed by Bekker (Bekker, 1969), was used to estimate the Cone index value for various Bekker parameter values. The Bekker parameter values for Upland sandy loam soil was used, the values were fetched from Wong's literature (Wong, 2010). Then sinkage value for a single wheel was estimated using Bekker's equation. With the calculated Cone index values, sinkage for the wheel was calculated with WES based models. Here, the soil parameter only changes, not the load acting on the wheel. The results of the analysis are shown in Figure 58. The relation connecting Cone index to Bekker model is given by the Equation 70..

$$CI = 1.625\left(\frac{k_c}{(n+1)}\left((z+1.5)^{n+1} - z^{n+1}\right) + 0.517k_\phi\left(\frac{(z+1.5)^{n+2}}{(n+1)(n+2)} + \frac{z^{n+2}}{n+2} - \frac{(z+1.5)z^{n+1}}{n+1}\right)\right) \quad (70)$$

Various values of moduli of soil deformation and sinkage exponent for Upland sandy loam has been used as shown in the Figure 57.

Terrain type	Constants for Bekker's equation			Constants for Reece's equation			Goodness-of-fit %	Wet density (kg/m³)	Moisture content %
	n	k_c (kN/m^{n+1})	k_ϕ (kN/m^{n+2})	n	k_c'' (kN/m^2)	k_ϕ'' (kN/m^3)			
LETE sand	0.705	6.94	505.8	0.705	39.1	779.8	95.3	~1600	
	0.611	1.16	475.0	0.611	28.2	1066	94.5		
	0.804	3.93	599.5	0.804	16.9	879.6	93.8		
	0.728		1348	0.728	18.3	2393	88.8		
	0.578	9.08	2166	0.578	197	4365	89.2		
	0.781	47.8	6076	0.781	229.7	8940	89.8		
	0.806	155.9	4526	0.806	413.5	5420	88.1		
Upland sandy loam	1.10	74.6	2080	1.10	42.0	1833	87.7	1557	51.6
	0.97	65.5	1418	0.97	77.4	1464	92.0	1542	49.2
	1.00	5.7	2293	1.00	5.3	2283	94.8	1570	49.1
	0.74	26.8	1522	0.74	121.7	2092	95.1	1519	44.3
	1.74	259.0	1643	1.74	−0·9	763	86.0	1696	50.0
	0.85	3.3	2529	0.85	42.4	3270	87.5	1471	28.6
	0.72	59.1	1856	0.72	231.4	2323	84.2	1592	34.3
	0.77	58.4	2761	0.77	214.1	3626	86.6	1559	35.1
	1.09	24.9	3573	1.09	6.7	2982	91.9	1716	31.2
	0.70	70.6	1426	0.70	279.3	1317	94.3	1470	27.3
	0.75	55.7	2464	0.75	213.6	3244	89.4	1526	32.6
Rubicon sandy loam	0.66	6.9	752	0.66	63.3	1176	92.6	1561	43.3
	0.65	10.5	880	0.65	88.2	1358	97.0	1588	44.2
North Gower clayey loam	0.73	41.6	2471	0.73	121.2	−4.2	88.8	1681	45.8
	0.85	6.8	1134	0.85	27.0	1430	90.0	1597	52.0
Grenville loam	1.01	0.06	5880	1.01	−1.3	5814	87.4	1326	24.1
	1.02	66.0	4486	1.02	55.3	4292	89.1	1339	18.2

Figure 57 Bekker parameters for various soils

The WES model used for evaluating is the one proposed by McLaurin, Rantala and Gee-Glough. The results of which are shown in Figure 58, the x axis shows the various soil conditions described by Bekker parameters. It can be seen that only the Gee-Glough model provides a ratio that is almost near to one, but as it does not experience a trend in the graph, it is hard to find a constant that connects both the models.

The WES equations used are:

Maclaurin:

$$z = d\left(\frac{0.224}{N_{CI}^{1.25}}\right) \quad (71)$$

Rantala's (2001) equations for soft soils and all soils:

$$z = d\left(\frac{0.224}{N_{CI}^{1.25}}\right) \quad (72)$$

$$z = 0.059 + \frac{0.490}{N_{CI}} \tag{73}$$

$$z = \frac{0.989}{N_{CI}^{1.23}} \tag{74}$$

Gee-Glough's:

$$z = \frac{\mu_R d}{\left(0.63 + 0.34\frac{b}{b}\right)^2} \tag{75}$$

$$\mu_R = \frac{0.287}{N_{CI}}$$

Where

z= sinkage in m

μ_R = rolling resistance coefficient

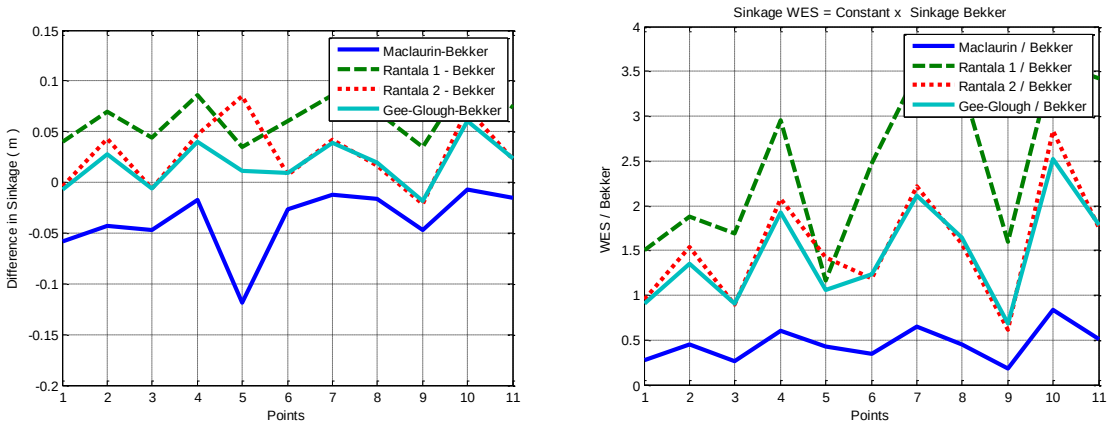

Figure 58 Correlating WES and Bekker model at different soil conditions

In the second approach, the ratio of sinkage calculated from WES and Bekker models for various load conditions were calculated. Here, the values of Bekker parameters used were obtained from the Bevameter tests carried at Tierp, the Cone index values were also obtained from test done at Tierp.

The results of the above mentioned analysis is shown in Figure 59, the x axis shows the various load conditions. Here also, it was hard to find a model that was equal or almost near to one.

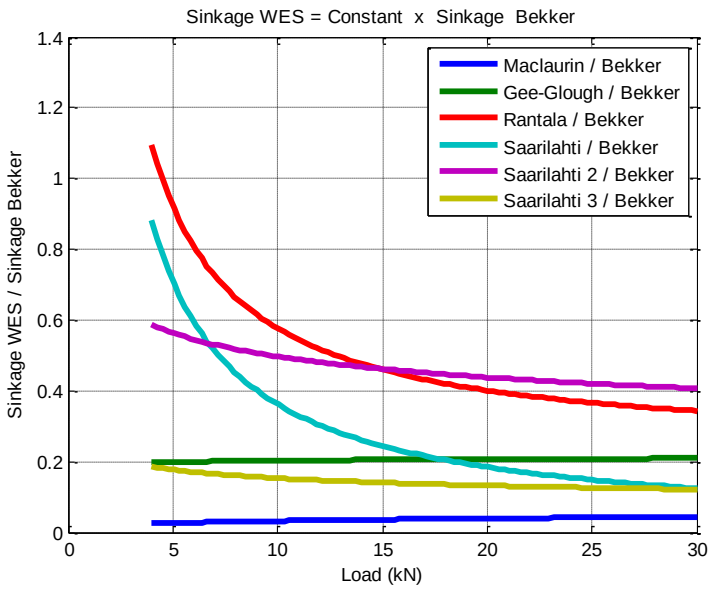

Figure 59 Correlating WES and Bekker model at different load conditions

11 ADAMS Multi-body Simulation

MSC Adams software has been used to simulate a full-scale forwarder models to see its effectiveness in predicting rut depths. Single wheel tests have also been carried out to estimate the effect of tire inflation pressure and velocity on rut depths.

As part of the master thesis work, MSC Adams is used to simulate the effect of multi-pass of the forwarder. Adams has a module called Soft-Soil tire model; this module can be used to simulate the interaction between tires and elastic/plastic grounds like sand, clay, snow and loam .This model uses a tire property file and a road data file with soil properties. Adams offer two types of tire soil contact models:

- Elastic-plastic soil deformation model
- Visco-Elastic soil deformation model

In the thesis work, elastic-plastic deformation mode has been used throughout the simulations.

11.1Adams Tire

Adams tire is a separate module that helps simulate tire-soil interaction. It computes the forces action on a tire moving over a roadway or irregular terrain. Dynamic response of vehicles performing activities like acceleration, steering braking etc. can be obtained (MSC Software, 2014).

Adams/Tire can be used with Adams/Car, Adams/Chassis, Adams/Solver or Adams/View. In this thesis work, Adams/Tire is employed in Adams/View. Adams/Tire consists of a set of shared libraries which Adams/Solver calls through subroutines. These subroutines, namely, DIFSUB, GFOSUB, GSESUB, compute the moments and force that the tire exert on the vehicle due to tire-terrain interaction. Adams/Tire has a set of tire modules that could be used to model rubber tires. The five modules present in Adams/Tire are (University of Bergamo, 2014).

- Adams/Tire Handling Module
- Adams/Tire 3D Spline Road Module
- Adams/Tire 3D Shell Road Module
- Specific Tire Models
- Features in Adams/Tire modules.

The basic steps involved in Adams/Tire are shown in Figure 60.

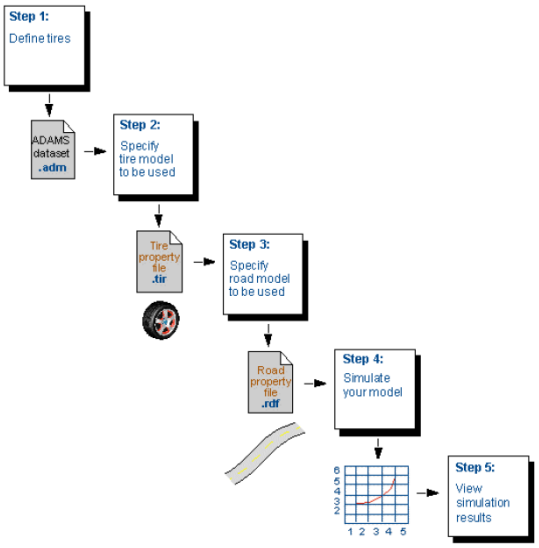

Figure 60 Basic steps followed by Adams/Tire

The three processes that occur when a tire is added to Adams model are (University of Bergamo, 2014):

- Adams/Solver activates Adams/Tire
- Adams/Tire determines the tire and road model to use
- Adams/Tire does the calculations for the tire model

The above mentioned process is graphically represented in Figure 61.

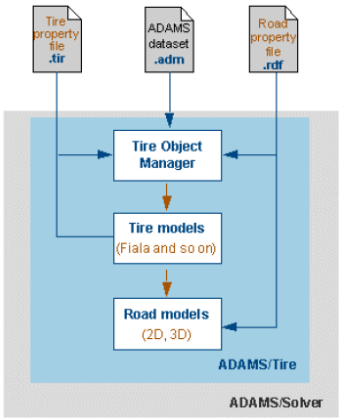

Figure 61 Processes that occur after tire is added to the model

Adams/Solver checks the .adm file to obtain elements that represent a tire; from the .adm file Adams/Solver obtains the tire property file (.tir) and road property file (.rdf). The Tire Object Manager in Adams/Tire examines the tire property file and road property file to determine the tire model and road model to use. The tire Object Manager calls the selected tire model to compute the tire forces and moments; the tire model then checks the road model to determine the relative position of tire with respect to the road model. Then road model obtains road data from road property file; further, the tire model returns the calculated forces and moments to Adams/Solver. Finally Adams/Solver applies the forces and moments to the wheel part. Avery detailed description of the above mentioned procedures and more can be found in the reference mentioned.

11.2 Soft-soil tire model

The Adams/Tire Soft Soil model can explain the tire-soil interaction forces acting on any tire operation on elastic surfaces, like sand, loam, clay and snow. It uses a tire property file and a road property file with extra soil properties.

11.3 Rigid wheel model

The soil characteristics employed in such a model is obtained through measurement and mathematical calculations. Rigid wheel comes in handy when problems associated with rovers/robotics come into picture. Figure 62shows the principle of rigid wheel motion.

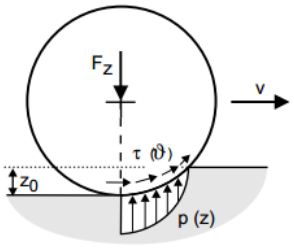

Figure 62 Rigid wheel motion

The stress under a wheel is computed with the help of local pressure under the wheel and local shear displacement. Integrating this local pressure over the specific contact area could provide the vertical reaction being acted upon the wheel. Lateral and horizontal forces can be obtained by integrating local shear stress over the contact area (AESCO, 2014).

11.4 Elastic tire model

Simulation of an elastic tire is a complicated task. Substitution circle method is employed to predict the deflection of the elastic tire; the substitution circle model is shown in Figure 63.

Equilibrium between the vertical reaction force from the soil and vertical reaction from tire is used to obtain the diameter of the substitute circle, D^* (AESCO, 2014).

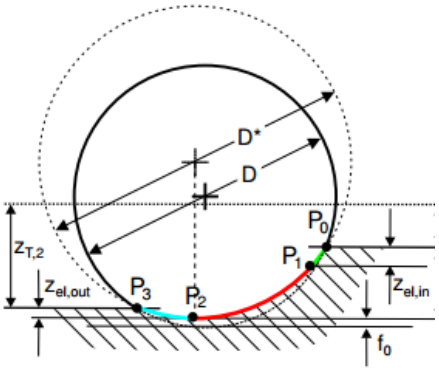

Figure 63 Substitution circle method

11.5 Elastic/plastic deformation of the soil

The deformation experienced by the soil as result of loading by tires consists of an elastic part and a plastic part (MSC Software, 2013).Soil elasticity values used are very important in such simulations, especially for multi-pass computations. As a result more exact and realistic values associated with pressure distribution under wheels can be obtained. Elastic behavior of soil in this module is adapted from Wong's work (Wong, 2010), here the stiffness is assumed to be linear over the entire range of sinkage (AESCO, 2014).

11.6 Visco-elastic tire soil contact

This is another mode of taking into account the tire-soil interaction in Adams soft-soil tire model. Here, for multi-pass effect, the deformation of the road at the exit of tire-soil contact is stored. The rut depth after a tire pass is obtained by correcting with relaxation effect the road deformation (MSC Software, 2013).

11.7 Observations in Adams soft soil

For the one wheel model as well as the full scale model of Komatsu 860, it was noticed that, when the models are in equilibrium position the tire/tires sink to a specific depth into the soil. It was observed that, this sinkage depend upon the amount of load applied to the respective wheel; as the load increases the sinkage increases as can be seen from the.

This position gives the static equilibrium position of the system and returns the static sinkage of the tires. When the simulation was carried out, for both single tire and the Komatsu model, it was observed that the output sinkage was the same as obtained in equilibrium.

This observation is something that is different from what is observed in reality, what can be interpreted from Adams results is that the sinkage value remains the same as observed during

static equilibrium. But in reality, the total sinkage due to a wheel pass/multiple wheel pass is greater than static sinkage; it is the combination of static and dynamic sinkage (Ding, et al., 2014).

Adams uses tire-soil terramechanical models published by Bekker, Wong, Janosi, Ishigami and Schmid. As mentioned before, in the thesis work, elastic/plastic mode in Adams soft-soil is used; for the elastic/plastic model, the soil deformation involves both plastic and elastic sinkage and Adams stores only the plastic deformation (MSC Software, 2013). In Figure 64, the red part represents the plastic deformation and the blue and green part show the elastic deformation (AESCO, 2014). The elastic deformation depends on the elastic stiffness of the soil and the plastic deformation is calculated on the basis of the works done by the Bekker (MSC Software, 2013) .

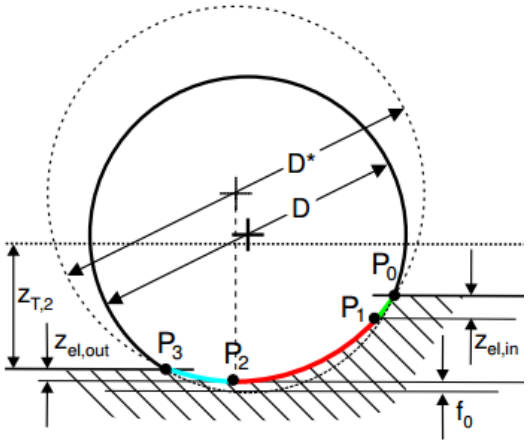

Figure 64 Elastic and plastic deformation of the soil

The plastic deformation is the difference between the total sinkage that depend solely on load, and the elastic deformation which depend on a constant soil elastic stiffness. Also, damping coefficient is not taken into account (AESCO, 2014); if taken into account, then there would have been variations in the graph of sinkage.

It can be inferred that the sinkage/plastic deformation provided by Adams at static equilibrium remains the same during the testing of the tire model. Because it does not take into account the changing soil properties (AESCO, 2014) and the plastic deformation provided solely depend on the wheel load. Adams does not take into account the dynamic sinkage provided by the slip, lugs etc... In the real situation, as each wheel passes the soil properties changes (Lyasko, 2009), this change in soil properties, that is k_c, $k\varphi$ and n, are not taken into account for simplification purposes.

When the soft-soil tire model available for the Komatsu machine was used, it did not give any sinkage, instead the tire just deflected, this was verified by plotting the loaded tire radius and distance of center of mass of the tire from the ground, both returned the same value as seen in Figure 65. The reason was unknown, so another tire property file available in Adams library,

''soft_soil_plastic_elastic'', was used with properties modified to suit the forwarder. This tire property file has option for multi-pass also, but contains certain parameters like low load stiffness effective rolling radius, peak value of effective rolling radius and high load stiffness effective rolling radius, that were unknown.

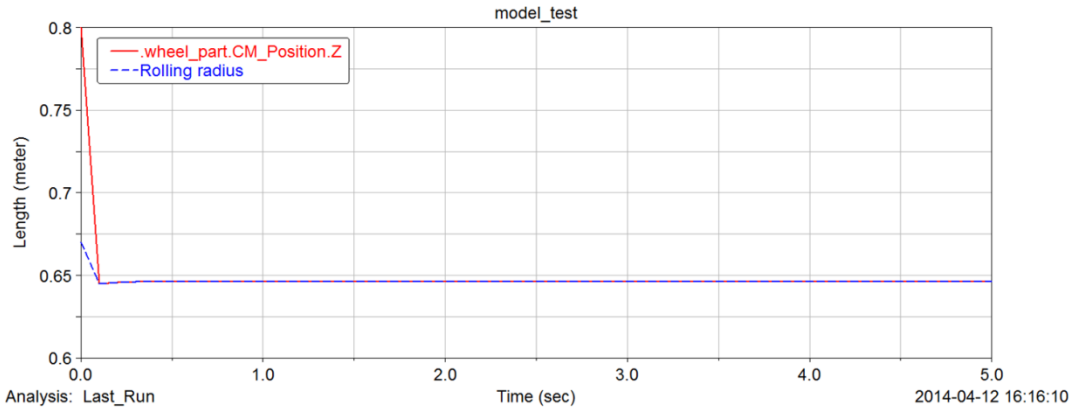

Figure 65 Adams results confirming the loaded tire radius and sinkage as the same

11.8 Multi-pass effect

This effect occurs when two or more wheels run in the same rut created initially by the first wheel. The soil will be compacted as a result of such passes and the consecutive wheel will encounter pre-compacted soil. Sinkage in such pre-compacted soil will be low when compared to the wheel/wheels passed before and as a result the rolling resistance also reduces. Adams soft-soil tire module takes into account the multi-pass effect. Road plastic deformation history stored is used while other tires pass through the exact spot. The second tire passing over a particular spot already traversed by the first tire will experience new soil properties when compared to the already passed first tire, but this fact is not taken into account in soft-soil model (AESCO, 2014). Soft soil model will store the plastic and elastic deformation of the point where the first tire has traversed as a function of the contact point coordinates (MSC Software, 2013). This concept is better explained in Figure 66.

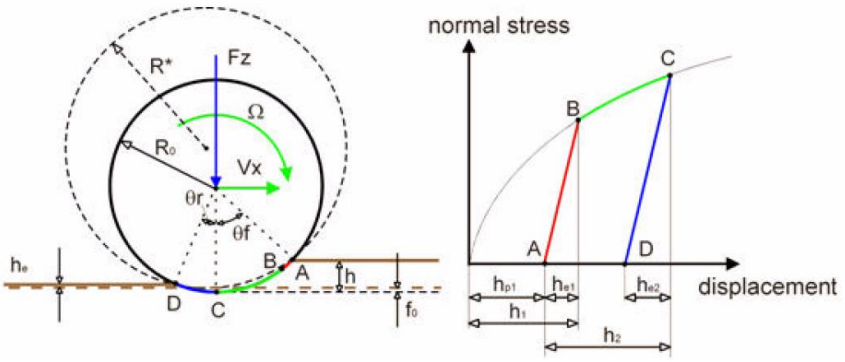

Figure 66 Sinkage estimation in Adams

Take into account two tires, one rolling after the other through the same spot. The first tire will produce an elastic deformation he_1 and a plastic deformation h_{p1}, adding to a total deformation of h_1.

The second tire passing over the same spot will produce an elastic deformation from A to B (=he_1). The plastic deformation of second tire h_{p2} is equal to the total deformation h_2 subtracted from the elastic deformation h_{e2}.

The plastic deformation is calculated as:

$$\text{Plastic deformation} = h - h_e$$

$$h_e = \frac{\sigma(\theta_m)}{C_s} \tag{76}$$

$$h = f(R^*, R_0, f_0) \tag{77}$$

Where,

h_e = elastic deformation

h = total sinkage

f_0 = tire deflection

The coordinates, as well as elastic and plastic deformation and tire width of each tire will be stored. Single point of contact approach is used in soft-soil tire model; the stored values of deformation will be used as a new tire comes into contact with the rut generated by the previous tire pass. So, when a tire encounters the point passed by another tire, the tire just encounters the same virgin terrain at a depth produced by the first terrain, without taking into account the changed soil properties. It has been assumed in the calculations that soil strength parameters will not be changed, in reality it does and can be seen in the work done by M. Lyasko 2009 and Sandu and Senatore 2011, this assumption has been made to simplify the computations and reduce the soil parameters (AESCO, 2014).

11.9 Connecting Adams results with WES models

An attempt was carried out to connect the results from Adams simulation with the WES models. A simple approach was experimented, loaded single wheel at various loads ranging from 10 kN to 24 kN was tested in Adams, the results of which was compared with the WES models.

The soil property values, namely, the cohesive modulus of sinkage (k_φ), friction modulus of sinkage (k_c) and the exponent of sinkage (n) obtained from the bevameter tests at Tierp, Sweden was used in the Adams soft soil road property file. Other values in the soil property file were left as such, because they were not known. The corresponding, value of Cone index

was used in WES calculations. The WES models used were the ones proposed by Maclaurin, Antilla, Gee-Glough and Rantala.

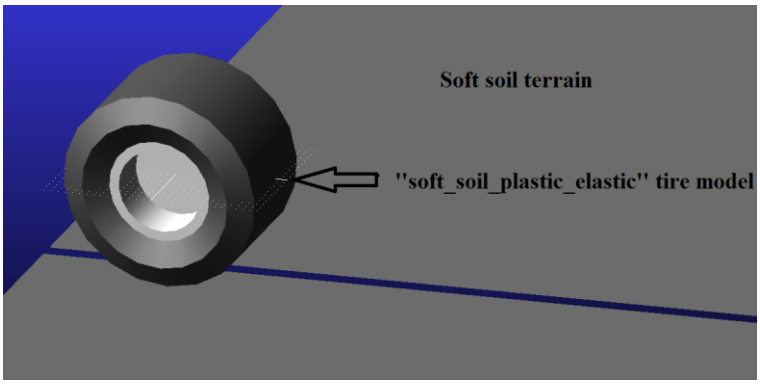

Figure 67 Soft-soil/Tire model in Adams

Results obtained from Adams were exported to Matlab and analyzed. The ratio of sinkage results at various loads from WES models and Adams results were taken to obtain a constant that connects both the results. From Figure 68 , it can be seen that the Antilla model connects well to the Adams results; the ratio is almost near to one. An average of the ratio between Antilla and Adams model, that is, 0.83, can be used to connect both the models. Here the soil condition is assumed to be same, while the load varies.

In the above analysis, the slip-sinkage effect has not been taken into account; it has already been discussed in Section 9 about the importance of slip-sinkage effect. Taking the slip into account in the WES model provides a more realistic result; for that, another comparison the same Adams results and WES model with slip-sinkage incorporated has been done and the results can be seen in Figure 68, here the constant 1.10 connects WES and Adams results.

It has to be noted that, bevameter tests for various soils has to be obtained, to determine the soil stiffness constants as well as exponent of sinkage and inputted to the soft soil road property file along with soil friction angles, soil cohesion stress, soil stiffness and soil deformation modulus to determine the reliability of the constants proposed. Sinkage for each load case starting from 10 kN till 24 kN, as measured from Adams results is shown in Figure 69.

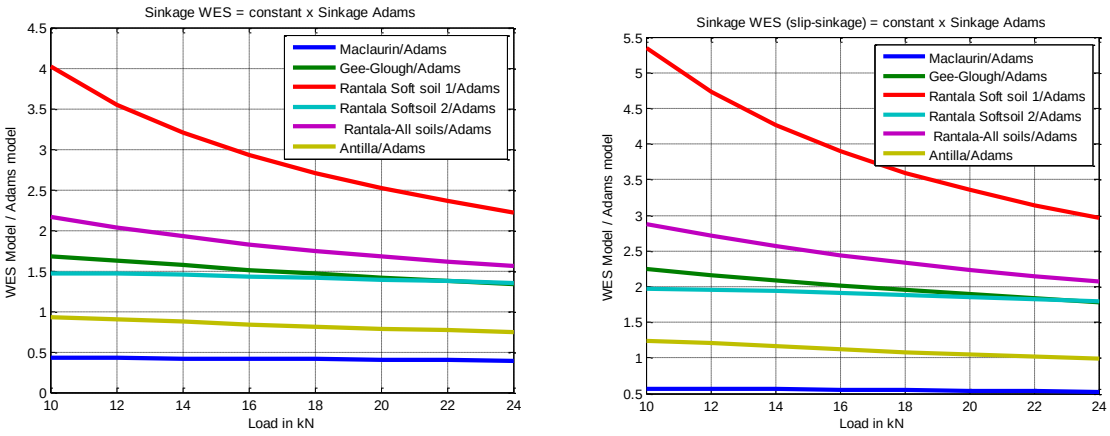

Figure 68 Comparison between Adams result and WES results with/without slip-sinkage

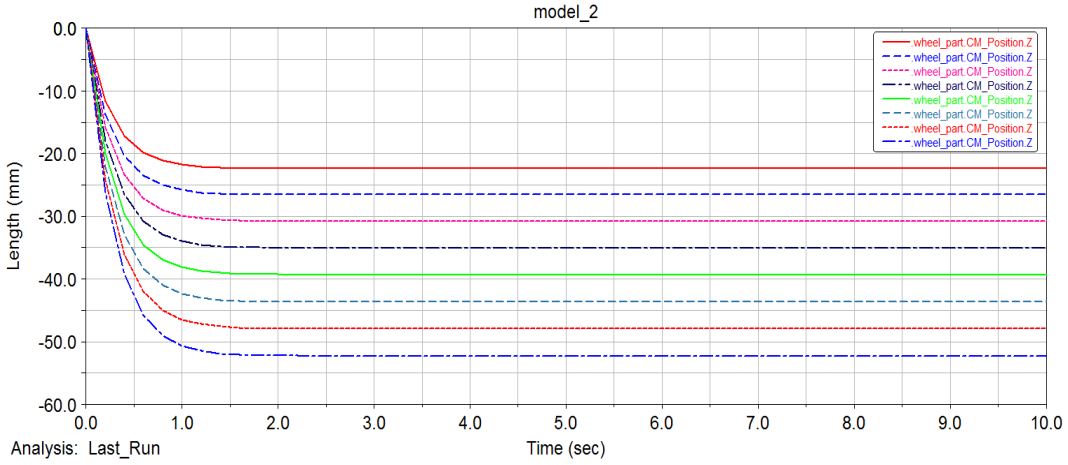

Figure 69 Single wheel test results for various loads from Adams

11.10 Simulation of the Komatsu 860.3 model

The Komatsu 860.3 CAD model was imported to Adams View 2012, then a simulation was run to determine the rut depth created by the vehicle pass.

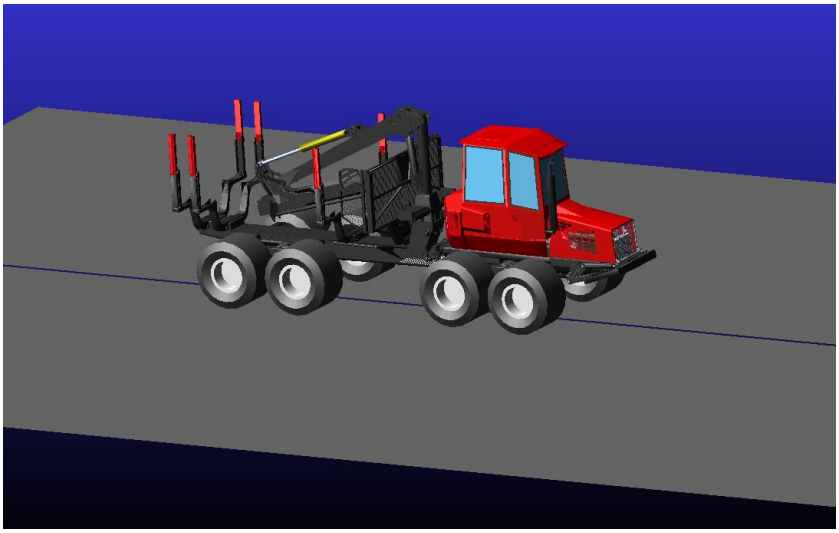

Figure 70 Komatsu 860.3 model imported to Adams View 2012

The model, as seen in Figure 70, was available for unloaded version of the forwarder; proper pressure value of 600 kPa was inputted to the tire property file. The machine was simulated; but the simulation was not as smooth and had issues with equilibrium. The model exhibited unstable behavior during major portion of the simulation time and then provided a stable sinkage value. The results of the simulation in Adams for the right side tires are shown below in Figure 71.

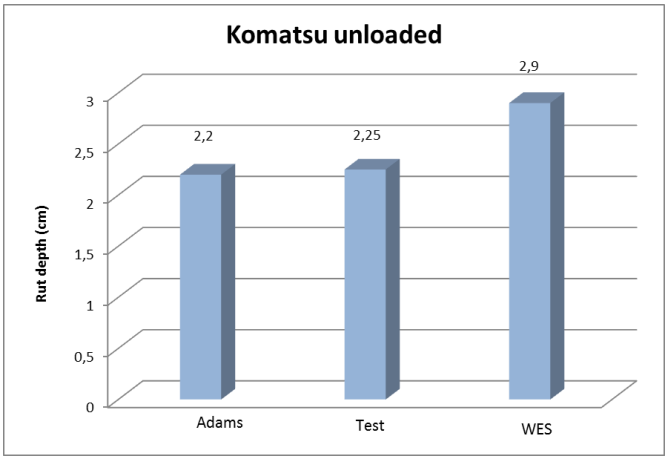

Figure 71 Comparison of Adams, WES and Test data for Komatsu unloaded 600 kPa

In the field test of Komatsu 860.3 for the machine configuration 600 kPa tire pressure unloaded, the rut depth generated was 2.25 cm average on the right side. In the Adams simulation, for the right side tires of the machine, the rut depth created by the after the 4th wheel pass is 2.2 cm as seen in Figure 71 . The same result has been compared with the WES model that takes the slip-sinkage into account.

Also, the Komatsu machine was simulated for loaded condition with 450 kPa by applying the specified load into the Adams model, the result of which is shown in Figure 72. It can be seen from the results that the WES model better predicts the rut depth.

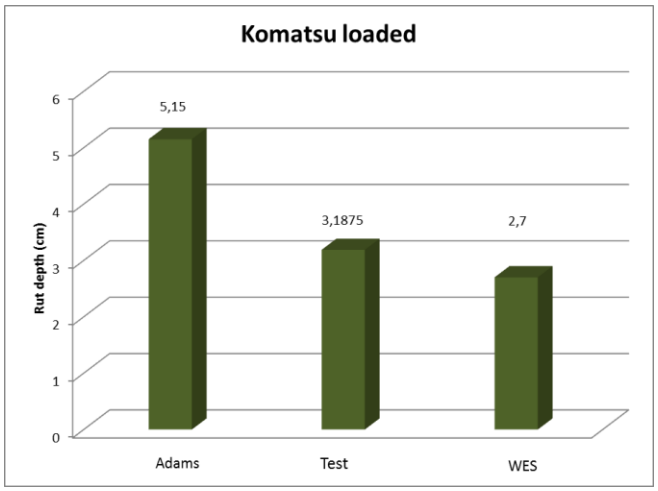

Figure 72 Comparison of Adams, WES and Test data for Komatsu loaded 450 kPa

From the analysis, it can be concluded that the Adams models and the WES model returns results that are similar to the test data. But it has to be kept in mind that Adams does not take the changing soil conditions into account. It would be good to do more simulation in Adams with other forwarder models and compare it with test data and WES models to confirm its suitability for rut depth prediction. The simulations are good for comparing machine configurations. This analysis implies the suitability of using the simple WES based model and demonstrates its capability in predicting rut depth at various machine configurations.

Issues with equilibrium were encountered when simulating the Komatsu model, the model when simulated was trying to obtain its equilibrium position till 200 seconds after which it returned a constant rut depth and this implies a wastage of simulation time. To run the model the default integrator and the permissible error had to be changed; this may also contribute to less accurate results. But still, Adams simulation after the equilibrium stability returns a sinkage value that is almost matching with the test data.

11.11 Effect of tire inflation pressure on sinkage

The tire inflation pressure can affect both the topsoil and upper subsoil stress distribution (Keller & Arvindsson, 2004). The tires are designed in such a way that they should be used at a specific inflation pressure and a specific load. It has been shown by Arvindsson & Ristic, 1996, that the rut depth will increase with the tire inflation pressure. It is evident from Bekker's work as well from other tests (Szymaniak & Pytka, u.d.) that, as the inflation pressure decreases the rut depth also decreases. At low inflation pressure, the tire deflects more due to increased contact area, as a result contact pressure reduces. Pronounced effect of inflation pressure is seen at lower velocities (Szymaniak & Pytka, u.d.).

The effect of tire inflation pressure on sinkage has been studied by simulating a single wheel tester. The wheels were simulated on conditions depicting Upland sandy loam and Rubicon sandy loam. Sinkage values were obtained for a constant load of 21.82 kN and for tire pressures, 270 kPa, 450 kPa and 600 kPa. Also, the sinkage values were compared to the sinkage obtained when the manufacturer prescribed tire pressure was used for the particular load. The results are shown in Figure 73 and Figure 74.

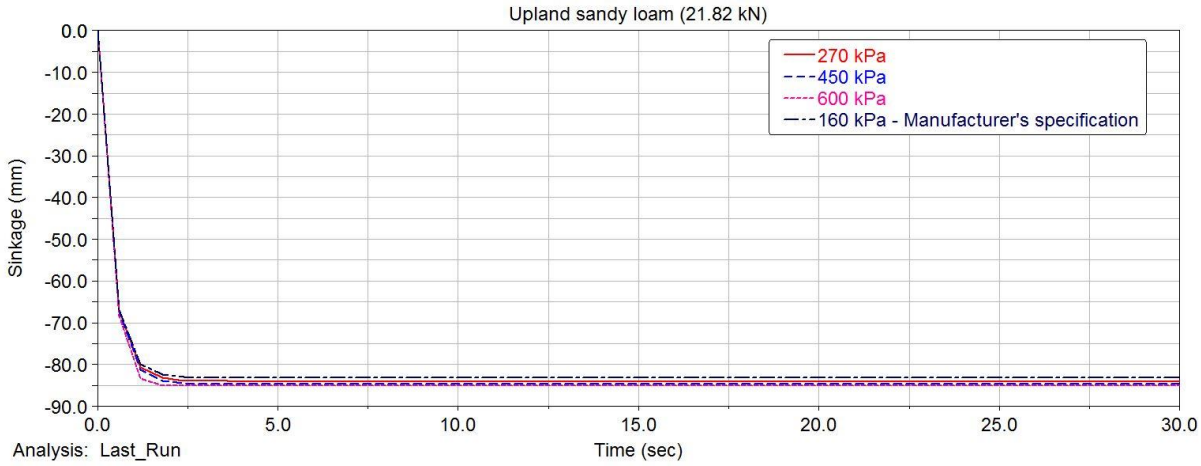

Figure 73 Sinkage for various tire inflation pressures in Upland sandy loam

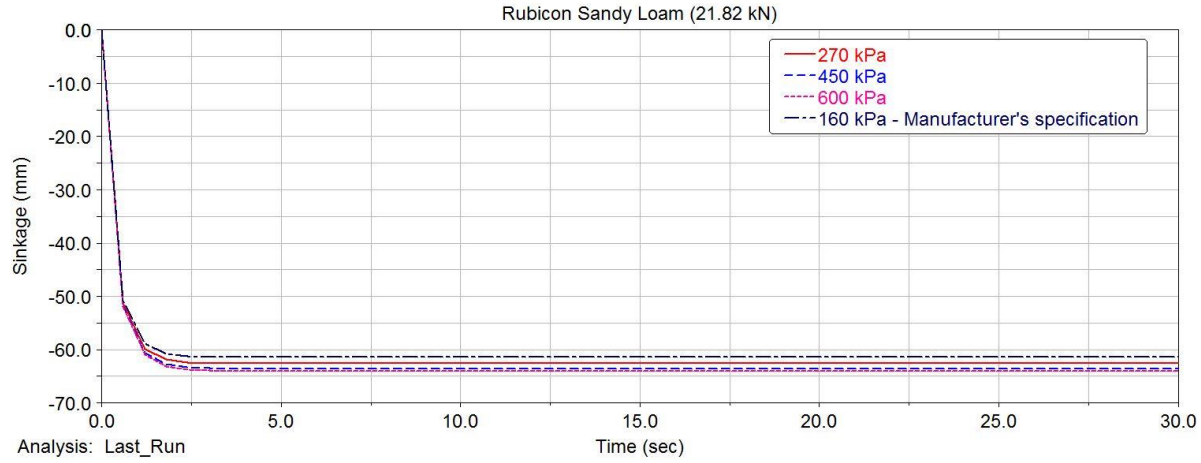

Figure 74 Sinkage for various tire inflation pressures in Rubicon sandy loam

From the results it can be inferred that, the sinkage increases as the tire inflation pressure increases. And, it is advisable to use the manufacturer specified tire inflation pressure to reduce the sinkage. The sinkage at pressures 200 kPa, 220 kPa, 300 kPa, 400 kPa, 450 kPa and 600 kPa was studied for Upland sandy loam as seen in Figure 75.

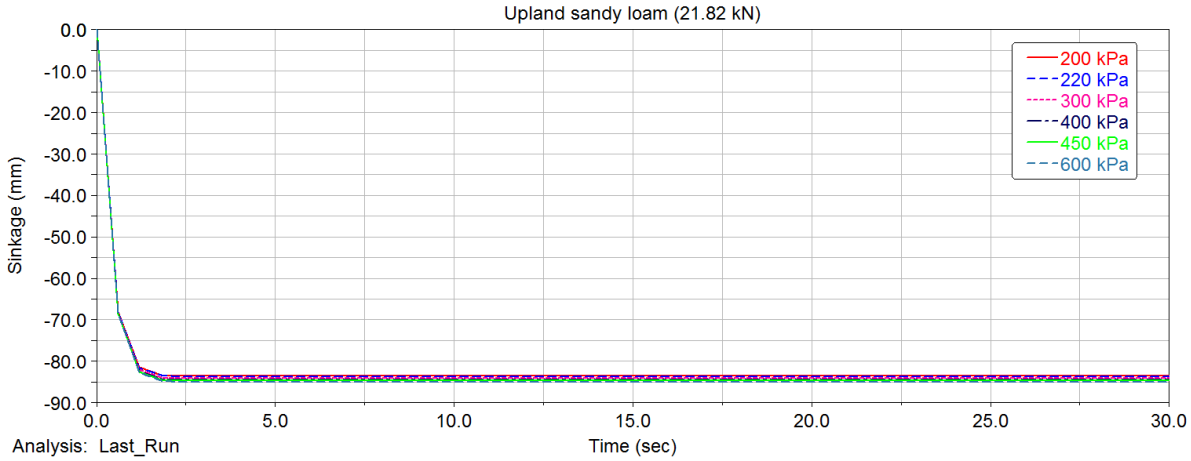

Figure 75 Sinkage for various tire inflation pressure in Upland sandy loam

After the simulation, the results were analyzed in Matlab and a linear relationship was found between the tire inflation pressure and sinkage, the relation can be described as:

$$y = 81 + 0.00359x \tag{78}$$

Where

y= sinkage in mm

x= tire inflation pressure in kPa

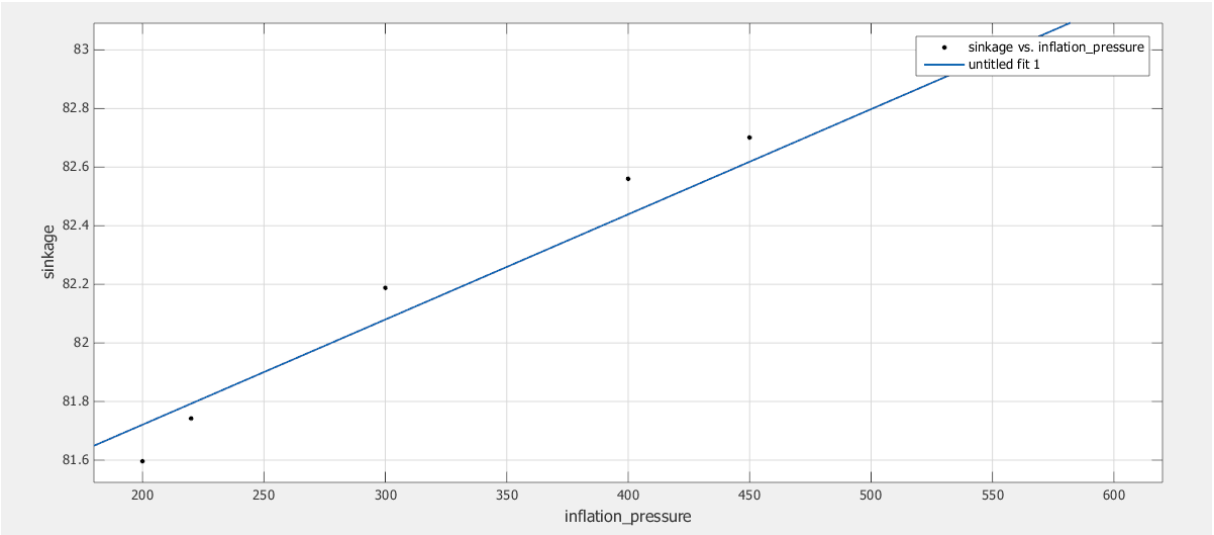

Figure 76 Linear relationship between tire inflation pressure and tire sinkage

11.12 Effect of velocity on rut depth

The velocity of the wheel affects factors like wheel sinkage, wheel slip, net tractive ratio, gross tractive ratio, tractive efficiency etc. From the works of many authors, it can be asserted that velocity should be taken into account while studying tire-soil interaction. To control the performance of off-road vehicles, a general model that is capable of taking into account the changing velocity is needed (Shmulevich, et al., 1998).

Grahn, 1991 concluded from his works on sandy loam that the rut depth decreases as the velocity increases. There are also other studies that indicate reduction in rut depths when the vehicle velocity increases (Szymaniak & Pytka, u.d.). Whereas, Liu, et al., 2009, from their field test on a Heavy Expanded Mobility Tactical Truck concluded that the rut depth increases as the velocity of the vehicle increases. The tests conducted by Crenshaw, 1972 showed that at high speed (higher than 93 km/h) and low speeds (0-37 km/h), as the velocity is increased the rut depth decreases; but at intermediate-speeds (0-37 km/h), as the velocity is increased the rut depth also increases.

So, to get an idea about how the wheel velocity affects the rut depth, a simulation was carried out in Adams. Single wheel with an inflation pressure of 160 kPa was tested in Upland sandy loam with a load of 21.82 kN at various velocities. The results of which are shown in Figure 77.From the results, it can be inferred that, Adams does not taken into account the effect of velocity. For all the velocities, it gives the same sinkage, unlike reality. As a result, the velocity effect on sinkage was not properly studied with Adams as it only takes into account the static sinkage This can be considered as flaw that needs to be rectified, if the software has to been used in prediciting accurate rut depths.

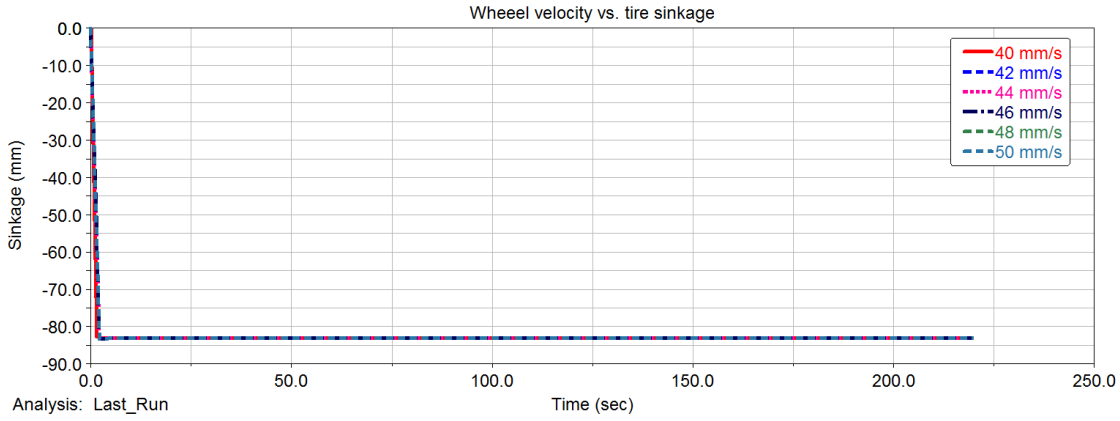

Figure 77 Wheel velocity vs. wheel sinkage simulated in Adams

12 DISCUSSION AND CONCLUSIONS

Various aspects of work done as part of the thesis and the conclusion derived from the study are discussed here.

12.1 Rut depth

From the analysis of the rut depths with the available models for single wheel pass, it can be concluded that, the single pass rut depth models are not suitable for estimating the rut depths caused by a forwarder.

To counter the above mentioned issue, new coefficient's has been obtained through regression analysis for the existing single wheel pass rut depth models to take care of the multi-pass effect of the forwarder's, Rottne 13S and Komatsu 860.3. It is suggested to use the existing WES based models with the new coefficient obtained through regression analysis. Maclaurin's, Antilla's model 1,2,3 and Rantala's model can be used to give a better prediction as those model gives the least mean square error. But it has to be noted that the new coefficients are applicable only for the specific terrain and machine conditions; it should not be extrapolated to other terrain and vehicle conditions.

With the application of the Novel wheel mobility number, the rut depth prediction was enhanced, especially for the Komatsu 860.3. With more test data, the capability of the model could be estimated. This model also has the drawback of being an empirical model and as a result cannot be extrapolated. But, from the results obtained, it can be inferred as a good model.

The variation of constants in WES based models has been studied. It was noted that the constants depend on the soil characteristics, the constants varied when the cone index/cone-index range was varied. The constants displayed the same value for a range of cone index values.

The Abebe model that takes into account the multi-pass effect of wheels has been studied. The original model developed by Abebe was for the multi-pass of same wheels with same load. As a result, that model cannot be applied in the case of the forwarders, due to the varying load on each wheel. So, non-linear regression analysis has been carried out to obtain new values of multi-pass coefficient's that could take care of the situation of varying wheel loads. The use of regression analysis to estimate the best fit parameters implies the use of the model only in the specific conditions. The Abebe model with the new coefficients can predict rut depth better than the single wheel pass models.

During multi-pass of wheels, each following wheel will experience a new soil condition different from the wheel passed before it. This issue has been taken into account by computing the new cone index after each wheel pass, and this new cone index values has been

used to estimate the rut depth after each wheel pass and the cumulative rut depth due to the vehicle pass has been estimated. From the analysis, it was noted that the model give results that are good be taken into account, even though not accurate. This is due to the inherent assumptions applicable to the model that computes the varying cone index. But, this model takes into account the realistic situation of changing soil parameters that are not available in other models.

The Kharkhuta's model was employed to estimate the rut depth due to multi-pass effect of wheels primarily because of the simplicity of the model. But, it was found that the model gives poor results. The Kharkhuta's coefficient should be determined after tests in soil, but here, the coefficient used has been the average of values obtained from literature. This is considered as the primary reason for unsatisfactory results.

An empirical equation to connect the change in rut depth percentage with changing cone index has been obtained. This empirical relation can be used in the future for estimating the change in rut depth percentage with change in cone index percentage. It is suggested to evaluate the efficiency of the relation by doing more multi-pass tests and cross-checking the test data with the calculated results.

Finally, an empirical relation connecting the cone index with depth of measurement has been obtained. From the analysis, the range of values that the coefficients can take has been found out. This equation has the potential to act a good empirical model for finding the cone index at Tierp provided the depth of measurement till 21 cm. Liner equations were proposed even though the trend exhibited was not exactly linear; the reason is to make the equations simpler and reduce the coefficients.

All the empirical models discussed, with the new coefficients can be used to determine the rut depth's with reasonable accuracy and these models can be used as yardstick to select various machine configurations. None of the models can act as a general equation to determine the rut depth; this is mentioned to show that the empirical models cannot act as general model in any parameter analysis. As a suggestion, to estimate the effectiveness of all the approaches and analysis carried out, more field tests with varying loads, machine conditions and soil conditions has to be carried out.

According to Jun, et al., 2004, the soil compaction is dependent on the tire-soil contact pressure. Edlund, et al., 2012, has shown that the forwarder steering and transmission drive system also affects the rut depths. Liu, et al., 2009 has demonstrated the effects of vehicle weight, type, velocity, turning radius, soil texture and soil moisture content affetcs the depth of ruts. A comprehensive model that takes all these factors into account, as well as varying soil conditions, would be more realistic and may provide accurate result. Incorporating the shearing effect due to trailer tires in forwarder has to be addressed by looking into the relation between the trailer turning radius and the wheel torque.

12.2 Pressure

The surface pressure felt by the soil due to wheel load has been studied. Various models proposed by Saarilahti, 2002, has been analysed. It was observed that the Schwanghart (1990) model was in line with the pressure predicted by dividing the wheel load with measured area for Rottne. In case of Komatsu, , MMP Moist clay 1, MMP Moist clay 2, Disern's (2008) 1, Disern's 2008 (2) and Duttmann (2012) provided similar results. Whereas, the model Per (2010) provided similar result to the pressure measured at 15 cm below ground level for Rottne. Ground pressure index, Empirical, Keller (2005) and Disern's (2011) 2 models provided similar result to the measured pressure value at 15 cm for Komatsu. It has been understood that no model could predict the exact value at the tire soil interface and there was no measured value also to compare with. Reviewing various literatures showed that, still there exist confusions in measuring accurate surface pressure values.

It would be good to obtain the pressure at tire-soil interface, and make a comparison with the available models. Values obtained from pressure cells that are placed at low depth give more insight into the contact pressure values. The pressure sensor can be configured in a way similar to placing the load cells as suggested by Lamande, et al., 2007, the sensor can be placed in a specially made cylinder so that it has more contact area and better measurements can be made. Figure 78 shows the construction of the cylinder.

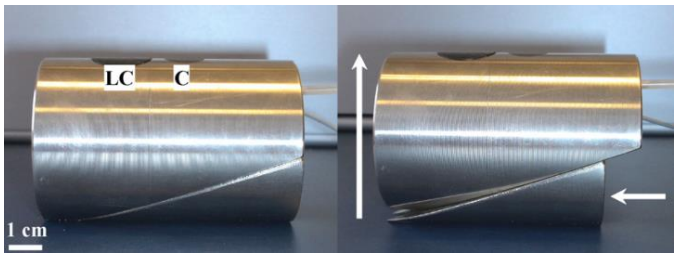

Figure 78 Cylinder designed by Lamande, et al., 2007

The cylinder is made up of two parts, when one part is pushed it displaces relative to the other part and results in a wider diameter. Such an action could cause a good contact between the soil and the load cell.

Also, the load cell arrangement as used by Lamande´ & Schjønning, 2011, can be used to get a better estimate of the contact pressure at the tire-soil interface. This would provide more realistic values to compare the pressure obtained through various models. Also, the suitability of the models for predicting pressure in the specific terrain can be assesed.

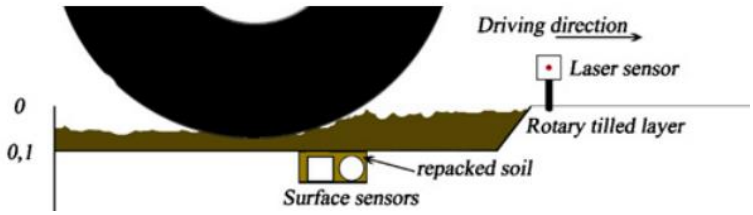

Figure 79 Surface sensor arrangement by Lamande et al., 2007

One of the best methods that can be employed to get an almost accurate value of surface is the one used by Cirello, et al., (2009) were chromatic impression technology is employed. The chromatic filim, know as Prescale film (brand name), is attached between the tire and ground. When the load is applied, the film varies among various shadings of magenta, the internsity of which is directly proportional to the applied load/pressure: the darker color corresponds to higher pressure and vive-versa. The value of pressure can be obtained with the help of a special software. A series of tests at various load levels and at a constant pressure can be done and an empirical relation can be derived, to aid in the surface pressure prediction in Noridic soil conditions.

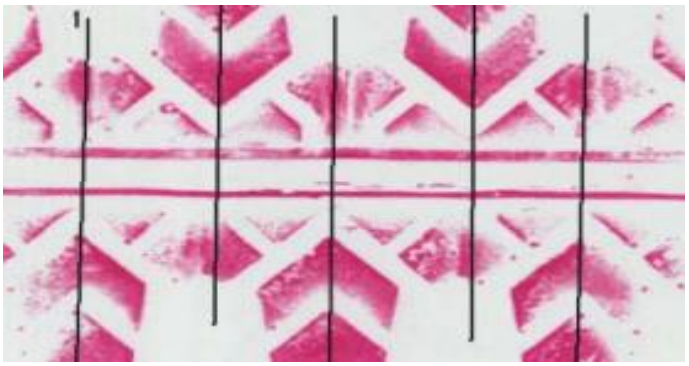

Figure 80 Tire footprint on a Prescale paper

Figure 81 Color density of magenta

The pressure distribution is always not uniform under a tire, the work done by Jun, et al., 2004, demonstrates that when the correct combination of dynamic load and inflation pressure exist, the pressure distribution is relatively uniform. The same work emphasises the use of correct inflation pressure for the specific load to reduce tire-soil contact pressure as well as soil compaction.

The surface pressure also depends on the tire load and tire inflation pressure. But as the tire load increases, the recommended tire inflation pressure increases. This creates a situation where both the parameters cannot be studied independently.

If the pressure value at a certain depth can be considered as standard value to compare the soil damage induced due to heavy machines, measurement's would be easy as compared to surface pressure measurement.

The cone index value at a particular depth along a line has to be measured, along the same line at the same depth, the pressure can also be measured by load cells. Such an analysis at various types of soils has to be carried out. It would be good to connect the cone index and measured pressured to gain an insight about the dependence of cone index and pressure.

12.3 Contact area

Various models have been analyzed to predict the tire-soil contact area of the forwarders. The results have been compared with the measured area, by multiplying the measured length and breadth of the contact patch. It has to be noted that, the measured contact area does not provide the accurate contact patch area, but a rough value only suitable for comparison. Finally, the super-ellipse model was also studied the results were compared with the measured value.

Few models provided values that are close to the measured values. But they cannot completely be regarded as good predictor, as the measured area is only a rough estimate and not an accurate value. By using image processing techniques the real contact area can be calculated, it would be good to compare various models with this original area and determine the best models.

Work done by various researchers suggests the use of the super-ellipse model as good indicator of accurate contact patch area. The study with super ellipse in the thesis also point to that direction. It can therefore be concluded that, super-ellipse model is good predictor of tire-soil contact area.

To exactly determine the contact area, advanced technologies like image processing can be used. The technology is promising and good results have been obtained by applying such technology to obtain the tire soil contact area in a single wheel tester at Urmia University (Mardani & Taghavifar, 2013). Also techniques involving capturing the images of contact area and further analyzing it in an image processing software and finally using a planimeter to obtain the area is also being used and provides a good estimate of the contact area, this method has been explored by Mardani & Taghavifar, 2012.

12.4 Mobility parameters

From the results obtained for the wheel numerics of the both Rottne and Komatsu; for Rottne, the models Turnage (1972a), WESLAB, Wismer and Luth (1973), Maclaurin (1990), Maclaurin (1990_rounded wheel numeric gives similar result for drawbar pull coefficient. For

Komatsu, the models, N.I.A.E Model, Brixiuis (1987), Maclaurin (1990) and Maclaurin (1990_rounded wheel numeric) gives similar results for drawbar pull coefficient.

The rolling resistance provided by most of the models except, N.I.A.E Models and Ashmore et al (1987) for Rottne gives similar results. For Komatsu also, both N.I.A.E Models and Ashmore et al (1987) provide results that are dissimilar to other models.

When cone index range from 200 kPa to 1160 kPa are taken into account, it can been seen that the models Wismer and Luth, Rummer and Ashmore, Maclaurin, Maclaurin new, McAllister and Bruce Maclaurin gives similar results.

As the models, Maclaurin (1990) and Maclaurin (1990_rounded wheel numeric/new), provide reliable results for both drawbar pull coefficient and rolling resistance coefficient, these two models can be used to find out the mobility parameters of the machines at all times. As a word of caution, it has to be noted that the models are empirical.

It would be good to do field tests in real machines in the specified cone index range and compare the results with the theoretical model, so that certain models can be always be used to predict the mobility parameters.

12.5 Roots

Laboratory tests have been carried out to study the reinforcement effect provided by roots to the soil. Two types of soils were used along with branches and roots of pine trees to evaluate their strengthening effects. The results showed variation in the characteristics of the shear force measured; the sandy textured soil with pine branches exhibited higher shear resistance when compared to the other soil with pine roots. It was concluded from the tests that the combination of soil and roots affect the shear strength of the roots. The shear resistance offered by the soil also depends on the root number and configuration; it was evident from the analysis that when the number of root were 2, the vertical arrangement offered more shear resistance; while the horizontal arrangement offered more shear resistance when the number of roots were 4.

The measured shear force obtained from the machined designed by Pirnazarov, et al., (2013) was compared to the results obtained from the perpendicular model, Abe & Ziemer, (1991) model and finally the root strech model. The perpendicular models over estimated the values when compared to the measured data.The perpendiucular model used by both Andre, et al., (2011) and Hudek, et al., (2010) had already received comments from various authors about its overestimation trend, plus the model is only suitable when the root breaks

The model developed by Abe & Ziemer, (1991) has been based on one shear plane, but test rig used for the experiment has two shear planes. The values of cohesion and internal angle of friction for the soils were obtained from laboratory tests in the equipment designed by Pirnazarov, et al., (2013). Also a constant in the model has been obtained from literature. It is assuemd that these may be the reasons that contributed to the oversetimation by the model.

The root stretch model provided good results. This model simulated the exact conditions in the test carried out; because the roots didn’t break and it only stretched. The results, even

though comparable, was not accurate. The possbile resasons include, usage of general fiber tensile modulus for pine roots, assumed shear displacement and the coefficient of friction.

The soil cohesion and friction angle has to be determined through lab tests that follow the standard ASTM D3080 to obatin the accurate value. Similar tests have to be carried out to find the Youngs modulus, coeffcient of friction between roots and soil and finally the shear displacement of roots; this will help to bring the results more close to test data.

It was noticed that the equations used to predict the reinforcement due to roots cannot differentiate between the orientation of the roots that is whether they are horizontal or vertical. This is a major flaw in the equations. One remedy can be to obtain an average value of ratio between the horizontal and vertical arrangement, then apply this ratio to a best fit equation that describes the reinforcement effects due to roots.

When using the perpendicular model, the root average root tensile strength has to be measured by tensile tests and it has to be utilized to obtain the correct value of average tensile strength of roots per unit area (T. Hubble & Docker, 2008). It has also to be taken into account that while calculating the reinforcement effect due to roots, the root diameter has to be divided into classes and analyzed, as is done by Zhou, et al., (1998), Hudek, et al., (2010) etc.

It can be concluded that the perpendicular reinforcement model and Abe & Ziermer model with the available value of cohesion and internal friction angle of soil cannot be used to calculate the reinforcement provided by roots to soil when the soil-root combination is tested in the machine available. But, the root stretch model is promising and can determine the extra reinforcement provided by the roots.

As a solution to the above mentioned issue of incompatibility perperndicular root model and Abe & Ziemer model; a set of empirical equations has been developed for the second set of soil similar to forest soil and pine roots. These equations can be used to predict the shear resistance offered by the specific soil with pine roots when tested in the machien designed by Pirnazarov, et al., (2013).

It is highly recommended that more design features has to be incorporated into the machine designed by Pirnazarov, et al., (2013) such as an actuator to apply a fixed force, proper fixing mechanism, sheat test apparatus etc. so that it could also act as machine that could be used to estimate cohesion and internal friction angle values, and this could make the machine more flexible so that all experiments can be done in a single machine. Data acquisition system can be programmed to directly output the cohesion and friction angle values.

WES based models was used for the calculation of rut depths with and without roots. The root of *Casuarina glauca* was taken into account for the analysis. The results implies a reduction in rut depth with roots when for the forwarder travel. This shows the importance of root systems in reducing the rut depths. Rut depth reduction also depend on root architecture and root distribution .

Roots were modelled as circular plate under elastic foundation and plate under semi-infinite solid. The results suggest the same rut depth for various load combinations in both cases. The

feasibility of the model can only be determined by evaluating the results after a single wheel test on a pine root matrix at various loads.

Thomas & Bankhead, (2009), suggest the use of fiber-bundle models (FBM) to estimate the root reinforcment values exactly. According to the works of Thomas & Bankhead (2009), the constant '1.2' used in the Equation 29 is too large and the value can only be attained if friction angle is greater than 35^0. Pollen & Simon (2005) and Pollen, (2007) developed the fiber bundle model where they take into account the more realistic progressive root failure. The total load applied to the fiber is allotted to a bundle of N parallel fibers in FBM; then the fibers are monitored whether the load applied to the *n*th fivber exceed its strength. Once a fiber has been broken, then the total load is again redistributed among the remaining fibers. This approach has provided more accurate estimate of root reinforcement by taking into consideration the progressive root failure. And even in cases where all the roots break simultaneously, Pollen & Simon, (2005) found that the perpendicular root model overestimates the root reinforcement .

In the light of the given root tests, result analysis and from the various works, it can be concluded that more importance has to be given to FBM models to predict the extra root reinforcement. FBM analysis on roots growing in the nordic soils would give a new dimension to reinforcement modelling, as most of the works have been done in North-American soil.

12.6 Slip-Sinkage

The slip-sinkage effect was studied for a single wheel at various slip to evaluate the effect of slip on sinkage. Both WES and Bekker based models have been used in the calculations. It can be concluded that the sinkage will rise as the slip increases.

Another approach to determine the rut depth of the forwarder, Komatsu 860.3, by using slip-sinkage concept was tried. The slip-sinkage concept proposed by Lyasko, (2009) was used with the wheel carrying the highest load in the forwarder. The results obtained were quite satisfactory, even though not accurate, except for S-shaped curves. The suitabilty of the approach can only be evalauted after comparing results from various tests only. This approach takes into account the slip also, while other WES based model's do not. But, within the frame work of avilable data, the model seems to be promising without involving the complexities associated with estimatimg multi-pass coeffcient's.

12.7 WES-Bekker correlation

One of the main challenges in terramechanics is to connect WES model with the Bekker model. A small step towards solving this problem was taken and a completely new set of equations has been derived for connecting, the cone index individually with sinkage exponent, and friction modulus of deformation and cohesive modulus of deformation. One of the equations can be applied only to sandy textured soils and the other to forest soils. The

equations derived have not been verified by lab tests. It is highly recommended to do field tests in order to see the suitability of the equations.

Bekker has already derived a relation expressing cone index as a function of sinkage exponent, friction modulus of deformation and cohesive modulus of deformation. This relation has been assessed for various soil conditions as well as loads and the results showed that only Gee-Glough WES model complied well with the relation, but not exactly. But more tests in various soil conditions needs to be done to get a complete picture of which models could correlate well.

12.8 Multi-body simulation

A detailed investigation into the feasibility of using multi-body simulation software MSC Adams was done. The various aspects of the soft-soil/tire model were studied and its various drawbacks were determined. The results from Adams were connected to certain WES models using a constant.

The software MSC Adams was used to analyze a single wheel in soft-soil condition and also the full scale Komatsu 860.3 model was simulated to obtain the rut depths created by the vehicle pass. Only one vehicle pass simulation was carried out on the Komatsu machine, also the effect of inflation pressure and vehicle velocity on rut depths were studied with the help of the software.

The results of a single wheel test at various loads were studied and the results were connected to the WES model proposed by Antilla through a ratio. Analysis was carried by taking into account sinkage with and without slip. After carrying out a real world test with single wheel tester, the same approach can be carried out to connect Adams results with test data; as well as with WES models, this would provide more realistic results by taking care of any error presented by Adams results. Such an approach would help to create more realistic results without creating any sub-routine to take care of various changing conditions of soil, but it involves the job of setting up a single wheel test and applies only to a specific soil type. The approaches, single wheel test and writing a subroutine has to be evaluated on the basis of time, complexity and reliability and follow the one that is less demanding on the resources.

Few issues with Adams soft-soil/tire module have been identified. The main issue is that, the package does not take into account the changing soil parameters due to multipass of wheels; this is in stark contrast to what happens in reality. During multipass, it provides rut depths that are actually the static sinkage of the wheels.

During the simulation of the Komatsu model, it was found that the soft-soil module had issues with equilibrium, it displayed unrealistic behavior for the first 200 seconds as highlighted in Figure 82, this necessitate the need to delve more into the root cause behind the issue.

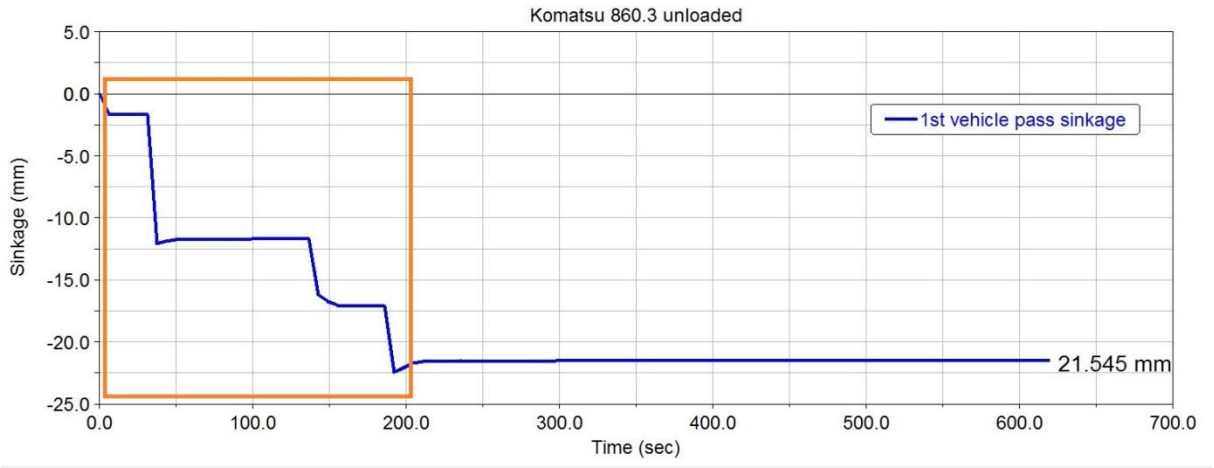

Figure 82 Adams simulation result showing the equilibrium issue

Simulation with both unloaded and loaded condition has been carried out and the results were comparable to the test data and WES model results. This indicates that the both Adams and WES models could be used for rut depth estimation, but the WES models are simple and does not involve the intricacies of Adams.

The tire property file in Adams contains certain parameters like low load stiffness effective rolling radius, peak value of effective rolling radius and high load stiffness effective rolling radius, that were unknown. Such complications can be avoided by taking into consideration the WES models, where the only input parameter is the Cone Index. This reinforces the usage of WES model based subroutines in Adams to tackle the issues associated with tire-soil interaction. The WES models do not need any parameters that are usually fed to the Adams soft soil property files also. The Bekker based approach provides a more detailed overview about calculating various variables like normal stress, longitudinal shear stress, lateral shear stress, bulldozing effect, grouser effect etc. A subroutine that could incorporate both the models, even though time consuming, would be appropriate in taking care of multi-pass effect as well as determining the forces acting on the vehicle traversing on soft soil. But if rut depth estimation and mobility parameters are given high importance, then a WES based subroutine is good enough.

Digital elevation model (DEM) techniques can also be taken into account to tackle the issue of changing soil parameters due to multi-pass effect. With DEM, the soil surface can be portrayed as a digital elevation grid DEM. Through subroutines the soil parameters of each grid can be changed as each wheel passes through a set of grids, so that the following wheel experiences a set of grids with modified soil parameters and simulates non-homogeneous soil condition. Similar kind of analysis with DEM has been done by Trease, et al (2011) as well as in the research carried out at the Institute of Robotics and Mechatronics in the German Aerospace Center (Krenn & Hirzinger, 2009).

The process of changing the grid parameters has been implemented by Pan, et al.(2004) in their work focussing on creating a complete simulation environment by taking into account all the models and mobility analysis of vehicles operating in soft-terrain. The same has been

implemented by Madesn, et al. (2013) when they developed a model that could take care of three dimensional deformable terrain in mobility simulation software. Madsen, et al., (2012) in their work dealing with simulating a terrain vehicle interaction model for a vehicle simulator has taken care of changing soil parameters by modifying the density of the soil; the soil density modification has been done by taking into account the time the tire has been in contact with the soil. In the aforementioned work, the tire soil interaction has been modelled by physics based analysis where visco-elastic-plastic regimes are taken into account. It would be good to implement the varying cone index approach for the same mehod mentioned above and compare the results with test data.

Generating DEM of nordic forest terrain using methods like interferometric synthetic aperture radar and digital image correlation method and connecting it to Adams to generate terrain would provide more reliable high fidelity simulations, as it depicts the exact terrain rather than a user-created terrain.

Adams has been used to study the effect of varying inflation pressure on rut depths at a constant load with the help of a single wheel. From the analysis, it can be concluded that at a certain load, the manufacturer recommended tire inflation pressure returns the lowest rut depth.

An attempt to study the effect of velocity on rut depth was initiated, but the outputs were same for all the velocities tried. This implies that the software does not take into account the velocity effects of the wheel.

Fixing the inherent problems with the software are integrating it with more realistic terrain models, tire models and a subroutine that could take care of varying soil parameters would assist in improving the performance of high fidelity simulations, which in-turn could generate more realistic model based designs.

13 RECOMMENDATIONS AND FUTURE WORK

Recommendations and areas of future work intended to take elevate the tire-soil interaction analysis to a more detailed level is discussed in this chapter.

Effect of factors like turning radius, velocity and moisture content on rut depth should be studied. They should be independently studied in various soil conditions to get a broad idea. The effect of turning radius of trailers and the torque acting on the wheel should be carried out in various soil conditions as well a machine conditions to get a grip of the various factors affecting the rut depth in the S-shaped portion. A generalized equation based on such studies can be developed; implementation of the developed relation into the available WES model could aid in predicting rut depth accurately in the S-shaped curves.

Soil properties like cohesion and internal friction angle should be obtained through proper laboratory tests, it is not recommended to use values available from literatures, as soil properties vary from place to place.

Similarly, the Bekker parameter's (cohesive modulus of deformation, friction modulus of deformation and sinkage exponent) used should be obtained through proper bevameter tests. Using already existing values for similar soil types is not recommended. This helps in giving proper inputs to Adams road file, which can have a bearing on the predictions.

Contact pressure acting in the tire-soil interface can be studied in detailed by carrying out field tests. With such tests, the relation of contact pressure on tire inflation pressure, tire contact area, soil conditions etc.. can be studied in relation to the Nordic conditions. It is highly recommended to follow the approach intoduced by Cirello, et al., (2009).

Finite element analysis can be carried out to study in detail about the shear stress reinforcement occurring when the roots are tested in the machine designed by Pirnazarov, et al., (2013). This will help to derive suitable analytical equations to predict the extra reinforcement provided by the roots in the soil; this can aid in making the machine a standardized instrument to test various roots in diffrent soils.

Taking into account the complex calculations of Bevameter approach going into the software; it is highly recommended to implement a WES based sub-routine that could take care of various terramechanic parameters in Adams. It also has the advantage of using only the cone index as the input variable, instead of using the Bekker parameter's as well as other soil property values. Implementing the changing soil conditions through a proper subroutine, either the changing Bekker parameters or the changing Cone index values, in Adams is highly advocated, this will take the simulation to a more realistic level. If such a subroutine procedure is developed, it has to be ensured that proper contacts with the MSC experts have to be maintained to avoid future incompatibilities. The existing issue equilibrium has to be studied in detail and work can be initiated to fix the problem.

The forwarder while doing its work has to be studied in detail and its behavior while traversing various terrains as well as obstacles has to be noted. This knowledge should be taken into account while creating an Adams based model, so that a more refined Adams model that captures real world behavior can be implemented. Such a two way interaction could produce a refined simulation model.

Implementation of DEM based approach in Adams has the potential to take care of the changing soil conditions during multi-pass. Simulating the forwarder over realistic terrains that takes into account DEM and variable soil characteristics opens a new chapter to take forwarder simulations to a new level. Varying cone index calculations can be implemented in such a platform to yield better simulation models that can take care of reality better when compared to the existing models.

The effect of tire lug on tractive performance is not taken care by any commercially available terramechanic software. The soil flow effects like bulldozing and slip-sinkage are also dealt in an ad-hoc manner. This is an area where more study can be carried out to further refine the existing terramechanic software's capability, especially Adams.

14 REFERENCES

Abebe, A. T., Tanaka, T. & Yamazaki, M., 1989. Soil compaction by multiple passes of a rigid wheel relevant for optimization of traffic.. *Journal of Terramechanics.*

Abe, K. & Ziemer, R. R., 1991. Effect of tree roots on a shear zone: modling reinforced shear stress. *Canadian Journal of Forest Research.*

Abe, K. & Ziemer, R. R., 1991. *Effect of Tree Roots on Shallow-Seated Landslides,* CA,USA: USDA Pacific Southwest Research Station.

AESCO,2014.[Online]
http://www.tire-soil.de/Demo/Version-1.13/UserGuide.pdf
[Accessed 2 April 2014].

Affleck, R. T., July 2005. *Disturbance Measurements from Off-Road vehicles on Seasonal Terrain* , Washington: US Army Corps of Engineers .

Akay, A. E., Sessions, J. & Aruga, K., 2006. Designing a forwarder operation considering tolerable soil disturbance and minimum total cost. *Journal of Terramechanics.*

Andre, L. S. o.a., 2011. Engineering ecological protection against landslides in diverse mountain forests: Choosing cohesion models. *Ecological Engineering.*

Ansorge, D., 2007. *Soil Reaction to Heavily Loaded Rubber.* u.o.:Cranfield University, School of Applid Science.

Arvindsson, J. & Keller, T., 2007. Soil stress as affedted by wheel load and tyre inflation pressure. *Soil & Tillage Research.*

Arvindsson, J. & Ristic, S., 1996. Soil stress and compaction effects for four tractor tyres. *Journal of Terramechanics.*

Baladi, G. Y. & Rohani, B., 1981. *Correlation of mobility cone index with fundamental engineering properties of soil,* u.o.: U.S.Army Waterways Experiment Station.

Bekker, M. G., 1956. *Theory of land locomotion.* Ann Arbor: University of Michigan Press.

Bekker, M. G., 1969. *Introduction to Terrain-Vehicle Systems.* u.o.:University of Michigan Press, USA.

Berglund, K. & Berglund, Ö., 2008. Distribution and cultivation intensity of agricultural organic soils in Sweden and an estimation of greenhouse gas emissions.. *Geoderma.*

Bishop, D. M. & Stevens, M. E., 1964. *Landslides on Logged Areas in South-east Alaska,* u.o.: US Department of Agriculture, Juneau, Alaska.

Botta, G. F. o.a., 2008. Soil compaction produced by tractor with radial and cross-oly tyres in two tillage regimes.. *Soil & Tillage Research.*

Brown, C. B. & Sheu, M. S., 1975. Effects of Deforestation on Slopes. *Journal of Geotechnical Engineering Division.*

Choi, J. H., Woo, J. S., Kim, K. W. & Cho, J. R., 2012. Numerical investigation os snow traction characteristics of 3-D patterned tire. *Journal of Terramechanics.*

Cirello, A., Marannano, G. & Mariotti, G. V., 2009. Experimental analysis of the contact pressure distribution in an off-road tyre. *The Journal of Strain Analysis for Engineering Design.*

Cofie, P., 2001. *Mechanical properties of tree roots for soil reinforcement models, Doctoral Thesis,* The Netherlands: Wageningen University.

Crenshaw, M. B., 1972. Soil/wheel interaction at high speed. *Journal of Terramechanics.*

Defossez, P. & Richard, G., 2002. Models of soil compaction due to traffic and their evaluation.. *Soil Tillage.*

Ding, L. o.a., 2014. New perspective on characterizing pressure-sinkage relationship of terrains for estimating interaction mechanics. *Journal of Terramechanics.*

Diserens , E., Defossez b, P., Duboisset, A. & Alaoui, A., 2011. Prediction of the contact area of agricultural traction tyres. *Biosystems Engineering.*

Diserns, E., 2008. Calculating the contact area of trailer tyres in the field. *Soil and Tillage Research.*

Diserns, E., Defossez, P., Duboisset, A. & Alaoui, A., 2011. Prediction of the contact area of agricultural traction tyres on firm soil. *Biosystems Engineering.*

Docker, B. B. & Hubble, T. C., 2008. Quantifying root-reinforcement of river bank soils by four Australian tree species.. *Geomorphology.*

Duttmann, R., Brunotte, J. & Bachd, M., 2012. Spatial analyses of field traffic intensity and modeling of changes in wheel load. *Soil and Tillage Research.*

Döll, H., 2001. *Deformation-characterstics farm tyres-effect on the soil-pressure and plant - stress.* u.o., u.n.

Edlund, J., Bergsten, U. & Löfgren, B., 2012. Effects of two diffrent forwarder steering and transmission drive systems on rut dimensions.. *Journal of Terramechanics.*

Edlund, J., Bergsten, U. & Löfgren, B., 2012. Effects of two diffrent steering and transmission drive systems on rut dimensions. *Journal of Terramechanics.*

ESA,u.d.[Online]
http://robotics.estec.esa.int/ASTRA/Astra2008/S08/08_01_Krenn.pdf
[Accessed 19 May 2014].

Genet, M. o.a., 2008. Root reinforcement in plantations of Cryptomeria japonica D. Don: effect of tree age and stand structure on slope stability. *Forest Ecology and Management.*

Genet, M. o.a., 2007. The influence of cellulose content on tensile strength in tree roots. i: *Eco-and Ground Bio-Engineering: The Use of Vegetation to Improve Slope Stability*. Netherlands: u.n.

Grahn, M., 1991. Prediciton of sinkage and rolling resistance for off-the road vehicles considering peneteration velocity.. *Journal of Terramechanics*.

Gray, D. H. & Barker, D., 2013. Root-Soil Mechanics and Interactions. i: *Riparian Vegetation and Fluvial Geomorphology*. u.o.:American Geophysical Union.

Gray, D. H. & Barker, D., 2013. Root-Soil Mechanics and Interactions. i: *Riparian Vegetation and Fluvial Geomorphology*. u.o.:u.n.

Gray, D. H. & Sotir, R. D., 1996. *Botechnical and Soil Bioengineering Slope Stabilization*. New York: Wiley.

Grecenko, A., 1995. TYRE FOOTPRINT AREA ON A HARD GROUND COMPUTED FROM CATALOGUE VALUES. *Journal of Terramechanics*.

Grecenko, A. & Prikner, P., 2013. Tire rating based on soil compaction capacity. *Journal of Terramechanics*.

Hallonborg, U., 1996. Super ellipse as tyre-ground contact area. *Journal of Terramechanics*.

Hambleton, J. P. & Drescher, A., 2009. Modelling wheel-induced rutting in soils: Indentation. *Journal of terramechanics*.

Hegazy, S. & Sandu, C., 2013. Experimental investigation of vehicle mobility using a novel wheel mobility number. *Journal of Terramechanics*.

Hetherington, J. G. & White, J. N., 2002. An investigation of pressure under wheeled vehicles. *Journal of Terramechanics*.

Holm, I. C., 1969. MULTI-PASS BEHAVIOUR OF PNEUMATIC TIRES. *Journal of Terramechanics*.

Horn, R., Vossbrink, J. & Becker, S., 2004. Modern forestry vehicles and their impacts on soil physical properties. *Soil & Tillage Research*.

Hudek, C., Burylo, M. & Rey, F., 2010. Root system traits of Mahonia acquifolium and its potential use in soil reinforcement in mountain horticulture practice.. *Scientia Horticulture*.

Hudek, C., Burylo, M. & Rey, F., 2010. Root system traits of Mahonia acquifoluim and its potential use in soil reinforcement in mountain horticulture practices. *Scientia Horticulturae* .

Hudek, C., Rey, F. & Burylo, M., 2010. Soil reinforcement by the roots of six dominant species on eroded mountainous marly slopes (Southern Alps, France). *Caten*.

Håkansson, I., 1994. Subsoil compaction caused by heavy vehicles-a long term threat to soil productivity. *Soil & Tillage Research*.

Iagnemma, K. o.a., 2011. *Terramechanics modelling of mars surface exploration rovers for simulation and parameter estimation.*. Washington, DC, USA, ASME.

Jun, H.-g.o.a., 2004. Dynamic load and inflation pressure effects on contact pressures of a forestry forwarder tire. *Journal of Terramechanics.*

Karafiath, L. L., 1975. *Development of mathematical model for pneumatic-tire soil interaction in layered soils.*, Michigan: U.S Army Tank Automotive Command.

Keller, T., 2005. A Model for the Prediction of the Contact Area and the Distribution of Vertical. *Biosystems Engineering.*

Keller, T. & Arvindsson, J., 2004. Technical solutions to reduce the risk of sunsoil compaction: effects of dual wheels,tandem wheels and tyre inflation pressure on stress propagation in soil.. *Soil & Tillage Research.*

Krenn,R.&Hirzinger,G.,2009.[Online]
http://robotics.estec.esa.int/ASTRA/Astra2008/S08/08_01_Krenn.pdf
[Accessed 19 May 2014].

Labell, E. R. & Jaeger, D., 2006. *Assessing Soil Disturbances Caused by Forest Machinery.* Idaho, u.n.

Lamande´, M. & Schjønning, P., 2011. Transmission of vertical stress in a real soil profile. Part I: Site description,. *Soil & Tillage Research.*

Lamande, M., Schjønning, P. & Tøgersen, F. A., 2007. Mechanical behaviour of an undisturbed soil subjected. *Soil & Tillage Research.*

Lindström, A. & Rune, G., 1999. Root deformation in plantations of container-grown Scots pine trees: effects on root growth, tree stability and stem straightness. *Plant and Soil.*

Liu, K., Ayers, P., Howard, H. & Anderson, A., 2009. Influence of soil and vehicle parameters on soil rut formation. *Journal of Terramechanics.*

Liu, K., Ayers, P., Howard, H. & Anderson, A., 2009. Influence of turning radius on wheeled military vehicle induced rut formation. *Journal of Terramechanics.*

Liu, K., Howard, H., Anderson, A. & Ayers, P., 2009. Influence of turning radius on wheeled military vehicle induced rut formation. *Journal of Terramechanics.*

Lyasko, M., 2009. LSA model for sinkage predictions. *Journal of Terramechanics.*

Lyasko, M., 2009. Slip sinkage effect in soil-vehicle mechanics. *Journal of Terramechanics.*

Lyasko, M., 2010. Multi-pass effect on off road vehicle performance. *Journal of Terramechanics.*

Lyasko, M. I., 1994. TEH DETERMINATION OF DEFLECTION AND CONTACT CHARACTERISTICS OF A PNEUMATIC TIRE ON A RIGID SURFACE. *Journal of Terramechanics.*

Lyasko, M., u.d. LSA model for sinkage predictions. *Journal of Terramechanics.*

Maclaurin, B., 2013. Using a modified version of the Magic Formula to describe the. *Journal of Terramechanics.*

Madesn, J., Seidl, A. & Negrut, D., 2013. *Off-road vehicle simulation with a compaction based deformable terrain model.* Oregon, ASME.

Madsen, J. o.a., 2012. A physics-based vehicle/terrain interaction model for soft soil off-road vehicle simulations. *SAE International.*

Mardani, A. & Taghavifar, H., 2012. CONTACT AREA DETERMINATION OF AGRICULTURAL TRACTOR WHEEL WITH SOIL. *Agronomical Research in Moldavia.*

Mardani, A. & Taghavifar, H., 2013. Potential of function image processing technique for the measurement of contact area and contact pressure of a radial ply tire in a soil bin testing facility.. *Measurement*.

McKyes, E., 1985. *Soil Cutting and Tillage*. New York: Elsevier.

Melanz, D. J., Mazhar, H. & Negrut, D., 2014. A multibody dynamics-enabled mobility analysis tool for military applications. *SAE International.*

Michigan.gov,2014.[Online]
http://www.michigan.gov/documents/dnr/9-Rutting_193281_7.pdf
[Accessed 6 April 2014].

MSCSoftware,2014.[Online]
http://simcompanion.mscsoftware.com/infocenter/index?page=content&id=DOC10409&cat=2013_ADAMS_DOCS&actp=LIST&showDraft=false
[Accessed 4 April 2014].

MSCSoftware,2014.[Online]
http://www.mscsoftware.com/en-nd/product/adams
[Accessed 6 April 2014].

MSCSoftware,2014.[Online]
http://www.mscsoftware.com/assets/1712_adm6_02_dat_tire_ee_r5.pdf
[Accessed 8 April 2014].

Onafeko, O. & Reece, A. R., 1964. Soil stresses and deformations beneath rigid wheels. *Journal of Terramechanics.*

Pan, W., Papelis, Y. & He, Y., 2004. *A vehicle-terrain system modeling and simulation approach to mobility analysis of vehicles on soft terrain.* Bellingham, u.n.

Picchio et al., 2012. Machinery-induced soil compaction in thinning two pine stands in central Italy. *Forest Ecology and Management*, p. 6.

Pirnazarov, A., Sellgren, U. & Löfgren, B., 2013. *Development of a methodology for predicting the bearing capacity of rooted soft soil.* Tampa, u.n.

Plackett, C. W., 1984. The ground pressure of some agricultural tyres at low load with zero sinkage. *Journal of Agricultural Engineering.*

Pollen, N., 2007. Temporal and spatial variability in root reinforcement of streambanks: accounting for soil shear strength and moisture.. *Catena.*

Pollen, N. & Simon, A., 2005. Estimating the mechanical effects of riparian vegetation on streambank stability using fiber bundle model.. *Water Resource Research*.

Pollen, N. & Simon, A., 2007. Estimating the mechanical effects of riparian vegetation on stream bank stability using a fiber bundle model. *Water Resources Research*.

R.L.Raper, 2005. Agricultural traffic impacts on soil. *Journal of Terramechanics*, p. 22.

Ronai, D. & Schmulevich, I., 1995. TIRE FOOTPRINT CHARACTERISTICS AS A FUNCTION OF SOIL PROPERTIES AND TIRE OPERATIONS. *Journal of Terramechanics*.

Saarilahti, M., 2002. *SOIL INTERACTION MODEL*, Helsinki: University of Helsinki, Department of Forest Resource Management.

Sakai, H. o.a., 2008. Soil compaction on forest soils from different kinds of tires and tracks and possibility of accurate estimate. *Croatian Journal of Forest Engineering*.

Sandu, C. & Senatore, C., 2011. Off-road tire modelling and the multi-pass effect for the vehicle dynamics simulation. *Journal of Terramechanics*.

Schjønning , P. o.a., 2007. Modelling effects of tyre inflation pressure on stress distribution near the soil-tyre interface. *Biosystems Engineering*.

Schjønning, P. & Lamande, M., 2010. A note on the vertical stresses near the soil-tyre interface. *Soil and Tillage Research*.

Schmidt, K. M. o.a., 2001. Root cohesion variablity and shallow landslide susceptibility in the Oregon Coast Range. *Canadian Geotechnical Journal*.

Schwanghart, H., 1991. MEASUREMENT OF CONTACT AREA, CONTACT PRESSURE AND COMPACTION UNDER TIRES IN SOFT SOIL. *Journal of Terramechanics*.

Sharma,A. K. & Pandey, K. P., 1996. A REVIEW ON CONTACT AREA MEASUREMENT OF PNEUMATIC TIRE ON RIGID AND DEFORMABLE SURFACES. *Journal of Terramechanics*.

Shioji, Y. o.a., 2010. Determining the angle of repose of sand under low-gravity conditions using discrete element method.. *Journal of Terramechanics*.

Shmulevich, I., Mussel, U. & Wolf, D., 1998. The effect of velocity on rigid wheel performance. *Journal of Terramechanics*.

Spenko, M. & Meirion-Griffith, G., 2011. A modified pressure-sinkage model for small,rigid wheels on deformable terrains.. *Journal of Terramechanics*.

Sutherland, B. J., 2003. *PREVENTING SOIL COMPACTION AND RUTTING IN THE BOREAL FOREST OF WESTERN CANADA*, u.o.: Forest Engineering Research Institute of Canada.

Szymaniak, G. & Pytka, J., u.d. *Effects of reduced inflation pressure and ride velocity on soil surface deformation*. u.o.:u.n.

T. Hubble, T. C. & Docker, B. B., 2008. Quantifying root-reinforcement of river banl soils by four Australian tree species. *GEOMORPHOLOGY*.

Thomas, R. E. & Bankhead, N. P., 2009. Modelling root-reinforcement with a fiber-bundle model and Monte Carlo simulation. *Ecological Engineering*.

Thomas, R. E. & Bankhead, N. P., 2009. Modelling root-reinforcement with a fiber-bundle model and Monte-Carlo simulation. *Ecological Engineering*.

Timoshenko, S. & Krieger, S. W., 1959. *Theory of Plates and Shells*. McGraw Hill: u.n.

Trease, B. o.a., 2011. *Dynamic modeling and soil mechanics for path planning of the mars exploration rovers*. Washington DC, ASME.

UniversityofBergamo,2014.[Online]
http://mech.unibg.it/~lorenzi/VD%26S/Matlab/Tire/tire_basics.pdf
[Accessed 8 April 2014].

Upadhyaya, S. K., Wulfsohn, D. & Mehlschau, J., 1993. An instrumented device to obatin traction related parameters.. *Journal of Terramechanics*.

Waldron, L. J., 1977. The shear resistance of root permeated homogeneous and stratified soil. *Soil Science*.

Waldron, L. J. & Dakessian, S., 1981. Soil reinforcement by roots: calculation of increased soil shear resistance from root properties. *Soil Science*.

Van Beek, L. P., Wint, J., Cammeraat, L. H. & Edwards, J. P., 2005. Observation and simulation of root reinforcement on abandoned Mediterranean slopes.. *Plant Soil*.

Wijekoon, M., 2012. *Forest machine tire-soil interaction*, Stockholm, Sweden: KTH Royal Institute, School of Industrail Engineering and Management.

Wong, J. Y., 1967. Behaviour of soil beneath rigid wheels. *Journal of agricultural engineering research*.

Wong, J. Y., 1984. An Introduction to Terramechanics. *Journal of Terramechanics*.

Wong, J. Y., 2010. *Terramechanics and Off-Road Vehicle Engineering*. UK: Elsevier.

Wu et al., 1988. Study of Soil-Root Interaction. *Journal of Geotechnical Engineering*, p. 25.

Wulfsohn, D. & Upadhyaya, S. K., 1992. Determination of dynamic three dimensional soil tyre contact profile.. *Journal of Terramechanics*.

Wu, T. H., 1976. *Investigation of landslides on Prince of Wales Island,Alska.*, Columbus, Ohio: Department of Civil Engineering, Ohio State University.

Wästerlund, I., 1989. STRENGTH COMPONENTS IN THE FOREST FLOOR RESTRICTING MAXIMUM TOLERABLE MACHINE FORCES. *Journal of Terramechanics*.

Xia, K., 2010. Finite element modelling of tire/terrain interaction: Application to predicting soil compaction and tire mobility. *Journal of Terramechanics*.

Yong, N. R., Fattah, A. E. & Skiadas, N., 1984. *Vehicle Traction Mechancis Developments in Agricultural Engineering*. Amsterdam: Elsevier.

Zhou, F. o.a., 2013. Simulations of Mars Rover Traverses. *Journal of Field Robotics*.

Zhou, Y., Watts, D., Li, Y. & Cheng, X., 1998. A case study of effect of lateral roots of Pinus yunnanensis on shallow soil reinforcement. *Forest Ecology and Management*.

APPENDIX A: EQUATIONS

A1.Wheel numerics

Model	Equation	Remarks
Wismer and Luth (1973)	$C_N = \frac{CIbd}{W}$	CI= Cone index
Freitag (1965)	$N_{CC} = \frac{CIbd}{W}\sqrt{\frac{\delta}{h}}$	
Freitag (1965) improved model	$N_{CI} = \frac{CIbd}{W}\sqrt{\frac{\delta}{h}}\frac{1}{1+\frac{b}{2d}}$	
Maclaurin (1997_Rounded wheel numeric)	$N_M = \frac{CIb^{0.85}d^{0.8}\delta^{0.4}}{W}$	
Brixius	$N_B = \frac{CIbd}{W}\left(\frac{1+5\frac{\delta}{h}}{1+3\frac{b}{d}}\right)$	

A2. Wheel Loads

	Komatsu 8600.3 (kN)				Rottne F13 (kN)			
	Unloaded		Loaded		Unloaded		Loaded	
1ST wheel	26.3	26.9	24.3	24.9	28.8	29.8	27.5	27.8
2nd wheel	26.3	27.1	24.5	24.7	28.1	29.1	27.7	27.7
3rd wheel	21.1	22	49.8	49.6	19	19.4	40.8	44.8
4th wheel	20.4	21.6	49	50	20.1	20.9	42.8	46.6
Total weight	191.7		296.8		195.2		285.7	
Payload	NA		105.1		NA		82.2	

A3. Rut depth models

Model	Equation	Remarks
Antilla 1	$z = d\left(0.003+\frac{0.910}{C_N}\right)$	
Antilla 2	$z = d\frac{0.248}{N_{CI}}$	

Antilla 3	$z = 0.003 + \frac{0.380}{N_{CC}}$	
Antilla 4	$z = 0.000 + \frac{0.328}{N_{CI}}$	
Antilla 5	$z = 0.005 + \frac{1.212}{C_N}$	
Antilla 6	$z = \left(0.001 + \frac{0.287}{N_{CC}} \right) d$	
Antilla 7	$z = \left(-0.001 + \frac{0.248}{N_{CI}} \right) d$	
Rantala 1	$z = 0.059 + \frac{0.490}{N_{CI}}$	Soft soil
Rantala 2	$z = \frac{0.989}{N_{CI}^{1.23}}$	Soft soil
Rantala 3	$z = 0.010 + \frac{0.610}{N_{CI}}$	
Saarilahti 1	$z = \frac{0.142}{N_{CI}^{0.83}} d$	
Maclaurin	$z = d \left(\frac{0.224}{N_{CI}^{1.25}} \right)$	
Gee-Glough	$z = \frac{\mu_R d}{\left(0.63 + 0.34 \frac{b}{d} \right)^2}$ $\mu_R = \frac{0.287}{N_{CI}}$	

A4. Mobility models

Model	Equation
Turnage (1972 b, WESFIELD)	$\mu_P = 0.8 - \frac{1.31}{N_{CI} - 2.45}$ $\mu_R = 0.04 + \frac{0.20}{N_{CI} - 2.50}$
Turnage (1972 a, WESLAB)	$\mu_P = 1.51 - \frac{12.37}{N_{CI} + 5.94}$ $\mu_R = 0.04 + \frac{0.20}{N_{CI} - 1.50}$

Wismer and Luth (1973)	$\mu_P = 0.75\left(1-e^{-0.3C_N S}\right)-\left(0.04+\frac{1.2}{C_N}\right)$ $\mu_R = 0.04+\frac{1.2}{C_N}$ $\mu_T = 0.75\left(1-e^{-0.3C_N S}\right)$
N.I.A.E models	$\mu_P = 0.56-\frac{0.47}{N_{CI}}$ $\mu_R = 0.07+\frac{0.2}{N_{CI}}$
Brixius (1987)	$\mu_P = 0.88\left(1-e^{-0.1N_B}\right)\left(1-e^{-7.5S}\right)-\left(\frac{1}{N_B}+\frac{0.05S}{\sqrt{N_B}}\right)$ $\mu_R = \frac{1}{N_B}+0.04+\frac{0.05}{\sqrt{N_B}}$ $\mu_T = 0.88\left(1-e^{-0.1N_B}\right)\left(1-e^{-7.5S}\right)+0.04$
Ashmore et.al (1987)	$\mu_P = 0.47\left(1-E^{-0.20N_C S}\right)+0.38\left(\frac{W}{W_R}\right)-\left(\frac{0.22}{N_C}+0.20\right)$ $\mu_R = -0.1\left(\frac{W}{W_R}\right)+\frac{0.22}{N_C}+0.20$ $\mu_T = 0.47\left(1-E^{-0.20N_C S}\right)+0.28\left(\frac{W}{W_R}\right)$
Rummer and Ashmore (1985)	$\mu_R = \frac{1.15}{C_N}+0.06\left(\frac{W}{W_R}\right)$
Maclaurin (1990)	$\mu_P = 0.8-\frac{3.2}{N_{CI}}+1.91$ $\mu_R = 0.017+\frac{0.453}{N_{CI}}$
Maclaurin (1990_Rounded wheel numeric)	$\mu_P = 0.8-\frac{3.2}{N_M}+1.91$ $\mu_R = 0.017+\frac{0.453}{N_M}$
Sharma and Pandey (1998)	$\mu_P = 0.76\left(1-e^{-0.07N_{CC}S}\right)$ $\mu_T = 0.36\left(1-e^{-0.35N_{CC}S}\right)$
McAllister (1983)	$\mu_R = 0.054+\frac{0.323}{N_{CI}}$

Bruce Maclaurin (2013)	$\mu_R = 0.01 + \frac{0.41}{N_{CM} - 0.14}$ $N_{CM} = \frac{CIb^{0.9} d^{1.1}}{W} \left(\frac{\delta}{d} \right)^{0.45}$

A5. Contact area equations

Model	Equation	Remarks
Pneumatic tire on hard surface	$A = cl_c b_c$ $l_c = 2\sqrt{d\delta - \delta^2}$ $b_c = 2\sqrt{2r_b\delta - \delta^2}$ $c = 1$ $c = 0.785$ $c = 0.85$	lc=contact patch length bc=contact patch width rb=tire transversal radius δ =tire deflection
Mikkonen and Wuolijoki	$A = b.r$	
Swedish formula	$A = l_c b_c$ $l_c = 1.235r$ $b_c = 1.02r$	
Schwanghart (1991)	$A = 0.77bl_c$ $l_c = \sqrt{d\left(z+\delta\right) - \left(z-\delta\right)^2} + \sqrt{d\delta - \delta^2}$	
Komadi (1990)	$A = \frac{cW^{0.7}\sqrt{\frac{b}{d}}}{p_i^{0.45}}$ $c = 0.31$	pi=tire inflation pressure
Silverside and Sundberg (1989)	$A = \frac{0.90W}{p_i}$	W=wheel load
Kemp (1990)	$A = \frac{W}{p_i}$	
Grecenko (1995)	$A = cbd$ $c = 0.245$	d=wheel diameter
Krick (1969)	$A = 8\delta h$ $A = 5.3h^2\delta\left(\frac{p_i}{W}db\right)^{0.8}$	
Pillai and Fielding (1986)	$A = 1.85\delta^{\frac{2}{3}} b.r^{\frac{1}{3}}$	

Godbole et al (1993)	$A = \pi\delta\sqrt{dh}$ $\delta = h.0.54\left(\frac{p_i dh}{W}\right)^{-0.79}$	
Dwyer (1984)	$A = \frac{W}{G}$ $G = \frac{W}{bd}\sqrt{\frac{h}{\delta}}\left(1+\frac{b}{2d}\right)$	G=ground pressure index
Febo (1987)	$A = \frac{\pi}{4} l_c b_c$ $l_c = 2\sqrt{d}\,\delta^{0.44}$ $b_c = b_w\left(1-e^{-36\delta}\right)$	
Söhne (1969)	$A = 2b\sqrt{dz}$	z=sinkage
Diserns (2008)	$A = \left(0.1174\times WD\right)+\left(4.5\times10^{-5}\times F\right)-\left(18.3\times10^{-5}\times P_i\right)$ $A = \left(0.1360\times WD\right)+\left(6.7\times10^{-5}\times F\right)-\left(32.2\times10^{-5}\times P_i\right)$	WD=b X d
Keller (2005)	$A = 0.43 w_{tyre} d_{tyre} - 0.0006152\, p_{tyre} + 0.0022 F_{wheel}$	w_{tyre} =tire with d_{tyre} =tire diameter p_{tyre} =tire inflation pressure F_{wheel} = wheel load
Duttmann (2012)	$A = \left(0.416.B.D\right)-\left(457.670 P_i\right)+\left(0.186.F\right)$	F=wheel load
Lyasko (1994)	$A = \frac{\pi}{4} ab$ $a = C_3\sqrt{Df - f^2}$ $b = 2\sqrt{D_p}\, f - f^2$ $D_p = \frac{\left(B+H\right)}{2.5}$ $C_3 = \frac{23}{\left(\lvert D/B-3.5\rvert+11.9\right)}$	
Diserns (2011)	$A = 0.2461.TS$ $TS = bd$	

Ronai and Schmulevich (1995)	$A = a_1 + a_2 F + a_3 p_i + a_4 w$ $A = a_5 + a_6 F + a_7 p_i + a_8 w + a_9 F p_i + a_{10} F w + a_{11} p_i w$ $+ a_{12} F^2 + a_{13} p_i^2 + a_{14} w^2$ $a_1 = 760, a_2 = 32.37, a_3 = 0.846, a_4 = 19.84$ $a_5 = -68.3, a_6 = 16.04, a_7 = -1.805, a_8 = 72.66$ $a_9 = -0.027, a_{10} = 0.0027, a_{11} = 0.0141, a_{12} = 0.5970$ $a_{13} = 0.0035, a_{14} = 0.9102$	
Geecenko and Prikner (2013)	$A = 0.927 + 0.761 \times AR - 1.215 \times AR^2$ $AR = \frac{h}{b}$	
Sharma and Pandey (1996)	$A = \frac{\pi l b}{4}$ $A = 4 f \sqrt{Dh}$ $l = 2\sqrt{Df}$	f=deflection
Grecenko (1995)	$A = 0.245 \times b \times d$ $A = 1.57 \times (d - 2r) \times \sqrt{db}$ $A = 0.926 \times b \times \left[d (d - 2r)^2 \right]^{1/3}$ $A = \frac{98.1W}{112.8 + 66.5p + 0.883 \times 10^{-2} W - 0.4d}$	
Per Schjønning (2010)	$A = 0.46^b$	b=wheel width

A6. Contact pressure equations

Model	Equation	Remark
MMP Moist clay	$MMP = \frac{3.3 W_{TW}}{2mbd\sqrt{\frac{\delta}{d}}}$ $MMP = \frac{k_1 W_{TW}}{2mbd}$ $k_1 = 9.1, 7.9$	
Koolen (1992)	$P = 2 p_i$	
Boling (1985)	$P = 40 + p_i$	
Steiner (1979)	$P = 112.8 + 665 p_i + 0.88W - 40d$	

Ground Pressure Index	$P = \frac{W}{b^{0.8} d^{0.8} \delta^{0.4}}$	
Empirical	$P = 45 + 0.32 p_i$	
Ziesak and Matthies (2001)	$P = -3947 + 0.000452.\frac{W.PR.p_i}{bd} + 29.4 \ln\left(\frac{W}{9.81}\right)$ $\frac{-4239}{p_i} - 253.3d^2 - \frac{1149.5}{b} - 2911.8.\ln(1000b)$ $+1807bd + \frac{1.295W}{bd} - 0.009W^2 - \frac{7117.3}{PR} - 440.6\ln(PR)$ $+\frac{1144.4}{h} + 3845\ln(h.1000) - \frac{2.26b}{1000}\left[\left(\frac{1000d}{2}\right)^2 - (500.d - 1000h)^2\right]$	PR=ply rating

All the other pressure models are obtained by dividing the load acting on the wheel by the corresponding area (that is mentioned in Appendix A5).

B1. Root testing in lab

Figure 83 Roots tested and root arrangement in horizontal and vertical orientation

Figure 84 Roots inside the test box and soil after test with 2 roots in horizontal orientation

Figure 85 After a test with single root

APPENDIX C: DEPTH OF MEASUREMENT vs. CI

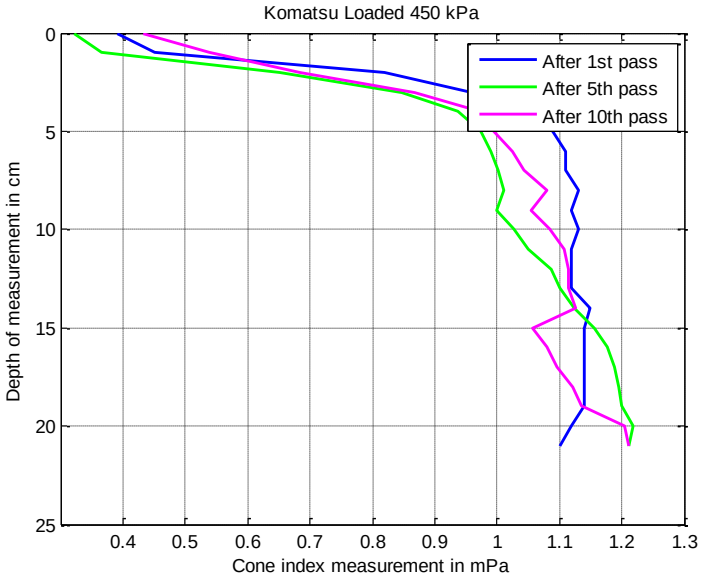

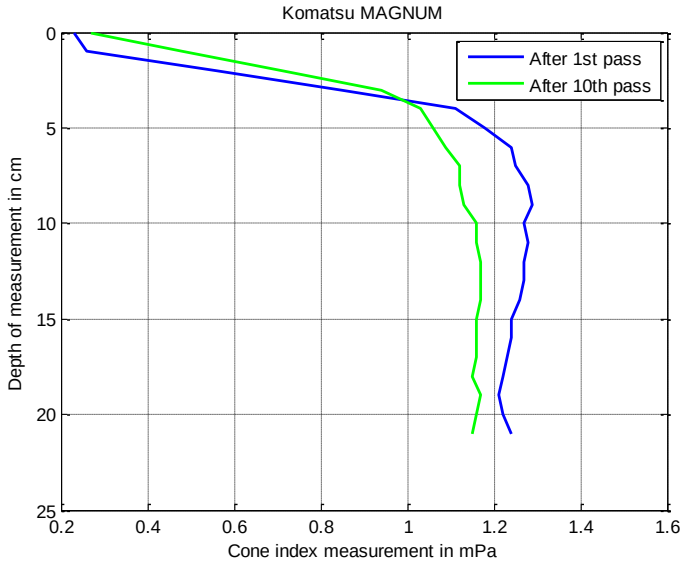

Figure 86 Depth of measurement vs. cone index for Komatsu and Komatsu with MAGNUM tracks

APPENDIX D: DIRECT SHEAR TEST RESULT

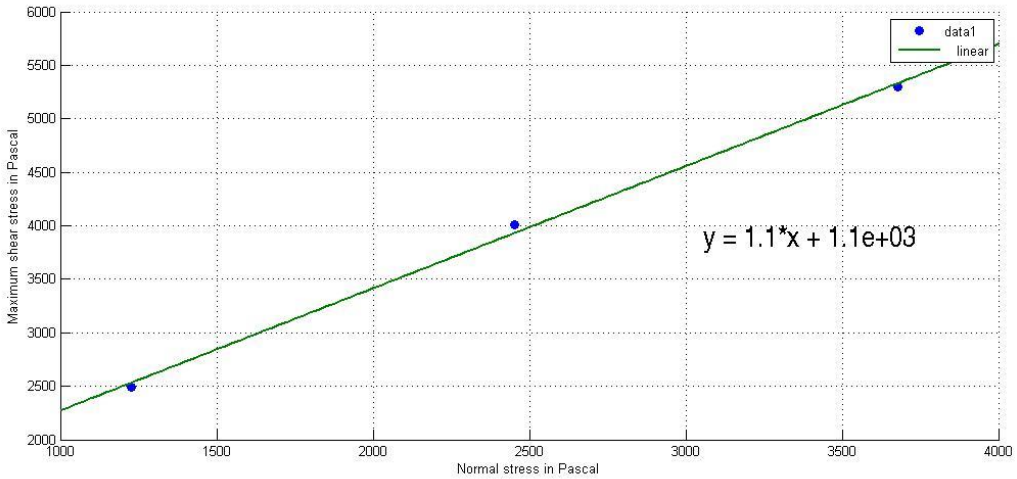

Figure 87 Result of direct shear test of the soil

APPENDIX E: ROOT DATA ANALYSIS

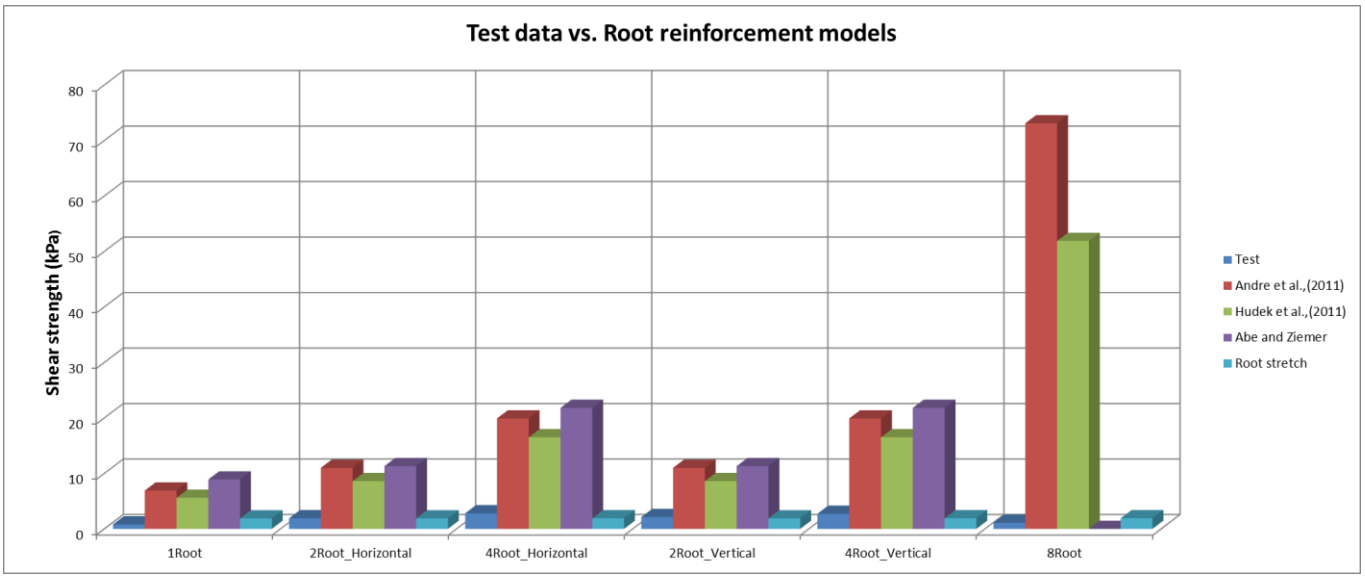

Figure 88 Comparison of shear strength test data vs. root reinforcement models